

Aus der Klinik und Poliklinik für Innere Medizin C (Direktor Univ.- Prof. Dr. Florian H. Heidel) der Universitätsmedizin der Universität Greifswald

**Identification of
functional vulnerabilities
in
acute myeloid leukemia**

Kumulative Inauguraldissertation zur Erlangung
des akademischen Grades Doctor of Philosophy (PhD)

der

Universitätsmedizin

der

Universität Greifswald

2023

vorgelegt von:

Tubío-Santamaría, Nuria

geb. am: 05.12.1992

in: Boiro, Spanien

Dekan: Prof. Dr. Karlhans Endlich

1. Gutachter(in): Prof. Dr. Florian H. Heidel, Universitätsmedizin Greifswald

2. Gutachter(in): Prof.Dr. Elke Krüger, Universitätsmedizin Greifswald

3. Gutachter(in): Prof.Dr. Jan Krönke, Charité Universitätsmedizin Berlin

Datum der Verteidigung: 20.11.2023

Ort, Raum: Hauptgebäude des Universitätsmedizin, Seminarraum J-04.34

The work presented in this thesis was performed under supervision of
Prof. Dr. Florian H. Heidel, University Medicine Greifswald,
Prof. Dr. Elke Krüger, University Medicine Greifswald, and
Prof. Dr. Jan Krönke, Charité University Medicine Berlin

Table of contents

1. List of abbreviations	5
2. Zusammenfassung	7
3. Summary	8
4. Introduction	9
4.1. Malignant transformation of hematopoietic cells	8
4.2. Cell polarity regulators in acute myeloid leukemia	10
4.3. Post-transcriptional regulation in acute myeloid leukemia	11
4.4. Dependency of KMT2A-rearranged leukemia on proteostasis	12
4.4.1. Sensitivity of KMT2A-rearranged leukemia to proteasome inhibition	14
5. Methods	15
6. Results	16
7. Discussion	20
8. Bibliography	23
9. Declaration of contribution to the publications	30
10. Original publications	31
11. Acknowledgements	66

1. List of abbreviations

ALL	Acute lymphoid leukemia
AML	Acute myeloid leukemia
BM	Bone marrow
BTZ	Bortezomib
cP	Constitutive proteasome
CSPs	Cold-shock proteins
Dlg	Discs large
DOT1L	Disruptor of telomeric silencing 1-like
FDA	Food and Drug Administration
FP	Fusion partner
HnRNP K	Heterogeneous nuclear ribonucleoprotein K
HSCs	Hematopoietic stem cells
HSPCs	Hematopoietic stem and progenitor cells
H2Bub	Histone H2B monoubiquitination
H3K4	Histone 3 lysine 4
H3K79	Histone 3 lysine 79
iP	Immunoproteasome
KMT2A-FP	KMT2A fusion-protein
KMT2Ar	KMT2A-rearranged
LBD	LEDGF-binding domain
LDA	Limiting dilution assay
LEDGF	Lens epithelium–derived growth factor
LLGL1	Lethal Giant Larvae Protein Homolog 1
LSCs	Leukemic stem cells
LSK	Lin ⁻ Kit ⁺ Sca1 ⁺
LT-HSCs	Long-term HSCs
MBM	Menin-binding motif
MEN1	Menin 1
MLL1	Mixed Lineage Leukemia 1
MM	Multiple myeloma
NPM1c	NPM1-mutant
PB	Peripheral blood
PDX	Patient derived xenografts
PIs	Proteasome inhibitors
P-TEFb	Positive transcription elongation factor b

RBP	RNA binding proteins
RNAi	RNA interference
Scrib	Scribble
SEC	Super elongation complex
SET	Su (Var)3-9, enhancer-of-zeste, trithorax
TCS1/2	Taspase1 cleavage sites 1/2
Ub	Ubiquitin
UPR	Unfolded protein response
UPS	Ubiquitin proteasome system
5-FU	5-Fluorouracil

2. Zusammenfassung

Obwohl sich das Outcome bei Patienten mit akuter myeloischer Leukämie (AML) in den letzten Jahrzehnten verbessert hat, liegt die Gesamtüberlebensrate jedoch immer noch unter 50 % [1, 2], und es besteht nach wie vor ein essentieller Bedarf an der Entwicklung neuer therapeutischer Strategien. In diesem Projekt haben wir funktionelle Vulnerabilitäten in der AML identifiziert und anschließend das therapeutische Potenzial von Zielstrukturen untersucht, die an der Proteostase, der Zellpolarität sowie an der RNA-Prozessierung bei verschiedenen Signalwegen beteiligt sind.

Dabei konnten wir zeigen, dass die genetische Inaktivierung des Zellpolaritätsregulators Scribble die Entwicklung der AML verzögert. Jedoch scheint die Deletion von Scribble auch die Proliferationsfähigkeit normaler hämatopoetischer Zellen zu beeinträchtigen, was ein Angehen von Scribble als therapeutisches Zielstruktur in der AML erschwert. Im Gegensatz dazu hemmt sowohl die Inaktivierung des pleiotropen DNA- und RNA-bindenden Proteins YBX1, welches zur Familie der Cold-shock Proteine zählt, als auch die Inaktivierung der katalytischen Untereinheit PSMB8/LMP7 des Immunoproteasom-Multiproteinkomplexes, der zum Ubiquitin-Proteasom-System (UPS) gehört, das Wachstum von Leukämie-Zellen, ohne dabei die Funktion normaler hämatopoetischer Stamm- und Vorläuferzellen zu beeinflussen. Diese Tatsache prädestiniert diese Zielstrukturen als potenzielle neue therapeutische Strategien, die bei der Behandlung von AML-Patienten Anwendung finden könnten.

Die genetische Inaktivierung von YBX1 führt zu einer verringerten Proliferation und Koloniebildungsfähigkeit in Leukämie-Zellen, unabhängig von der onkogenen Treibermutation, und verzögerte die Entwicklung einer AML *in vivo*. Mit Hilfe eines konditionalen Ybx1 Knockout-Modells konnten wir nachweisen, dass Ybx1 auch für die Aufrechterhaltung der AML *in vivo* eine Rolle spielt. Unsere Untersuchungen zeigen, dass YBX1 onkogene Transkripte, wie z.B. MYC, an die Polysomen rekrutiert und somit deren Translation verstärkt. Die Inaktivierung von YBX1 führt zu einer Verdrängung dieser Transkripte von den Polysomen und resultiert in einem Rückgang der onkogenen Proteinexpression.

Die genetische und pharmakologische Hemmung von PSMB8/LMP7 verringert selektiv die Proliferation und die Fähigkeit zur Koloniebildung in KMT2A (MLL)-

transformierten leukämischen Zellen. Die *in vivo* Behandlung mit einem PSMB8/LMP7-Inhibitor verzögert die Krankheitsentwicklung in einem KMT2A-transformierten Leukämie-Mausmodell ebenso wie in einem „Patient-derived“ Xenograft-Modell (PDX). In weiteren Untersuchungen konnten wir den transkriptionellen Korepressor BASP1 als funktionellen Effektor des Immunproteasoms identifizieren. Nach Hemmung von PSMB8/LMP7 kommt es zu einer Akkumulation von BASP1, welches dann an KMT2A-Zielgene bindet. Darüber hinaus führt die pharmakologische Hemmung von PSMB8/LMP7 zu einer verminderten Expression von KMT2A-Zielgenen sowie zu einer Anreicherung von Genen, die durch Inhibitoren der KMT2A-Komplexpartner DOT1L und MEN1 dereguliert wurden. Die Kombinationsbehandlung von KMT2A-transformierten AML-Zellen mit einem Immunproteasom-Inhibitor und einem Menin-Inhibitor führt im Vergleich zu der jeweiligen Mono-Behandlung zu einer deutlich verringerten Proliferation *in vitro* und einer erhöhten Überlebensrate *in vivo*. Diese Daten weisen auf ein therapeutisches Potenzial einer Kombinationbehandlung von Immunproteasom- und Menin-Inhibitoren hin.

3. Summary

Although the outcome of patients with acute myeloid leukemia (AML) has improved in the past decades, the overall survival is below 50% [1, 2] and there is still an unmet need for the development of new therapeutic strategies. Here, we aimed to identify functional vulnerabilities in AML and investigated the therapeutic potential of target structures involved in proteostasis, cell polarity and RNA-binding molecular pathways.

We determined that genetic deletion of the cell fate determinant and polarity regulator Scribble delays AML development, however, its deletion also seems to affect the proliferative capacity of normal hematopoietic cells, lowering its value as a therapeutic target. In contrast, inactivation of YBX1 (a pleiotropic protein with DNA/RNA binding capacity that excerpts post-transcriptional control on its targets) and PSMB8/LMP7 (a catalytic subunit of the immunoproteasome multi-protein complex that belongs to the ubiquitin-proteasome system (UPS)) inhibit leukemic cells without influencing normal hematopoietic stem and progenitor cell function, establishing these targets as potential novel therapeutic strategies against AML.

Genetic deletion of YBX1 caused reduced proliferation and colony forming capacity in leukemic cells independent of the oncogenic driver mutation and delayed AML development *in vivo*. The role of Ybx1 in leukemia maintenance was investigated using a conditional knockout model, confirming the functional requirement of Ybx1 in AML maintenance. Mechanistically, YBX1 recruited oncogenic transcripts to polysomes, increasing their translation. Displacement of these transcripts from polysomes after YBX1 deletion decreased their protein expression.

Genetic and pharmacologic inhibition of PSMB8/LMP7 decreased proliferation and colony forming capacity selectively in KMT2A (MLL)-rearranged leukemic cells. *In vivo* treatment with a PSMB8/LMP7 inhibitor delayed disease development in KMT2A-rearranged leukemic mice or patient derived xenografts (PDX). We identified the transcriptional corepressor BASP1 as a functional effector of the immunoproteasome. BASP1 was enriched after PSMB8/LMP7 inhibition and it was found binding to KMT2A-target genes. Moreover, pharmacologic inhibition of PSMB8/LMP7 led to decreased expression of bona-fide KMT2A-fusion target genes and enrichment for genes deregulated by inhibitors of the KMT2A complex partners DOT1L and MEN1. This prompted us to investigate a potential synergism between MEN1 inhibition and immunoproteasome inhibition. Combination treatment in AML cells revealed decreased proliferation *in vitro* and increased survival *in vivo* as compared to the single treatments, demonstrating the therapeutic potential of combining immunoproteasome and MEN1 inhibitors.

4. Introduction

4.1. Malignant transformation of hematopoietic cells

All types of mature blood cells are generated from multipotent hematopoietic stem cells (HSCs) through a hierarchical process called hematopoiesis [3]. In steady state conditions, HSCs are maintained in quiescence, but they can enter cell cycle and repopulate the hematopoietic system through differentiation and self-renewal, in response to stress [4]. Imbalance between quiescence, self-renewal and differentiation causes most of the malignancies of hematologic origin.

Acute myeloid leukemia (AML) is a hematologic malignancy characterized by clonal expansion of blasts originating from myeloid progenitors. AML can be initiated by corrupted HSCs or by more committed progenitors that acquire self-renewal capacity [5]. AML is hierarchically organized, with a subpopulation of leukemic stem cells (LSCs) at the top of the hierarchy that maintain self-renewal capacity, sustain the long-term AML growth and are drivers of disease relapse [6, 7]. AML is a highly heterogeneous disease with diverse cytogenetic and molecular abnormalities that are associated with distinct prognosis. These genetically defined subtypes show different oncogene-specific dependencies [8, 9].

The discovery of the heterogeneity of AML has led to the development of targeted and personalized therapeutic strategies and thereby improvement in prognosis. Several targeted therapies like the BCL-2 inhibitor venetoclax, FLT3 inhibitors, IDH inhibitors, and others have been approved for various AML subtypes in the last years [1, 10]. However, despite the improvement in the overall 5-year survival rates for AML patients in the past four decades [2], relapse is still the main driver of morbidity and mortality.

In this project, we aimed to unravel functional vulnerabilities of genetically defined AML subtypes and to explore the therapeutic possibilities of different molecular pathways, focusing on the regulators of cell fate, RNA-binding proteins and molecules of the UPS.

4.2. Cell polarity regulators in acute myeloid leukemia

Evolutionary conserved signaling pathways and cell fate determinants have been associated with the maintenance of the balance between self-renewal and differentiation of hematopoietic stem cells [11, 12]. It has been reported that genetic inactivation of cell polarity regulators can increase (Prox1, Llg1) or decrease (Pard6a, Prkcz, and Msi2) the repopulation capacity of HSCs [12, 13, 14].

In AML, the polarity regulator Msi2 (Musashi RNA binding protein 2) is highly expressed and its reduction leads to decreased proliferation and increased apoptosis [12]. Moreover, low expression of Llg1 (Lethal Giant Larvae Protein Homolog 1) correlated with decreased overall survival of AML patients, while Llg1 deletion by itself did not cause leukemia [13]. Llg1 is one of the four

homologues (Llgl1-4) of the *Drosophila melanogaster* *Lgl* gene, which is a member of the cell polarity complex Scribble, composed of *Lgl*, *Dlg* (Discs Large) and *Scribble*. Another *Lgl* homologue, Llgl2, appears mutated in the progression from severe congenital neutropenia to AML [15]. In contrast, the function of Llgl1 as a tumor suppressor is not conserved in murine models of lymphoid leukemia [16], suggesting that the role of Llgl1 in the hematopoietic lineage might be cell context specific. Moreover, *Dlg1* inactivation has been shown to promote the development of BCR-ABL and p53-driven B cell leukemia/lymphoma [17].

The role of the complex member Scribble has been less examined. In our studies, we have investigated the functional role of Scribble in the hematopoietic system and its potential role in AML transformation, in order to validate its use as a therapeutic target (Publication 1) [18].

4.3. Post-transcriptional regulation in acute myeloid leukemia

Post-transcriptional events that take place between RNA synthesis and protein production influence regulation of gene expression and cell fate. Non-coding RNAs and RNA binding proteins (RBPs) affect every aspect of post-transcriptional control, such as (alternative) splicing, RNA modification, nuclear export, localization, stability and turnover rates [19].

In AML, translocations of RBPs or somatic mutations in spliceosome components have been identified [20, 21, 22]. Furthermore, the expression of various RBPs is upregulated in AML [20, 21]. IGF2BP1 and IGF2BP2 (two components of the insulin-like growth factor 2 mRNA binding protein family) are overexpressed in AML and their depletion has negative effects on proliferation [23, 24]. Similarly, nucleolin, a protein mainly found in the nucleolus that associates with ribosomal DNA, is also overexpressed in AML and its deletion causes decreased proliferation and an increase in apoptosis [25]. HnRNP K (heterogeneous nuclear ribonucleoprotein K), which binds single stranded DNA and RNA and has the capacity for bi-directional transport across the nuclear envelope, has been suggested to act either as an oncogene or a tumor suppressor. In hematologic diseases, it seems to be mainly downregulated and reduced hnRNP K expression results in an increase in proliferation and defects in myeloid differentiation in a haploinsufficient mouse model, implying a role as a tumor suppressor (reviewed in [26]). Moreover, Wang et al. [27] discovered a network of RBPs whose expression is deregulated in AML and it is necessary for

leukemia survival. They further confirmed RBM39 as a targetable vulnerability of the RBP network that alters the splicing of mRNAs essential for AML.

Recently, our group identified YBX1, a member of the cold-shock protein (CSP) family that binds RNA/DNA, as a downstream effector of the mutated JAK2 kinase in myeloproliferative neoplasm (MPN) and uncovered its function in stabilizing MEK-ERK signaling to maintain JAK2-mutated clones under JAK-inhibitor treatment [28]. The role of YBX1 in AML, however, remained so far elusive. Here, we investigated the role of YBX1 as a potential therapeutic target in AML and defined its role as an RNA-binding protein and stabilizer of oncogenic mRNAs (Publication 2) [29].

4.4. Dependency of KMT2A-rearranged leukemia on proteostasis

Proteostasis includes a number of quality control mechanisms that are activated to stabilize the cellular proteome, including regulation of the protein synthesis, the unfolded protein response (UPR), the ubiquitin proteasome system (UPS) and autophagy. Appropriate performance of the hematopoietic system relies on several proteostatic mechanisms [30] and deregulation of the UPS has been previously associated with tumorigenesis [31, 32, 33, 34].

The UPS consists of a sequence of enzymatic processes that link multiple ubiquitin (Ub) molecules to a protein substrate for the recognition and subsequent degradation by the proteasome [35]. The proteasome is formed by a catalytic 20S core particle with three main peptidase activities (caspase-like, trypsin-like and chymotrypsin-like mediated by the β -subunits β 1, β 2 and β 5, respectively) and 19S regulatory particles that bind to one or both ends of the 20S proteasome composing the active 26S proteasome (Figure 1A) [36, 37].

The US Food and Drug Administration (FDA) has approved various proteasome inhibitors (PIs) for the treatment of hematologic malignancies, especially for multiple myeloma (MM) [38, 39, 40]. However, patients treated with PIs frequently acquire resistance and present with toxicities [39, 41].

Recently, our group detected proteostasis as an enriched cellular function in global proteome analysis of murine KMT2A-rearranged (KMT2Ar) leukemic stem cells (Figure 1A in Publication 3) [42]. The Mixed Lineage Leukemia 1 (*KMT2A*, *MLL1*) gene is a recurrent target of chromosomal translocations and can lead to acute lymphoblastic leukemia (ALL) or acute myeloid leukemia (AML) [43]. Of

note, Liu et al. [44] have described that proteasome inhibition leads to the accumulation of the KMT2A fusion-protein and triggers apoptosis and cell cycle arrest in KMT2Ar-ALL cell lines.

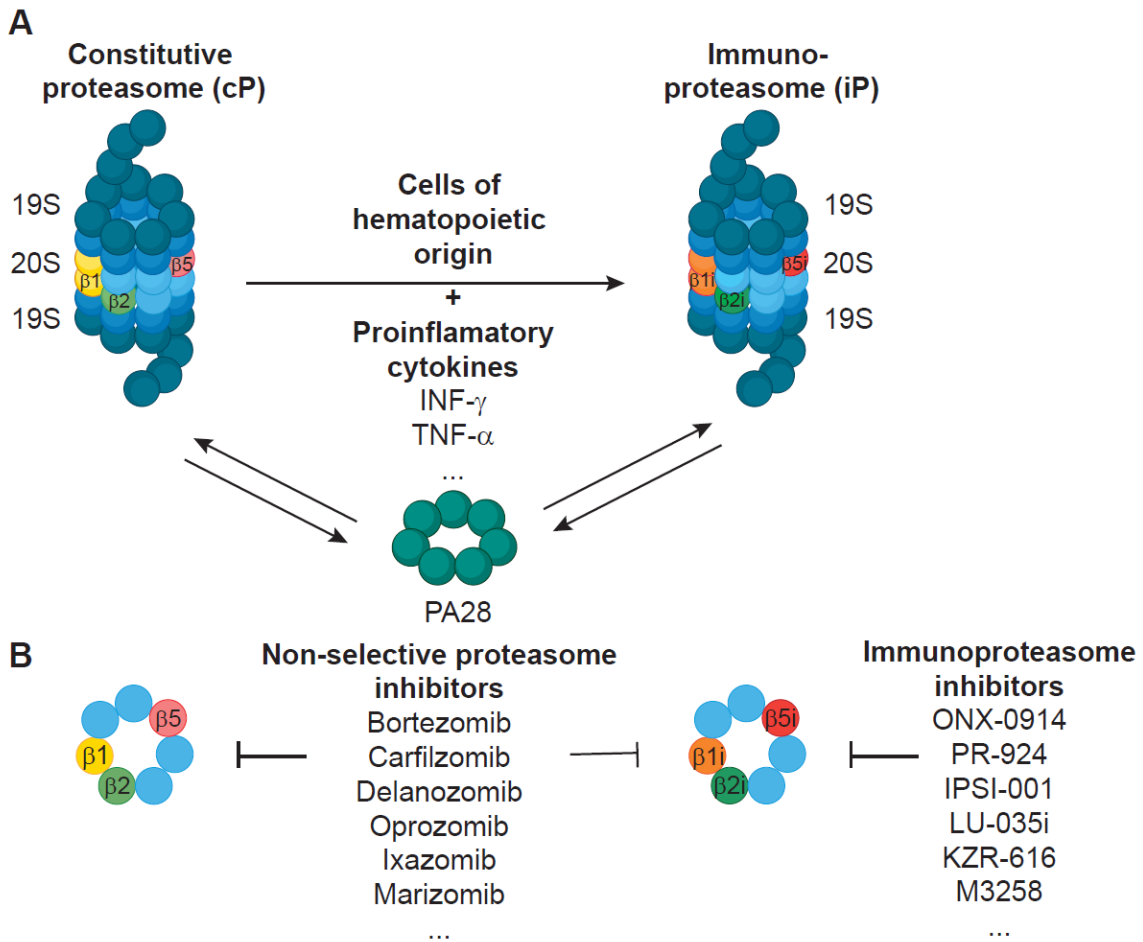


Fig.1. A) Structure of the constitutive proteasome (cP) and the immunoproteasome (iP). **B)** Inhibitors of the proteasome can be designed to target both the cP and the iP or to selectively target the iP. Adapted from [45].

Analysis of AML gene-expression datasets [46] (<http://servers.binf.ku.dk/bloodspot/>) determined that two out of the three main catalytic subunits of the constitutive proteasome (cP) were significantly higher expressed in KMT2Ar-leukemia compared to other AML subtypes. Interestingly, the three main catalytic subunits of the immunoproteasome, a proteasomal variant constitutively expressed in cells of hematopoietic origin or induced under pro-inflammatory cytokine stimulation [47, 48, 49, 50, 51], were higher expressed in KMT2Ar-AML and with higher significance than the cP (Figure 1B in Publication 3) [52].

Within the immunoproteasome (iP), the constitutive catalytic subunits $\beta 1$, $\beta 2$ and $\beta 5$ are replaced by their inducible counterparts $\beta 1i$, $\beta 2i$ and $\beta 5i$ [53, 54, 55] (Figure 1A) upon stimulation with inflammatory cytokines (e.g. IFN γ). Since the iP is expressed without additional stimulation in hematopoietic cells, including malignant hematopoietic cells [56, 57, 58, 59], this may indicate a dependency of these malignant cells on iP function. Moreover, specifically inhibiting the iP could overcome the problems of using non-selective PIs (which inhibit both the cP and the iP) (Figure 1B), while maintaining anti-leukemic effects. Immunoproteasome inhibitors have already proven their efficacy and safety against inflammatory and autoimmune diseases, but there are only some preliminary pre-clinical studies on their effects in hematologic malignancies, with one inhibitor currently being in clinical trials for the treatment of MM (reviewed in [45]).

The promising anti-tumoral effects of iP in hematologic malignancies added to the specific expression of iP in cells of hematopoietic origin, led us to explore the dependencies of a specific subtype of AML on immunoproteasome function. Here, evidence of the higher expression of iP in KMT2Ar-AML indicated an oncogene-specific dependency, which we have characterized in detail (Publication 3) [52].

4.4.1. Sensitivity of KMT2A-rearranged leukemia to proteasome inhibition

The *KMT2A/MLL1* gene encodes a histone H3 lysine 4 (H3K4) methyltransferase that regulates the expression of multiple *HOX* genes [60, 61]. In KMT2Ar-leukemia the N-terminus of KMT2A fuses to the C-terminus of one of more than 90 possible fusion partners (Figure 2A) [62]. Leukemias bearing an KMT2A rearrangement lose H3K4 methyltransferase activity, encoded by the SET domain in the C-terminus, but keep the capacity to bind chromatin through the Menin-binding motif (MBM) present in the N-terminus (Figure 2) [63, 64]. Menin 1 (MEN1) acts as an adaptor protein, interacting with DNA-binding proteins like Lens epithelium–derived growth factor (LEDGF) or directly binding DNA [64, 65] and it is essential for the regulation of *HOX* gene expression [66]. The relevance of MEN1 has been further confirmed by the development of MEN1 inhibitors that represent a promising treatment for KMT2Ar-leukemia [43, 67].

Moreover, KMT2A fusion partners belong or recruit the super elongation complex (SEC; composed of AFF1 or AFF4, MLLT3 (AF9) or MLLT1 (ENL), EAF, ELL and P-TEFb (positive transcription elongation factor b)) and the histone 3

lysine 79 (H3K79) methyltransferase disruptor of telomeric silencing 1-like (DOT1L) complex (consisting of DOT1L, MLLT3, MLLT10 and MLLT1). These complexes stimulate transcriptional elongation resulting in aberrant gene expression (Figure 2B) [63, 68, 69].

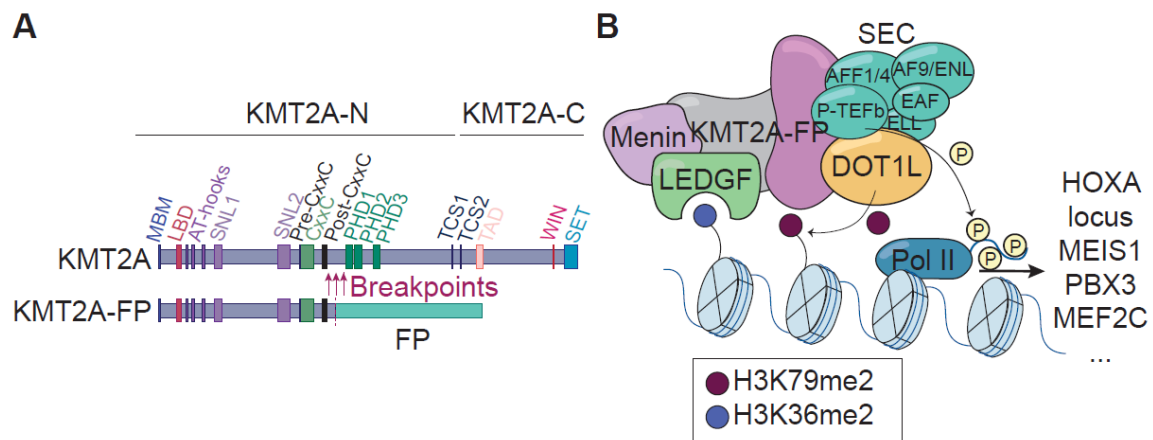


Fig.2. A) Schematic representation of the architecture of the KMT2A/MLL1 protein and KMT2A fusion-protein (KMT2A-FP). The KMT2A-N and KMT2A -C subunits are formed by Taspase 1 cleavage of the pre-KMT2A protein (at the Taspase1 cleavage sites 1/2; TCS1/2). In KMT2A-rearranged leukemia the N-terminus binds to one of the possible fusion partners (FP). **B)** The KMT2A-FP acquires a unique transcriptional machinery.

As described in the previous section, proteasome function is relevant for KMT2A (MLL)-rearranged leukemia (Figure 1A in Publication 3) [52] and has been already shown to be necessary for KMT2Ar-ALL maintenance [44]. Moreover, immunoproteasome is highly expressed in KMT2Ar-AML (Figure 1B-C in Publication 3) [52] indicating a possible dependency of this leukemia subtype on iP.

5. Methods

Murine and human AML cell lines containing different genetic aberrations were used for *in vitro* experiments [18, 29, 52]. Genetic inactivation by RNA interference (RNAi) and CRISPR-Cas9, CRISPR-Cas9 negative selection assays, proliferation, apoptosis and colony forming assays were performed in these cells. A detailed explanation of these techniques can be found in the Material and Methods of Publications 1-3 [18, 29, 52]. Moreover, primary AML patient samples were used for colony forming assays and proliferation [29, 52].

To study the effects of genetic inactivation or drug treatment *in vivo* in human leukemia, xenografts from human AML cell lines or PDX were performed [29, 52].

Previously published conventional and conditional knockout mouse models [28, 70, 71, 72] were used for competitive repopulation assays, serial transplantations and *in vivo* drug treatment in order to assess for normal hematopoiesis and leukemia development and maintenance.

Mechanistic properties were assessed by RNA-sequencing, proteome analysis, whole-genome CRISPR-Cas9 screens, ChIP-sequencing, ATAC-sequencing, Cut&Tag-sequencing and Cut&Run-sequencing. All these techniques are explained in detail in Publications 1-3 [18, 29, 52].

6. Results

The cell fate determinant Scribble is required for maintenance of hematopoietic stem cell function

Mohr J, Dash BP, Schnoeder TM, Wolleschak D, Herzog C, **Tubio Santamaria N**, Weinert S, Godavarthy S, Zanetti C, Naumann M, Hartleben B, Huber TB, Krause DS, Kähne T, Bullinger L, Heidel FH

In order to assess for the influence of Scribble (Scrib) on hematopoietic stem and progenitor cells (HSPCs), steady state hematopoiesis was studied by using a conditional Scrib knockout mouse model [70] and no significant changes were found between Scrib +/+ and Scrib -/- mice (Figure 1 in Publication 1).

The short-term repopulation capacity, assessed by the generation of colony forming unit spleen cells 12 days after transplantation of Scrib +/+ or Scrib -/- BM cells, was not affected by Scrib deletion, indicating that Scrib is dispensable for the multipotent progenitor function (Supplementary Figure S2A-B in Publication 1).

To assess for the long-term repopulation capacity, a competitive transplantation was performed. Scrib deficient cells were found to compete worse and the competitive disadvantage was more pronounced in secondary recipients (Figure 2A-B in Publication 1). Reduction of HSC frequency in a limiting dilution assay (LDA) confirmed the function of Scrib in HSCs (Figure 2C in Publication 1).

The decreased long-term repopulation capacity of Scrib deficient HSCs suggested that these cells might exhaust faster than normal long-term HSCs (LT-HSCs) under stress conditions. To corroborate these findings, Scrib +/+ or Scrib

-/- mice were treated with the cytotoxic agent 5-fluorouracil (5-FU). While short-term recovery was not affected, the regenerative capacity of LT-HSCs was decreased by Scrib deficiency (Figure 3 in Publication 1).

To study how Scrib affects LT-HSCs, global transcriptome analysis was performed in HSCs from Scrib +/+ or Scrib -/- mice. Gene ontology analysis showed regulation of stem cell proliferation, signaling pathways and motility as the most significantly enriched functions (Figure 4C in Publication 1).

In order to determine the function of Scrib on AML, KMT2A-MLLT3 (MLL-AF9) transfected Scrib +/+ or Scrib -/- Lin⁻Kit⁺Sca1⁺ (LSK) cells were injected into recipient mice. Scrib deletion prolonged survival and this negative effect on LSC function was evidenced by selection of partially and non-excised clones in secondary recipients (Figure 6 in Publication 1).

YBX1 mediates translation of oncogenic transcripts to control cell competition in AML

Perner F, Schnoeder TM, Xiong Y, Jayavelu AK, Mashamba N, **Santamaria NT**, Huber N, Todorova K, Hatton C, Perner B, Eifert T, Murphy C, Hartmann M, Hoell JI, Schröder N, Brandt S, Hochhaus A, Mertens PR, Mann M, Armstrong SA, Mandinova A, Heidel FH

Using publicly available genomic and proteomic datasets, YBX1 was found to be overexpressed in hematologic malignancies and AML cell lines were sensitive to its inactivation (Figure 1A-D, Supplementary Figure S1B-C in Publication 2). By CRISPR-Cas9 and RNAi, reduced proliferative capacity and cell cycle impairment was shown in YBX1 deficient cells (Figure 1H-I, Supplementary Figure S2A in Publication 2). Moreover, YBX1 depletion decreased colony forming capacity of primary AML patient samples (Figure 3 in Publication 2).

To investigate the effect of YBX1 depletion in human AML *in vivo*, YBX1 knockout or knockdown cells were transplanted into immunodeficient recipient mice and inactivation of YBX1 significantly increased survival (Figure 2K-M in Publication 2).

To determine the role of Ybx1 in AML development a conventional knockout mouse model [71] was used. Colony formation and self-renewal capacity *in vitro* and AML development *in vivo* were reduced after heterozygous loss of Ybx1 (Figure 2A-C in Publication 2). The function of Ybx1 in AML maintenance was assessed in a conditional knockout mouse model [28]. Ybx1 inactivation led to

increase in survival and this effect was even more pronounced in secondary recipients (Figure 2D-J in Publication 2). Together, these observations demonstrate an essential role of Ybx1 in AML development and maintenance.

In order to assess for the role of Ybx1 in HSPCs and for a potential therapeutic window, a competitive repopulation assay was performed using the conventional knockout mouse model. No loss of function in Ybx1 heterozygous deficient cells was found and neither an alteration of the HSPCs composition (Supplementary Figure S3C-D in Publication 2), indicating that loss of Ybx1 does not affect normal HSPC function.

Due to its role as an RNA-binding protein, we predicted that YBX1 impacts expression in AML by binding and stabilizing mRNAs. In agreement, by combining published mRNA binding data with RNA-sequencing data, we found that the majority of transcriptionally downregulated genes are targets of YBX1-mRNA binding (Figure 4F in Publication 2).

To confirm the ability of YBX1 to modulate translation of mRNAs, a transcriptome profiling of purified ribosomal fractions was performed (Figure 5G-H in Publication 2). Integration of this data with the respective functional dependencies from a genome-wide CRISPR-Cas9 screen identified relevant targets, with MYC among them (Figure 5K in Publication 2).

Taken together, these results suggest that YBX1 binds to target mRNAs, including MYC, and recruits them to polysomal chains, leading to their increased translation. YBX1 deletion in AML cells selectively modulates the abundance of proteins essential for AML maintenance and reduces proliferative capacity and competitive advantage (Figure 6G in Publication 2).

Immunoproteasome function maintains oncogenic gene expression in KMT2A-complex driven leukemia

Tubío-Santamaría N, Jayavelu AK, Schnoeder TM, Eifert T, Hsu C-J, Perner F, Zhang Q, Wenge DV, Hansen FM, Kirkpatrick JM, Jyotsana N, Lane SW, von Eyss B, Deshpande AJ, Kühn MWM, Schwaller J, Camman C, Seifert U, Ebstein F, Krüger E, Hochhaus A, Heuser M, Ori A, Mann M, Armstrong SA, Heidel FH

The functional relevance of the immunoproteasome subunit PSMB8 (human gene for the $\beta 5i$ subunit) in AML was investigated by genetic inactivation. PSMB8 deficiency reduced proliferative and colony forming capacity *in vitro* and prolonged survival in xenograft models of KMT2Ar-AML (Figure 1D-F in

Publication 3). Likewise, pharmacologic inhibition of PSMB8 using the inhibitor PR-957 (ONX-0914) reduced proliferative capacity in KMT2Ar-cell lines, leaving non-KMT2Ar-cells largely unaffected (Figure 2A in Publication 3). Moreover, *in vivo* PR-957 treatment prolonged survival of KMT2A-MLLT3 and KMT2A-AFF1 PDX (Figure 2B in Publication 3).

To assess the function of LMP7 (mouse gene for the $\beta 5i$ subunit) in AML development, a conventional knockout mouse model [72] was used. LMP7 deficiency decreased colony formation and self-renewal capacity *in vitro* and AML development *in vivo* in KMT2A transduced cells (Figure 3A-B, Supplementary Figure S3A in Publication 3)

To study the effects of pharmacologic inhibition of LMP7 in AML development and LSCs self-renewal, primary murine cells transformed with various oncogenic rearrangements were used. Pharmacologic inhibition of LMP7 reduced colony formation and self-renewal capacity in KMT2Ar-leukemic cells without affecting non-KMT2Ar-cells (Figure 4A in Publication 3). Serial transplantation showed a reduction of LSCs in the BM of recipient mice transplanted with KMT2A-MLLT3 transduced cells and treated *in vivo* with PR-957 compared with diluent treated mice (Figure 4E in Publication 3). Moreover, survival of secondary recipients of PR-957 treated mice was increased in comparison to control mice (Figure 4G in Publication 3). Reduction of LSC frequency after iP inhibition assessed by LDA (Figure 4H-I in Publication 3), confirm the effects of pharmacologic inhibition of LMP7 on attenuating leukemia initiating potential of KMT2Ar-AML.

In order to clarify a potential therapeutic window, we assess LMP7 function in HSPCs by performing a competitive repopulation assay (Figure 4J in Publication 3). No alteration in the HSPCs composition was found in recipients of the PR-957 treated mice, indicating that LMP7 is not necessary for the self-renewal of normal hematopoietic cells (Figure 4P-Q in Publication 3).

To identify functional effectors of the iP, we integrated data from a proteome assay and a CRISPR-Cas9 screen (Figure 5C-E in Publication 3). We identify the transcriptional repressor BASP1 as an immunoproteasome target that was upregulated following PSMB8 inhibition (Figure 5F in Publication 3). BASP1 binding to chromatin was found increase after PR-957 treatment (Figure 5G-H in Publication 3). Moreover, BASP1 overexpression reduced proliferation of AML

human cell lines *in vitro* and prolonged survival in xenograft models (Figure 5J-K in Publication 3).

The function of PSMB8 on transcriptional regulation was assessed by a global transcriptome analysis. Bona-fide targets of the KMT2A fusion-protein were found downregulated after PR-957 treatment, partially overlapping with deregulated genes after MEN1 and DOT1L inhibition (Figure 5A-B in Publication 3). This reveals a possible combination strategy that we explore by MI-503 (MEN1 inhibitor) and PR-957 treatment. Combination treatment further downregulated expression of KMT2A-fusion targets and had synergistic effects in proliferation reduction, survival prolongation and LSCs frequency reduction (Figure 6 in Publication 3). Furthermore, PR-957 treatment reduced the proliferative capacity of MEN1 mutated cells (resistant to MEN1 inhibition) to the same extent as wild-type cells (Figure 7A in Publication 3) and combination of MEN1 inhibition and immunoproteasome inhibition prevented the outgrowth of resistant cells compared with single MEN1 inhibition in an *in vivo* cell competition assay (Figure 7B-E in Publication 3). Taken together these results indicate the therapeutic value of combining MEN1 and PSMB8 inhibition.

7. Discussion

Understanding the diversity of AML and investigating molecular pathways with relevance for its development and maintenance is crucial to identify novel therapeutic targets. There is a requirement for new therapeutic strategies that 1) are frequently targeted to genetically defined AML subtypes, unraveling oncogene-specific vulnerabilities; 2) have less toxicity and side effects and can spare normal hematopoietic cells while affecting the malignant ones; 3) can overcome relapse by targeting LSCs that have low division rates and are difficult to eradicate [10, 73, 74]. Therefore, in my PhD thesis, I investigated different molecular pathways that have been previously related to hematopoiesis and AML with the purpose of assessing their therapeutic value in AML treatment.

In Publication 1 we found that the polarity regulator Scribble influences self-renewal capacity of LSCs, while it does not affect steady state hematopoiesis or short-term repopulation capacity in normal hematopoietic stem cells. However, the LT-HSCs showed impaired self-renewal capacity after genetic deletion of Scrib. LT-HSCs are a rare population required for the full long-term (>4 months) reconstitution capacity of the hematopoietic system [75, 76]. A recent report

showed that the way Scrib influences HSPCs is by altering adhesion and decreasing migration [77]. Disturbance of the HSPCs by Scribble deletion dismisses its potential application as a therapeutic target in AML.

Unexpectedly, we found that binding of Scrib to any of the other members of the Scribble complex was not detected in hematopoietic cells (Figure 5B in Publication 1) and that Scrib and Llg1 do not have an overlapping function in the hematopoietic system (Figure 4B in Publication 1). Moreover, Llg1 has potential therapeutic value, since its expression is correlated with AML survival [13]. Currently, Llg1 is being investigated in our group to characterize its function in the normal hematopoietic system and in AML and to explore its value as a possible therapeutic target.

In Publication 2 we determined that the cold-shock protein YBX1 is required for AML development and maintenance in human and murine cells. Despite the fact that LSC frequency in primary recipients of *Ybx1*^{-/-} leukemic cells was not reduced compared to the control mice, secondary transplantation decreased disease penetrance in 30% of the recipients indicating an impairment in the self-renewal capacity of LSCs after *Ybx1* deletion. In contrast, normal HSPCs were not affected, implying a potential therapeutic window and placing YBX1 as a selective vulnerability in AML. Besides, the recent development of an inhibitor that pharmacologically targets YBX1 [78] increases its value as a tractable target. The YBX1 inhibitor SU056 was developed and initially characterized in ovarian cancer models and resulted in a decrease of proliferative capacity *in vitro* and of tumor development *in vivo*. Currently, our group in collaboration with scientists from the United States, is investigating whether SU056 treatment has the same beneficial effects in AML as genetic deletion of YBX1, in which case it is expected that SU056 enters clinical trials for its use in AML treatment.

In Publication 3 we identified the catalytic iP subunit PSMB8/LMP7 as a selective dependency in KMT2Ar-leukemia by genetic and pharmacologic inhibition in human and murine cells. Pharmacologic inhibition of LMP7 using the inhibitor PR-957 in an *in vivo* KMT2Ar-mouse model, revealed that LMP7 is required for LSC function in KMT2Ar-leukemia while it seems to be dispensable for normal HSPCs, highlighting the therapeutic potential of iP inhibition. Although identified as a vulnerability in KMT2Ar-leukemia, PSMB8 inhibition also reduced proliferation in NPM1-mutant (NPM1c) AML cell lines (Figure 2A in Publication

3). This finding is explained by the fact that NPM1 co-occupies KMT2A targets [79], leading to NPM1c-AML sharing oncogenic transcriptional programs with KMT2Ar-leukemia [80]. Since NPM1c is the most common mutation in AML, appearing in 20-30% of all AML cases, this amplifies the therapeutic value of pharmacologic inhibition of the iP.

Previous publications have reported an accumulation of the KMT2A fusion-protein after proteasome inhibition in KMT2Ar-ALL cell lines [44, 81]. However, they fail to find the same effect in KMT2Ar-AML. Our data describes increased abundance of BASP1 as a previously unidentified mechanism after inactivation of the catalytic immunoproteasome subunit PSMB8 in the context of KMT2Ar-AML. BASP1 can act as a transcriptional co-suppressor [82, 83] and its silencing has been reported to be essential for MYC-induced leukemogenesis [84]. In agreement with its role as a transcriptional suppressor, increased BASP1 abundance after PR-957 treatment leads to repression of KMT2A-target genes.

From the perspective of clinical translation, combination therapies are frequently superior to monotherapies, since they can target genes with redundant functions in a transcriptional network. Pharmacologic inhibition of KMT2A-associated epigenetic complexes (DOT1L and MEN1) has demonstrated significant anti-leukemic effects *in vitro* [85, 86], however, translation into clinical trials shows transient responses [85, 86] and a recent report showed development of resistance in one third of patients on prolonged MEN1 inhibitor treatment [87]. We have determined that PSMB8 inhibition produces transcriptional changes on KMT2Ar-target genes without affecting chromatin conformation. Combination of this alternative non-epigenetic mechanism with inhibition of the epigenetic regulator MEN1 resulted in synergistic effects against KMT2Ar-AML *in vitro* and in pre-clinical PDX models. We confirmed a preserved class-effect, by recapitulating the anti-proliferative effects using (immuno-) proteasome inhibitors with different specificity and second-generation MEN1 inhibitors (Figure 6D-G in Publication 3). Moreover, mutant cells with acquired Menin-inhibition resistance [87] were still sensitive to the non-epigenetic mechanism of immunoproteasome inhibition.

8. Bibliography

1. Kantarjian, H.; Kadia, T.; DiNardo, C.; Daver, N.; Borthakur, G.; Jabbour, E.; Garcia-Manero, G.; Konopleva, M.; Ravandi, F., Acute myeloid leukemia: current progress and future directions. *Blood Cancer J* **2021**, *11* (2), 41.
2. Sasaki, K.; Ravandi, F.; Kadia, T. M.; DiNardo, C. D.; Short, N. J.; Borthakur, G.; Jabbour, E.; Kantarjian, H. M., De novo acute myeloid leukemia: A population-based study of outcome in the United States based on the Surveillance, Epidemiology, and End Results (SEER) database, 1980 to 2017. *Cancer* **2021**, *127* (12), 2049-2061.
3. Orkin, S. H.; Zon, L. I., Hematopoiesis: an evolving paradigm for stem cell biology. *Cell* **2008**, *132* (4), 631-44.
4. Kohli, L.; Passegue, E., Surviving change: the metabolic journey of hematopoietic stem cells. *Trends Cell Biol* **2014**, *24* (8), 479-87.
5. Passegue, E.; Jamieson, C. H.; Ailles, L. E.; Weissman, I. L., Normal and leukemic hematopoiesis: are leukemias a stem cell disorder or a reacquisition of stem cell characteristics? *Proc Natl Acad Sci U S A* **2003**, *100* Suppl 1, 11842-9.
6. Kreso, A.; Dick, J. E., Evolution of the cancer stem cell model. *Cell Stem Cell* **2014**, *14* (3), 275-91.
7. Lapidot, T.; Sirard, C.; Vormoor, J.; Murdoch, B.; Hoang, T.; Caceres-Cortes, J.; Minden, M.; Paterson, B.; Caligiuri, M. A.; Dick, J. E., A cell initiating human acute myeloid leukaemia after transplantation into SCID mice. *Nature* **1994**, *367* (6464), 645-8.
8. Dohner, H.; Weisdorf, D. J.; Bloomfield, C. D., Acute Myeloid Leukemia. *N Engl J Med* **2015**, *373* (12), 1136-52.
9. Papaemmanuil, E.; Gerstung, M.; Bullinger, L.; Gaidzik, V. I.; Paschka, P.; Roberts, N. D.; Potter, N. E.; Heuser, M.; Thol, F.; Bolli, N.; Gundem, G.; Van Loo, P.; Martincorena, I.; Ganly, P.; Mudie, L.; McLaren, S.; O'Meara, S.; Raine, K.; Jones, D. R.; Teague, J. W.; Butler, A. P.; Greaves, M. F.; Ganser, A.; Dohner, K.; Schlenk, R. F.; Dohner, H.; Campbell, P. J., Genomic Classification and Prognosis in Acute Myeloid Leukemia. *N Engl J Med* **2016**, *374* (23), 2209-2221.
10. Carter, J. L.; Hege, K.; Yang, J.; Kalpage, H. A.; Su, Y.; Edwards, H.; Huttemann, M.; Taub, J. W.; Ge, Y., Targeting multiple signaling pathways: the new approach to acute myeloid leukemia therapy. *Signal Transduct Target Ther* **2020**, *5* (1), 288.
11. Duncan, A. W.; Rattis, F. M.; DiMascio, L. N.; Congdon, K. L.; Pazianos, G.; Zhao, C.; Yoon, K.; Cook, J. M.; Willert, K.; Gaiano, N.; Reya, T., Integration of Notch and Wnt signaling in hematopoietic stem cell maintenance. *Nat Immunol* **2005**, *6* (3), 314-22.
12. Kharas, M. G.; Lengner, C. J.; Al-Shahrour, F.; Bullinger, L.; Ball, B.; Zaidi, S.; Morgan, K.; Tam, W.; Paktinat, M.; Okabe, R.; Gozo, M.; Einhorn, W.; Lane, S. W.; Scholl, C.; Frohling, S.; Fleming, M.; Ebert, B. L.; Gilliland, D. G.; Jaenisch, R.; Daley, G. Q., Musashi-2 regulates normal hematopoiesis and promotes aggressive myeloid leukemia. *Nat Med* **2010**, *16* (8), 903-8.
13. Heidel, F. H.; Bullinger, L.; Arriba-Tutusaus, P.; Wang, Z.; Gaebel, J.; Hirt, C.; Niederwieser, D.; Lane, S. W.; Dohner, K.; Vasioukhin, V.; Fischer, T.; Armstrong, S. A., The cell fate determinant *lgl1* influences HSC fitness and prognosis in AML. *J Exp Med* **2013**, *210* (1), 15-22.
14. Hope, K. J.; Cellot, S.; Ting, S. B.; MacRae, T.; Mayotte, N.; Iscove, N. N.; Sauvageau, G., An RNAi screen identifies *Msi2* and *Prox1* as having opposite

- roles in the regulation of hematopoietic stem cell activity. *Cell Stem Cell* **2010**, *7* (1), 101-13.
15. Beekman, R.; Valkhof, M. G.; Sanders, M. A.; van Strien, P. M.; Haanstra, J. R.; Broeders, L.; Geertsma-Kleinekoort, W. M.; Veerman, A. J.; Valk, P. J.; Verhaak, R. G.; Lowenberg, B.; Touw, I. P., Sequential gain of mutations in severe congenital neutropenia progressing to acute myeloid leukemia. *Blood* **2012**, *119* (22), 5071-7.
 16. Hawkins, E. D.; Oliaro, J.; Ramsbottom, K. M.; Ting, S. B.; Sacirbegovic, F.; Harvey, M.; Kinwell, T.; Ghysdael, J.; Johnstone, R. W.; Humbert, P. O.; Russell, S. M., Lethal giant larvae 1 tumour suppressor activity is not conserved in models of mammalian T and B cell leukaemia. *PLoS One* **2014**, *9* (1), e87376.
 17. Sandoval, G. J.; Graham, D. B.; Gmyrek, G. B.; Akilesh, H. M.; Fujikawa, K.; Sammut, B.; Bhattacharya, D.; Srivatsan, S.; Kim, A.; Shaw, A. S.; Yanglott, K.; Bassing, C. H.; Duncavage, E.; Xavier, R. J.; Swat, W., Novel mechanism of tumor suppression by polarity gene discs large 1 (DLG1) revealed in a murine model of pediatric B-ALL. *Cancer Immunol Res* **2013**, *1* (6), 426-37.
 18. Mohr, J.; Dash, B. P.; Schroeder, T. M.; Wolleschak, D.; Herzog, C.; Tubio Santamaria, N.; Weinert, S.; Godavarthy, S.; Zanetti, C.; Naumann, M.; Hartleben, B.; Huber, T. B.; Krause, D. S.; Kahne, T.; Bullinger, L.; Heide, H., The cell fate determinant Scribble is required for maintenance of hematopoietic stem cell function. *Leukemia* **2018**, *32* (5), 1211-1221.
 19. Glisovic, T.; Bachorik, J. L.; Yong, J.; Dreyfuss, G., RNA-binding proteins and post-transcriptional gene regulation. *FEBS Lett* **2008**, *582* (14), 1977-86.
 20. Elcheva, I. A.; Spiegelman, V. S., Targeting RNA-binding proteins in acute and chronic leukemia. *Leukemia* **2021**, *35* (2), 360-376.
 21. Schuschel, K.; Helwig, M.; Huttelmaier, S.; Heckl, D.; Klusmann, J. H.; Hoell, J. I., RNA-Binding Proteins in Acute Leukemias. *Int J Mol Sci* **2020**, *21* (10).
 22. Taylor, J.; Lee, S. C., Mutations in spliceosome genes and therapeutic opportunities in myeloid malignancies. *Genes Chromosomes Cancer* **2019**, *58* (12), 889-902.
 23. Elcheva, I. A.; Wood, T.; Chiarolanzio, K.; Chim, B.; Wong, M.; Singh, V.; Gowda, C. P.; Lu, Q.; Hafner, M.; Dovat, S.; Liu, Z.; Muljo, S. A.; Spiegelman, V. S., RNA-binding protein IGF2BP1 maintains leukemia stem cell properties by regulating HOXB4, MYB, and ALDH1A1. *Leukemia* **2020**, *34* (5), 1354-1363.
 24. He, X.; Li, W.; Liang, X.; Zhu, X.; Zhang, L.; Huang, Y.; Yu, T.; Li, S.; Chen, Z., IGF2BP2 Overexpression Indicates Poor Survival in Patients with Acute Myelocytic Leukemia. *Cell Physiol Biochem* **2018**, *51* (4), 1945-1956.
 25. Shen, N.; Yan, F.; Pang, J.; Wu, L. C.; Al-Kali, A.; Litzow, M. R.; Liu, S., A nucleolin-DNMT1 regulatory axis in acute myeloid leukemogenesis. *Oncotarget* **2014**, *5* (14), 5494-509.
 26. Gallardo, M.; Hornbaker, M. J.; Zhang, X.; Hu, P.; Bueso-Ramos, C.; Post, S. M., Aberrant hnRNP K expression: All roads lead to cancer. *Cell Cycle* **2016**, *15* (12), 1552-7.
 27. Wang, E.; Lu, S. X.; Pastore, A.; Chen, X.; Imig, J.; Chun-Wei Lee, S.; Hockemeyer, K.; Ghebrechristos, Y. E.; Yoshimi, A.; Inoue, D.; Ki, M.; Cho, H.; Bitner, L.; Kloetgen, A.; Lin, K. T.; Uehara, T.; Owa, T.; Tibes, R.; Krainer, A. R.; Abdel-Wahab, O.; Aifantis, I., Targeting an RNA-Binding Protein Network in Acute Myeloid Leukemia. *Cancer Cell* **2019**, *35* (3), 369-384 e7.
 28. Jayavelu, A. K.; Schnoder, T. M.; Perner, F.; Herzog, C.; Meiler, A.; Krishnamoorthy, G.; Huber, N.; Mohr, J.; Edelmann-Stephan, B.; Austin, R.; Brandt, S.; Palandri, F.; Schroder, N.; Isermann, B.; Edlich, F.; Sinha, A. U.

- Ungelenk, M.; Hubner, C. A.; Zeiser, R.; Rahmig, S.; Waskow, C.; Coldham, I.; Ernst, T.; Hochhaus, A.; Jilg, S.; Jost, P. J.; Mullally, A.; Bullinger, L.; Mertens, P. R.; Lane, S. W.; Mann, M.; Heidel, F. H., Splicing factor YBX1 mediates persistence of JAK2-mutated neoplasms. *Nature* **2020**, *588* (7836), 157-163.
29. Perner, F.; Schnoeder, T. M.; Xiong, Y.; Jayavelu, A. K.; Mashamba, N.; Santamaria, N. T.; Huber, N.; Todorova, K.; Hatton, C.; Perner, B.; Eifert, T.; Murphy, C.; Hartmann, M.; Hoell, J. I.; Schroder, N.; Brandt, S.; Hochhaus, A.; Mertens, P. R.; Mann, M.; Armstrong, S. A.; Mandinova, A.; Heidel, F. H., YBX1 mediates translation of oncogenic transcripts to control cell competition in AML. *Leukemia* **2022**, *36* (2), 426-437.
30. Garcia-Prat, L.; Sousa-Victor, P.; Munoz-Canoves, P., Proteostatic and Metabolic Control of Stemness. *Cell Stem Cell* **2017**, *20* (5), 593-608.
31. Brooks, C. L.; Gu, W., p53 ubiquitination: Mdm2 and beyond. *Mol Cell* **2006**, *21* (3), 307-15.
32. Cardozo, T.; Pagano, M., The SCF ubiquitin ligase: insights into a molecular machine. *Nat Rev Mol Cell Biol* **2004**, *5* (9), 739-51.
33. Nakayama, K. I.; Nakayama, K., Ubiquitin ligases: cell-cycle control and cancer. *Nat Rev Cancer* **2006**, *6* (5), 369-81.
34. Schmidt, M. H. H.; Dikic, I., The Cbl interactome and its functions. *Nat Rev Mol Cell Biol* **2005**, *6* (12), 907-18.
35. Lecker, S. H.; Goldberg, A. L.; Mitch, W. E., Protein degradation by the ubiquitin-proteasome pathway in normal and disease states. *J Am Soc Nephrol* **2006**, *17* (7), 1807-19.
36. Coux, O.; Tanaka, K.; Goldberg, A. L., Structure and functions of the 20S and 26S proteasomes. *Annu Rev Biochem* **1996**, *65*, 801-47.
37. Tanaka, K., The proteasome: overview of structure and functions. *Proc Jpn Acad Ser B Phys Biol Sci* **2009**, *85* (1), 12-36.
38. Fisher, R. I.; Bernstein, S. H.; Kahl, B. S.; Djulbegovic, B.; Robertson, M. J.; de Vos, S.; Epner, E.; Krishnan, A.; Leonard, J. P.; Lonial, S.; Stadtmauer, E. A.; O'Connor, O. A.; Shi, H.; Boral, A. L.; Goy, A., Multicenter phase II study of bortezomib in patients with relapsed or refractory mantle cell lymphoma. *J Clin Oncol* **2006**, *24* (30), 4867-74.
39. Park, J. E.; Miller, Z.; Jun, Y.; Lee, W.; Kim, K. B., Next-generation proteasome inhibitors for cancer therapy. *Transl Res* **2018**, *198*, 1-16.
40. Richardson, P. G.; Barlogie, B.; Berenson, J.; Singhal, S.; Jagannath, S.; Irwin, D.; Rajkumar, S. V.; Srkalovic, G.; Alsina, M.; Alexanian, R.; Siegel, D.; Orlovski, R. Z.; Kuter, D.; Limentani, S. A.; Lee, S.; Hideshima, T.; Esseltine, D. L.; Kauffman, M.; Adams, J.; Schenkein, D. P.; Anderson, K. C., A phase 2 study of bortezomib in relapsed, refractory myeloma. *N Engl J Med* **2003**, *348* (26), 2609-17.
41. Chauhan, D.; Hideshima, T.; Mitsiades, C.; Richardson, P.; Anderson, K. C., Proteasome inhibitor therapy in multiple myeloma. *Mol Cancer Ther* **2005**, *4* (4), 686-92.
42. Schnoeder, T. M.; Schwarzer, A.; Jayavelu, A. K.; Hsu, C. J.; Kirkpatrick, J.; Dohner, K.; Perner, F.; Eifert, T.; Huber, N.; Arriba-Tutusa, P.; Dolnik, A.; Assi, S. A.; Nafria, M.; Jiang, L.; Dai, Y. T.; Chen, Z.; Chen, S. J.; Kellaway, S. G.; Ptasinska, A.; Ng, E. S.; Stanley, E. G.; Elefanty, A. G.; Buschbeck, M.; Bierhoff, H.; Brodt, S.; Matziolis, G.; Fischer, K. D.; Hochhaus, A.; Chen, C. W.; Heidenreich, O.; Mann, M.; Lane, S. W.; Bullinger, L.; Ori, A.; von Eyss, B.; Bonifer, C.; Heidel, F. H., PLCG1 is required for AML1-ETO leukemia stem cell self-renewal. *Blood* **2022**, *139* (7), 1080-1097.

43. Krivtsov, A. V.; Evans, K.; Gadrey, J. Y.; Eschle, B. K.; Hatton, C.; Uckelmann, H. J.; Ross, K. N.; Perner, F.; Olsen, S. N.; Pritchard, T.; McDermott, L.; Jones, C. D.; Jing, D.; Braytee, A.; Chacon, D.; Earley, E.; McKeever, B. M.; Claremon, D.; Gifford, A. J.; Lee, H. J.; Teicher, B. A.; Pimanda, J. E.; Beck, D.; Perry, J. A.; Smith, M. A.; McGeehan, G. M.; Lock, R. B.; Armstrong, S. A., A Menin-MLL Inhibitor Induces Specific Chromatin Changes and Eradicates Disease in Models of MLL-Rearranged Leukemia. *Cancer Cell* **2019**, *36* (6), 660-673 e11.
44. Liu, H.; Westergard, T. D.; Cashen, A.; Piwnica-Worms, D. R.; Kunkle, L.; Vij, R.; Pham, C. G.; DiPersio, J.; Cheng, E. H.; Hsieh, J. J., Proteasome inhibitors evoke latent tumor suppression programs in pro-B MLL leukemias through MLL-AF4. *Cancer Cell* **2014**, *25* (4), 530-42.
45. Tubio-Santamaria, N.; Ebstein, F.; Heidel, F. H.; Kruger, E., Immunoproteasome Function in Normal and Malignant Hematopoiesis. *Cells* **2021**, *10* (7).
46. Bagger, F. O.; Kinalis, S.; Rapin, N., BloodSpot: a database of healthy and malignant haematopoiesis updated with purified and single cell mRNA sequencing profiles. *Nucleic Acids Res* **2019**, *47* (D1), D881-D885.
47. Fruh, K.; Gossen, M.; Wang, K.; Bujard, H.; Peterson, P. A.; Yang, Y., Displacement of housekeeping proteasome subunits by MHC-encoded LMPs: a newly discovered mechanism for modulating the multicatalytic proteinase complex. *EMBO J* **1994**, *13* (14), 3236-44.
48. Akiyama, K.; Yokota, K.; Kagawa, S.; Shimbara, N.; Tamura, T.; Akioka, H.; Nothwang, H. G.; Noda, C.; Tanaka, K.; Ichihara, A., cDNA cloning and interferon gamma down-regulation of proteasomal subunits X and Y. *Science* **1994**, *265* (5176), 1231-4.
49. Noda, C.; Tanahashi, N.; Shimbara, N.; Hendil, K. B.; Tanaka, K., Tissue distribution of constitutive proteasomes, immunoproteasomes, and PA28 in rats. *Biochem Biophys Res Commun* **2000**, *277* (2), 348-54.
50. Eleuteri, A. M.; Angeletti, M.; Lupidi, G.; Tacconi, R.; Bini, L.; Fioretti, E., Isolation and characterization of bovine thymus multicatalytic proteinase complex. *Protein Expr Purif* **2000**, *18* (2), 160-8.
51. Haorah, J.; Heilman, D.; Diekmann, C.; Osna, N.; Donohue, T. M., Jr.; Ghorpade, A.; Persidsky, Y., Alcohol and HIV decrease proteasome and immunoproteasome function in macrophages: implications for impaired immune function during disease. *Cell Immunol* **2004**, *229* (2), 139-48.
52. Tubio Santamaria, N.; Jayavelu, A.K.; Schnoeder, T.M.; Eifert, T.; Hsu, C-J.; Perner, F.; Zhang, Q.; Wenge, D.V.; Hansen, F.M.; Kirkpatrick, J.M.; Jyotsana, N.; Lane, S.W.; von Eyss, B.; Deshpande, A.J.; Kühn, M.W.M.; Schwaller, J.; Camman, C.; Seifert, U.; Ebstein, F.; Krüger, E.; Hochhaus, A.; Heuser, M.; Ori, A.; Mann, M.; Armstrong, S.A.; Heidel F.H., Immunoproteasome function maintains oncogenic gene expression in KMT2A-complex driven leukemia. To be published in *Mol Cancer* **2023**, under review.
53. Groettrup, M.; Kraft, R.; Kostka, S.; Standera, S.; Stohwasser, R.; Kloetzel, P. M., A third interferon-gamma-induced subunit exchange in the 20S proteasome. *Eur J Immunol* **1996**, *26* (4), 863-9.
54. Ortiz-Navarrete, V.; Seelig, A.; Gernold, M.; Frentzel, S.; Kloetzel, P. M.; Hammerling, G. J., Subunit of the '20S' proteasome (multicatalytic proteinase) encoded by the major histocompatibility complex. *Nature* **1991**, *353* (6345), 662-4.

55. Yang, Y.; Waters, J. B.; Fruh, K.; Peterson, P. A., Proteasomes are regulated by interferon gamma: implications for antigen processing. *Proc Natl Acad Sci U S A* **1992**, *89* (11), 4928-32.
56. Parlati, F.; Lee, S. J.; Aujay, M.; Suzuki, E.; Levitsky, K.; Lorens, J. B.; Micklem, D. R.; Ruurs, P.; Sylvain, C.; Lu, Y.; Shenk, K. D.; Bennett, M. K., Carfilzomib can induce tumor cell death through selective inhibition of the chymotrypsin-like activity of the proteasome. *Blood* **2009**, *114* (16), 3439-47.
57. Niewerth, D.; Franke, N. E.; Jansen, G.; Assaraf, Y. G.; van Meerloo, J.; Kirk, C. J.; Degenhardt, J.; Anderl, J.; Schimmer, A. D.; Zweegman, S.; de Haas, V.; Horton, T. M.; Kaspers, G. J.; Cloos, J., Higher ratio immune versus constitutive proteasome level as novel indicator of sensitivity of pediatric acute leukemia cells to proteasome inhibitors. *Haematologica* **2013**, *98* (12), 1896-904.
58. Niewerth, D.; Kaspers, G. J.; Jansen, G.; van Meerloo, J.; Zweegman, S.; Jenkins, G.; Whitlock, J. A.; Hunger, S. P.; Lu, X.; Alonzo, T. A.; van de Ven, P. M.; Horton, T. M.; Cloos, J., Proteasome subunit expression analysis and chemosensitivity in relapsed paediatric acute leukaemia patients receiving bortezomib-containing chemotherapy. *J Hematol Oncol* **2016**, *9* (1), 82.
59. Di Rosa, M.; Giallongo, C.; Romano, A.; Tibullo, D.; Li Volti, G.; Musumeci, G.; Barbagallo, I.; Imbesi, R.; Castrogiovanni, P.; Palumbo, G. A., Immunoproteasome Genes Are Modulated in CD34(+) JAK2(V617F) Mutated Cells from Primary Myelofibrosis Patients. *Int J Mol Sci* **2020**, *21* (8).
60. Guenther, M. G.; Jenner, R. G.; Chevalier, B.; Nakamura, T.; Croce, C. M.; Canaani, E.; Young, R. A., Global and Hox-specific roles for the MLL1 methyltransferase. *Proc Natl Acad Sci U S A* **2005**, *102* (24), 8603-8.
61. Wang, P.; Lin, C.; Smith, E. R.; Guo, H.; Sanderson, B. W.; Wu, M.; Gogol, M.; Alexander, T.; Seidel, C.; Wiedemann, L. M.; Ge, K.; Krumlauf, R.; Shilatifard, A., Global analysis of H3K4 methylation defines MLL family member targets and points to a role for MLL1-mediated H3K4 methylation in the regulation of transcriptional initiation by RNA polymerase II. *Mol Cell Biol* **2009**, *29* (22), 6074-85.
62. Meyer, C.; Burmeister, T.; Groger, D.; Tsaur, G.; Fechina, L.; Renneville, A.; Sutton, R.; Venn, N. C.; Emerenciano, M.; Pombo-de-Oliveira, M. S.; Barbieri Blunck, C.; Almeida Lopes, B.; Zuna, J.; Trka, J.; Ballerini, P.; Lapillonne, H.; De Braekeleer, M.; Cazzaniga, G.; Corral Abascal, L.; van der Velden, V. H. J.; Delabesse, E.; Park, T. S.; Oh, S. H.; Silva, M. L. M.; Lund-Aho, T.; Juvonen, V.; Moore, A. S.; Heidenreich, O.; Vormoor, J.; Zerkalenkova, E.; Olshanskaya, Y.; Bueno, C.; Menendez, P.; Teigler-Schlegel, A.; Zur Stadt, U.; Lentjes, J.; Gohring, G.; Kustanovich, A.; Aleinikova, O.; Schafer, B. W.; Kubetzko, S.; Madsen, H. O.; Gruhn, B.; Duarte, X.; Gameiro, P.; Lippert, E.; Bidet, A.; Cayuela, J. M.; Clappier, E.; Alonso, C. N.; Zwaan, C. M.; van den Heuvel-Eibrink, M. M.; Izraeli, S.; Trakhtenbrot, L.; Archer, P.; Hancock, J.; Moricke, A.; Alten, J.; Schrappe, M.; Stanulla, M.; Strehl, S.; Attarbaschi, A.; Dworzak, M.; Haas, O. A.; Panzer-Grumayer, R.; Sedek, L.; Szczepanski, T.; Caye, A.; Suarez, L.; Cave, H.; Marschalek, R., The MLL recombinome of acute leukemias in 2017. *Leukemia* **2018**, *32* (2), 273-284.
63. Chan, A. K. N.; Chen, C. W., Rewiring the Epigenetic Networks in MLL-Rearranged Leukemias: Epigenetic Dysregulation and Pharmacological Interventions. *Front Cell Dev Biol* **2019**, *7*, 81.
64. Yokoyama, A.; Cleary, M. L., Menin critically links MLL proteins with LEDGF on cancer-associated target genes. *Cancer Cell* **2008**, *14* (1), 36-46.

65. La, P.; Silva, A. C.; Hou, Z.; Wang, H.; Schnepp, R. W.; Yan, N.; Shi, Y.; Hua, X., Direct binding of DNA by tumor suppressor menin. *J Biol Chem* **2004**, *279* (47), 49045-54.
66. Yokoyama, A.; Somerville, T. C.; Smith, K. S.; Rozenblatt-Rosen, O.; Meyerson, M.; Cleary, M. L., The menin tumor suppressor protein is an essential oncogenic cofactor for MLL-associated leukemogenesis. *Cell* **2005**, *123* (2), 207-18.
67. Borkin, D.; He, S.; Miao, H.; Kempinska, K.; Pollock, J.; Chase, J.; Purohit, T.; Malik, B.; Zhao, T.; Wang, J.; Wen, B.; Zong, H.; Jones, M.; Danet-Desnoyers, G.; Guzman, M. L.; Talpaz, M.; Bixby, D. L.; Sun, D.; Hess, J. L.; Muntean, A. G.; Maillard, I.; Cierpicki, T.; Grembecka, J., Pharmacologic inhibition of the Menin-MLL interaction blocks progression of MLL leukemia in vivo. *Cancer Cell* **2015**, *27* (4), 589-602.
68. Luo, Z.; Lin, C.; Shilatfard, A., The super elongation complex (SEC) family in transcriptional control. *Nat Rev Mol Cell Biol* **2012**, *13* (9), 543-7.
69. Bernt, K. M.; Zhu, N.; Sinha, A. U.; Vempati, S.; Faber, J.; Krivtsov, A. V.; Feng, Z.; Punt, N.; Daigle, A.; Bullinger, L.; Pollock, R. M.; Richon, V. M.; Kung, A. L.; Armstrong, S. A., MLL-rearranged leukemia is dependent on aberrant H3K79 methylation by DOT1L. *Cancer Cell* **2011**, *20* (1), 66-78.
70. Hartleben, B.; Widmeier, E.; Wanner, N.; Schmidts, M.; Kim, S. T.; Schneider, L.; Mayer, B.; Kerjaschki, D.; Miner, J. H.; Walz, G.; Huber, T. B., Role of the polarity protein Scribble for podocyte differentiation and maintenance. *PLoS One* **2012**, *7* (5), e36705.
71. Lu, Z. H.; Books, J. T.; Ley, T. J., YB-1 is important for late-stage embryonic development, optimal cellular stress responses, and the prevention of premature senescence. *Mol Cell Biol* **2005**, *25* (11), 4625-37.
72. Fehling, H. J.; Swat, W.; Laplace, C.; Kuhn, R.; Rajewsky, K.; Muller, U.; von Boehmer, H., MHC class I expression in mice lacking the proteasome subunit LMP-7. *Science* **1994**, *265* (5176), 1234-7.
73. Yu, J.; Jiang, P. Y. Z.; Sun, H.; Zhang, X.; Jiang, Z.; Li, Y.; Song, Y., Advances in targeted therapy for acute myeloid leukemia. *Biomark Res* **2020**, *8*, 17.
74. van Gils, N.; Denkers, F.; Smit, L., Escape From Treatment; the Different Faces of Leukemic Stem Cells and Therapy Resistance in Acute Myeloid Leukemia. *Front Oncol* **2021**, *11*, 659253.
75. Eaves, C. J., Hematopoietic stem cells: concepts, definitions, and the new reality. *Blood* **2015**, *125* (17), 2605-13.
76. Morrison, S. J.; Weissman, I. L., The long-term repopulating subset of hematopoietic stem cells is deterministic and isolatable by phenotype. *Immunity* **1994**, *1* (8), 661-73.
77. Dash, B. P.; Schnoder, T. M.; Kathner, C.; Mohr, J.; Weinert, S.; Herzog, C.; Godavarthy, P. S.; Zanetti, C.; Perner, F.; Braun-Dullaeus, R.; Hartleben, B.; Huber, T. B.; Walz, G.; Naumann, M.; Ellis, S.; Vasioukhin, V.; Kahne, T.; Krause, D. S.; Heidel, F. H., Diverging impact of cell fate determinants Scrib and Lgl1 on adhesion and migration of hematopoietic stem cells. *J Cancer Res Clin Oncol* **2018**, *144* (10), 1933-1944.
78. Tailor, D.; Resendez, A.; Garcia-Marques, F. J.; Pandrala, M.; Going, C. C.; Bermudez, A.; Kumar, V.; Rafat, M.; Nambiar, D. K.; Honkala, A.; Le, Q. T.; Sledge, G. W.; Graves, E.; Pitteri, S. J.; Malhotra, S. V., Y box binding protein 1 inhibition as a targeted therapy for ovarian cancer. *Cell Chem Biol* **2021**, *28* (8), 1206-1220 e6.

79. Uckelmann, H. J.; Kim, S. M.; Wong, E. M.; Hatton, C.; Giovinazzo, H.; Gadrey, J. Y.; Krivtsov, A. V.; Rucker, F. G.; Dohner, K.; McGeehan, G. M.; Levine, R. L.; Bullinger, L.; Vassiliou, G. S.; Armstrong, S. A., Therapeutic targeting of preleukemia cells in a mouse model of NPM1 mutant acute myeloid leukemia. *Science* **2020**, *367* (6477), 586-590.
80. Kuhn, M. W.; Song, E.; Feng, Z.; Sinha, A.; Chen, C. W.; Deshpande, A. J.; Cusan, M.; Farnoud, N.; Mupo, A.; Grove, C.; Koche, R.; Bradner, J. E.; de Stanchina, E.; Vassiliou, G. S.; Hoshii, T.; Armstrong, S. A., Targeting Chromatin Regulators Inhibits Leukemogenic Gene Expression in NPM1 Mutant Leukemia. *Cancer Discov* **2016**, *6* (10), 1166-1181.
81. Ge, M.; Li, D.; Qiao, Z.; Sun, Y.; Kang, T.; Zhu, S.; Wang, S.; Xiao, H.; Zhao, C.; Shen, S.; Xu, Z.; Liu, H., Restoring MLL reactivates latent tumor suppression-mediated vulnerability to proteasome inhibitors. *Oncogene* **2020**, *39* (36), 5888-5901.
82. Goodfellow, S. J.; Rebello, M. R.; Toska, E.; Zeef, L. A.; Rudd, S. G.; Medler, K. F.; Roberts, S. G., WT1 and its transcriptional cofactor BASP1 redirect the differentiation pathway of an established blood cell line. *Biochem J* **2011**, *435* (1), 113-25.
83. Toska, E.; Campbell, H. A.; Shandilya, J.; Goodfellow, S. J.; Shore, P.; Medler, K. F.; Roberts, S. G., Repression of transcription by WT1-BASP1 requires the myristoylation of BASP1 and the PIP2-dependent recruitment of histone deacetylase. *Cell Rep* **2012**, *2* (3), 462-9.
84. Hartl, M.; Nist, A.; Khan, M. I.; Valovka, T.; Bister, K., Inhibition of Myc-induced cell transformation by brain acid-soluble protein 1 (BASP1). *Proc Natl Acad Sci U S A* **2009**, *106* (14), 5604-9.
85. Brien, G. L.; Stegmaier, K.; Armstrong, S. A., Targeting chromatin complexes in fusion protein-driven malignancies. *Nat Rev Cancer* **2019**, *19* (5), 255-269.
86. Stein, E. M.; Garcia-Manero, G.; Rizzieri, D. A.; Tibes, R.; Berdeja, J. G.; Savona, M. R.; Jongen-Lavrenic, M.; Altman, J. K.; Thomson, B.; Blakemore, S. J.; Daigle, S. R.; Waters, N. J.; Suttle, A. B.; Clawson, A.; Pollock, R.; Krivtsov, A.; Armstrong, S. A.; DiMartino, J.; Hedrick, E.; Lowenberg, B.; Tallman, M. S., The DOT1L inhibitor pinometostat reduces H3K79 methylation and has modest clinical activity in adult acute leukemia. *Blood* **2018**, *131* (24), 2661-2669.
87. Perner, F.; Stein, E. M.; Wenge, D. V.; Singh, S.; Kim, J.; Apazidis, A.; Rahnamoun, H.; Anand, D.; Marinaccio, C.; Hatton, C.; Wen, Y.; Stone, R. M.; Schaller, D.; Mowla, S.; Xiao, W.; Gamlen, H. A.; Stonestrom, A. J.; Persaud, S.; Ener, E.; Cutler, J. A.; Doench, J. G.; McGeehan, G. M.; Volkamer, A.; Chodera, J. D.; Nowak, R. P.; Fischer, E. S.; Levine, R. L.; Armstrong, S. A.; Cai, S. F., MEN1 mutations mediate clinical resistance to menin inhibition. *Nature* **2023**.

9. Declaration of contribution to the publications

Mohr, J.; Dash, B. P.; Schnoeder, T. M.; Wolleschak, D.; Herzog, C.; **Tubio Santamaria, N.**; Weinert, S.; Godavarthy, S.; Zanetti, C.; Naumann, M.; Hartleben, B.; Huber, T. B.; Krause, D. S.; Kahne, T.; Bullinger, L.; Heidel, F. H., The cell fate determinant Scribble is required for maintenance of hematopoietic stem cell function. *Leukemia* **2018**, 32 (5), 1211-1221.

This investigation was carried out during my time as a PhD student at the University Hospital Jena in the laboratory of Prof. Florian Heidel.

- I contributed to the analysis of gene-expression profiling data and the conception of the corresponding figure.

Perner, F.; Schnoeder, T. M.; Xiong, Y.; Jayavelu, A. K.; Mashamba, N.; **Santamaria, N. T.**; Huber, N.; Todorova, K.; Hatton, C.; Perner, B.; Eifert, T.; Murphy, C.; Hartmann, M.; Hoell, J. I.; Schroder, N.; Brandt, S.; Hochhaus, A.; Mertens, P. R.; Mann, M.; Armstrong, S. A.; Mandinova, A.; Heidel, F. H., YBX1 mediates translation of oncogenic transcripts to control cell competition in AML. *Leukemia* **2022**, 36 (2), 426-437.

This investigation was carried out during my time as a PhD student at the University Hospital Jena and at the University Medicine Greifswald in the laboratory of Prof. Florian Heidel.

- I performed cell culture experiments and contributed to the xenograft model experiments including the respective data analysis.

Tubío-Santamaría, N.; Jayavelu, A.K.; Schnoeder, T.M.; Eifert, T.; Hsu, C-J.; Perner, F.; Zhang, Q.; Wenge, D.V.; Hansen, F.M.; Kirkpatrick, J.M.; Jyotsana, N.; Lane, S.W.; von Eyss, B.; Deshpande, A.J.; Kühn, M.W.M.; Schwaller, J.; Cammann, C.; Seifert, U.; Ebstein, F.; Krüger, E.; Hochhaus, A.; Heuser, M.; Ori, A.; Mann, M.; Armstrong, S.A.; Heidel, F.H., Immunoproteasome function maintains oncogenic gene expression in KMT2A-complex driven leukemia. *Mol Cancer* **2023**, 22 (196).

This investigation was carried out during my time as a PhD student at the University Hospital Jena and at the University Medicine Greifswald in the laboratory of Prof. Florian Heidel.

- I performed the majority of the *in vitro* experiments and processed the samples derived from the *in vivo* mouse experiments.
- I analyzed and interpreted the data from the *in vitro* and *in vivo* experiments.
- I contributed to the sample preparation for RNA-sequencing, ATAC-sequencing, Cut&Tag and Cut&Run and I participated in the analysis of these samples.
- I contributed to the preparation of the proteome samples.
- I created the figures for the manuscript.

Greifswald,

Unterschrift

10. Original publications

Publication 1:

Mohr, J.; Dash, B. P.; Schnoeder, T. M.; Wolleschak, D.; Herzog, C.; **Tubio Santamaria, N.**; Weinert, S.; Godavarthy, S.; Zanetti, C.; Naumann, M.; Hartleben, B.; Huber, T. B.; Krause, D. S.; Kahne, T.; Bullinger, L.; Heidel, F. H., The cell fate determinant Scribble is required for maintenance of hematopoietic stem cell function. *Leukemia* **2018**, 32 (5), 1211-1221.

Publication 2:

Perner, F.; Schnoeder, T. M.; Xiong, Y.; Jayavelu, A. K.; Mashamba, N.; **Santamaria, N. T.**; Huber, N.; Todorova, K.; Hatton, C.; Perner, B.; Eifert, T.; Murphy, C.; Hartmann, M.; Hoell, J. I.; Schroder, N.; Brandt, S.; Hochhaus, A.; Mertens, P. R.; Mann, M.; Armstrong, S. A.; Mandinova, A.; Heidel, F. H., YBX1 mediates translation of oncogenic transcripts to control cell competition in AML. *Leukemia* **2022**, 36 (2), 426-437.

Publication 3:

Tubío-Santamaría, N.; Jayavelu, A.K.; Schnoeder, T.M.; Eifert, T.; Hsu, C-J.; Perner, F.; Zhang, Q.; Wenge, D.V.; Hansen, F.M.; Kirkpatrick, J.M.; Jyotsana, N.; Lane, S.W.; von Eyss, B.; Deshpande, A.J.; Kühn, M.W.M.; Schwaller, J.; Cammann, C.; Seifert, U.; Ebstein, F.; Krüger, E.; Hochhaus, A.; Heuser, M.; Ori, A.; Mann, M.; Armstrong, S.A.; Heidel F.H., Immunoproteasome function maintains oncogenic gene expression in KMT2A-complex driven leukemia. *Mol Cancer* **2023**, 22 (196)



Stem cell biology

The cell fate determinant Scribble is required for maintenance of hematopoietic stem cell function

Juliane Mohr¹ · Banaja P. Dash¹ · Tina M. Schnoeder^{1,2} · Denise Wolleschak³ · Carolin Herzog³ · Nuria Tubio Santamaria^{1,2} · Sönke Weinert⁴ · Sonika Godavarthy⁵ · Costanza Zanetti⁵ · Michael Naumann⁶ · Björn Hartleben⁷ · Tobias B. Huber⁸ · Daniela S. Krause⁵ · Thilo Kähne⁶ · Lars Bullinger⁹ · Florian H. Heidel^{1,2}

Received: 18 December 2017 / Accepted: 2 January 2018 / Published online: 30 January 2018
© Macmillan Publishers Limited, part of Springer Nature 2018

Abstract

Cell fate determinants influence self-renewal potential of hematopoietic stem cells. Scribble and Lgl1 belong to the Scribble polarity complex and reveal tumor-suppressor function in drosophila. In hematopoietic cells, genetic inactivation of Lgl1 leads to expansion of the stem cell pool and increases self-renewal capacity without conferring malignant transformation. Here we show that genetic inactivation of its putative complex partner Scribble results in functional impairment of hematopoietic stem cells (HSC) over serial transplantation and during stress. Although loss of Scribble deregulates transcriptional downstream effectors involved in stem cell proliferation, cell signaling, and cell motility, these effectors do not overlap with transcriptional targets of Lgl1. Binding partner analysis of Scribble in hematopoietic cells using affinity purification followed by mass spectrometry confirms its role in cell signaling and motility but not for binding to polarity modules described in drosophila. Finally, requirement of Scribble for self-renewal capacity also affects leukemia stem cell function. Thus, Scribble is a regulator of adult HSCs, essential for maintenance of HSCs during phases of cell stress.

Electronic supplementary material The online version of this article (<https://doi.org/10.1038/s41375-018-0025-0>) contains supplementary material, which is available to authorized users.

✉ Florian H. Heidel florian.heidel@med.uni-jena.de

¹ Innere Medizin II, Hämatologie und Onkologie, Universitätsklinikum Jena, Jena, Germany

² Leibniz Institute on Aging, Fritz-Lipmann Institute, Jena, Germany

³ Department of Hematology and Oncology, Otto-von-Guericke University Medical Center, Magdeburg, Germany

⁴ Department of Cardiology, Otto-von-Guericke University Medical Center, Magdeburg, Germany

⁵ Georg-Speyer-Haus, Institute for Tumor Biology and Experimental Therapy, 60596 Frankfurt am Main, Germany

⁶ Institute of Experimental Internal Medicine, Otto-von-Guericke University Magdeburg, Magdeburg, Germany

⁷ Institute of Pathology, Medizinische Hochschule Hannover, Hannover, Germany

⁸ III Medical Department, University Medical Center Hamburg-Eppendorf, Hamburg, Germany

⁹ Medical Clinic for Hematology, Oncology and Tumor Biology, Charite University Hospital, Berlin, Germany

ARTICLE OPEN



ACUTE MYELOID LEUKEMIA

YBX1 mediates translation of oncogenic transcripts to control cell competition in AML

Florian Perner^{1,2,3}, Tina M. Schnoeder³, Yijun Xiong¹, Ashok Kumar Jayavelu^{4,5,6}, Nomusa Mashamba⁷, Nuria Tubio Santamaria³, Nicolas Huber³, Kristina Todorova⁸, Charles Hatton¹, Birgit Perner^{9,10}, Theresa Eifert³, Ciara Murphy¹, Maximilian Hartmann², Jessica I. Hoell¹¹, Nicolas Schröder¹², Sabine Brandt¹³, Andreas Hochhaus², Peter R. Mertens¹³, Matthias Mann⁴, Scott A. Armstrong¹, Anna Mandinova⁸ and Florian H. Heidel^{2,3,14}

© The Author(s) 2021

Persistence of malignant clones is a major determinant of adverse outcome in patients with hematologic malignancies. Despite the fact that the majority of patients with acute myeloid leukemia (AML) achieve complete remission after chemotherapy, a large proportion of them relapse as a result of residual malignant cells. These persistent clones have a competitive advantage and can re-establish disease. Therefore, targeting strategies that specifically diminish cell competition of malignant cells while leaving normal cells unaffected are clearly warranted. Recently, our group identified YBX1 as a mediator of disease persistence in *JAK2*-mutated myeloproliferative neoplasms. The role of YBX1 in AML, however, remained so far elusive. Here, inactivation of *YBX1* confirms its role as an essential driver of leukemia development and maintenance. We identify its ability to amplify the translation of oncogenic transcripts, including *MYC*, by recruitment to polysomal chains. Genetic inactivation of *YBX1* disrupts this regulatory circuit and displaces oncogenic drivers from polysomes, with subsequent depletion of protein levels. As a consequence, leukemia cells show reduced proliferation and are out-competed in vitro and in vivo, while normal cells remain largely unaffected. Collectively, these data establish YBX1 as a specific dependency and therapeutic target in AML that is essential for oncogenic protein expression.

Leukemia (2022) 36:426–437; <https://doi.org/10.1038/s41375-021-01393-0>

INTRODUCTION

Cold-shock proteins (CSPs) are a family of multifunctional DNA/RNA binding proteins that contain a highly conserved nucleic acid binding domain called the cold shock domain. YBX1 is a pleiotropic DNA and RNA binding protein that modulates translation, RNA-stability, mRNA splicing, transcription or cell signaling depending on cell type and genetic background [1–10]. In humans, eight members of the CSP-family are described: YBX1, YBX2, YBX3, CARHSP1, CSDC2, CSDE1, LIN28A and LIN28B [6]. Several of the mammalian CSP-family members promote malignant transformation or cancer progression [1–3, 11] and impact diverse inflammatory processes [6, 7]. Initially, the CSP family had been identified in bacteria as proteins required for stress responses. Upon rapid temperature decline CSPs facilitate resistance to translational stress as a consequence of changes in mRNA secondary structures [12–14]. One of the most highlighted

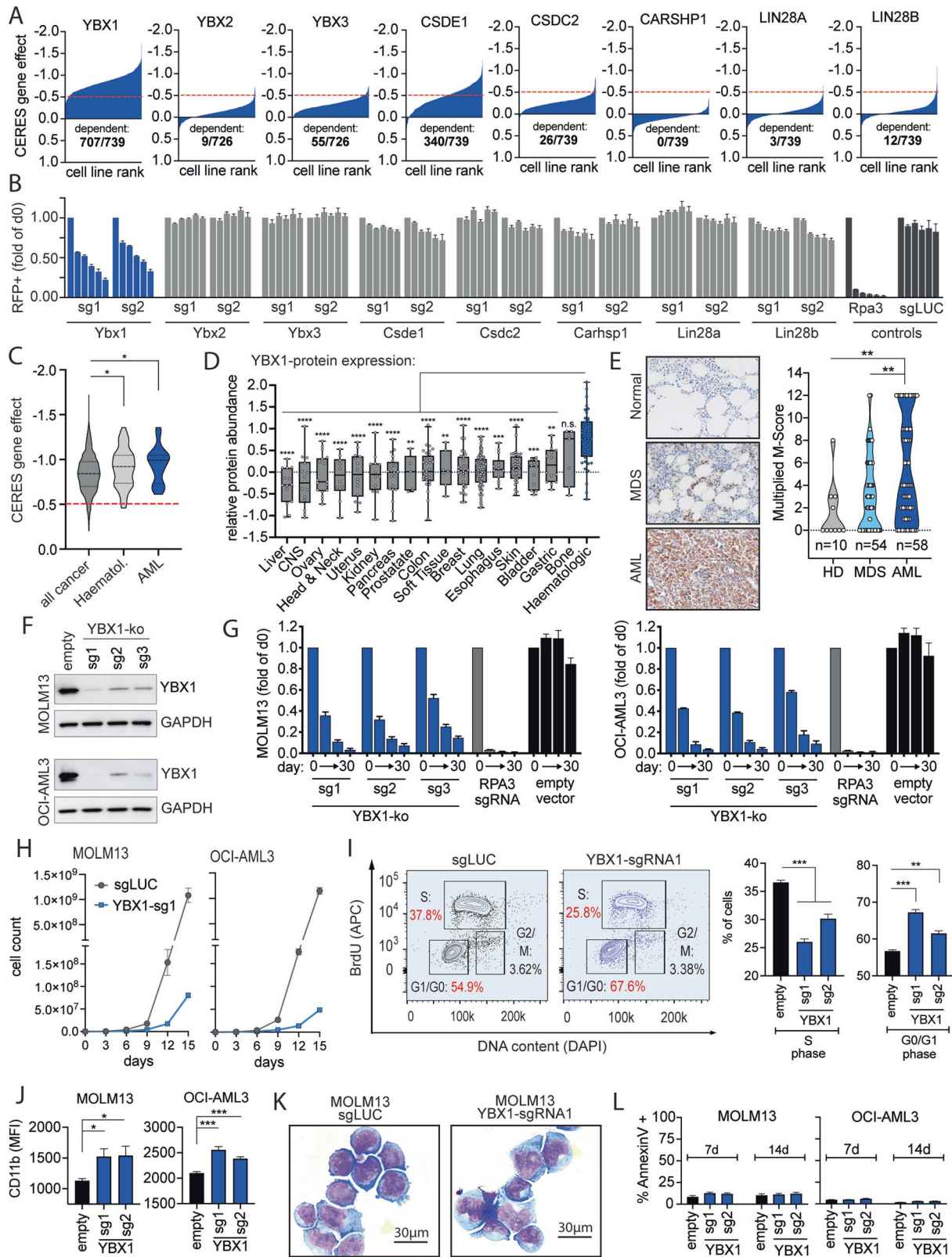
functions of YBX1 is its ability to adapt malignant cells to hypoxic stress [1, 2, 15]. YBX1 binds and stabilizes oncogenic RNAs in the context of hypoxia [2] and directly mediates translation of HIF1a transcripts [1, 15]. Recently, our group reported on a novel role of YBX1 in *JAK2*-mutated myeloproliferative neoplasms (MPN) [16]. During *JAK*-inhibitor treatment, YBX1 safeguarded splicing of transcripts essential for signal transduction. Genetic inactivation of *YBX1* led to a significant increase in mis-splicing of *MAPK/ERK* pathway members and to eradication of otherwise persistent MPN cells [16]. Of note, YBX1 was not primarily required for proliferation or survival of *JAK2*-mutated cells.

So far, the functional role of cold-shock proteins in AML had not been investigated in detail. Here, we aim to assess the functional relevance and mechanistic role of cold shock proteins, and specifically YBX1, in acute myeloid leukemia (AML) in vitro and in vivo.

¹Department of Pediatric Oncology, Dana Farber Cancer Institute, Harvard Medical School, Boston, MA, USA. ²Innere Medizin 2, Hämatologie und Onkologie, Universitätsklinikum Jena, Jena, Germany. ³Innere Medizin C, Universitätsmedizin Greifswald, Greifswald, Germany. ⁴Max-Planck-Institute for Biochemistry, Munich, Germany. ⁵Department of Pediatric Oncology, Hematology and Immunology, University of Heidelberg, Heidelberg, Germany. ⁶Clinical Cooperation Unit Pediatric Leukemia, DKFZ, Heidelberg, Germany. ⁷Department of Hematology and Oncology, Otto-von-Guericke Medical Center Magdeburg, Magdeburg, Germany. ⁸Cutaneous Biology Research Center, Massachusetts General Hospital, Harvard Medical School, Boston, MA, USA. ⁹Molecular Genetics Laboratory, Leibniz Institute on Aging-Fritz Lipmann Institute (FLI), Jena, Germany. ¹⁰Core Facility, Imaging, Leibniz Institute on Aging-Fritz Lipmann Institute (FLI), Jena, Germany. ¹¹Department of Pediatrics 1, Martin Luther University Halle-Wittenberg, Halle, Germany. ¹²Gemeinschaftspraxis für Pathologie, Schlosspark-Klinik, Berlin, Germany. ¹³Clinic of Nephrology and Hypertension, Diabetes and Endocrinology, Otto-von-Guericke University, Magdeburg, Germany. ¹⁴Leibniz Institute on Aging-Fritz-Lipmann Institute, Jena, Germany. ✉email: Florian_Perner@DFCI.harvard.edu; Florian.heidel@uni-greifswald.de

Received: 22 April 2021 Revised: 16 August 2021 Accepted: 18 August 2021

Published online: 31 August 2021



MATERIALS AND METHODS

Animal models

Mice were housed under pathogen-free conditions in the Animal Research Facility OvGU, Magdeburg and University Hospital Jena, Germany. All experiments were conducted after approval by the Landesverwaltungsamt Sachsen-Anhalt (42502-2-1279 UniMD) and Thüringen (02-030/2016).

Generation of conventional [17] and conditional [16] mouse models for genetic inactivation of *Ybx1* has been described before. Retroviral induction of leukemia was performed as published previously [18, 19]. The experimental details for the experiments conducted in murine leukemias and xenograft systems are outlined in detail in the supplementary methods section.

Fig. 1 YBX1 is a pan-cancer dependency and drives cell proliferation in AML. **A** Waterfall plots depicting the gene-dependency of each cold-shock protein coding gene in cell lines from the cancer dependency map portal (Achilles program, depmap.org). Cell lines are sorted by dependency rank (increasing dependency along the x axis), the CERES gene-effect score is shown on the Y axis. The red dotted lines display the arbitrary CERES score of -0.5 , which is generally considered as a cutoff for a relevant gene-dependency. **B** Bar graphs displaying the data from a CRISPR-Cas9 cell competition assay showing the effect of deletion of each cold-shock protein family member over time. Members of the CSP-family were knocked out using single guide RNAs in murine MLL-AF9 transformed AML cells and the chimerism of knockout and wild-type cells over time is visualized in the graphs. The bars within a block of each guide RNA represent the chimerism at day 0, 3, 6, 9, 12 and 15. A decrease in the % of RFP + cells (shown on the Y axis) over time, as seen for YBX1, reflects a competitive disadvantage of cells that harbor the respective knockout. **C** Violin plots showing the gene-dependency of YBX1 (Achilles program, depmap.org) in all cancer types compared to all hematologic cancers and AML. Statistical analysis via unpaired t test, $*p < 0.05$. **D** Box plots showing YBX1 relative protein expression among cell lines from the cancer cell line encyclopedia (Mass-spec proteome analysis, data derived from depmap.org). Statistical analysis via unpaired t test, $**p < 0.01$, $***p < 0.001$, $****p < 0.0001$. **E** Immunohistochemistry for YBX1 in bone marrow of healthy donors (HD), patients with myelodysplastic syndrome (MDS) and patients with AML. Left side: representative pictures of the analyzed bone marrow histology sections (brown color: anti-YBX1). Right side: Violin-plot showing the respective pathological scoring (Multiplied M-scores) among all specimens analyzed. Statistical analysis was performed using Mann-Whitney U Test, $**p < 0.01$. **F** Western-blot showing YBX1-protein levels in MOLM13 and OCI-AML3 cells after knockout using 3 different sgRNAs compared to empty vector control. **G** Bar graphs showing data from a CRISPR-Cas9 cell competition assay in MOLM13 and OCI-AML3 cells after YBX1 deletion using 3 different sgRNAs compared to knockout of RPA3 (positive control) or empty vector (negative control) at 0, 10, 20 and 30 days after starting the competition assay. **H** Growth curves of MOLM13 and OCI-AML3 cells after deleting YBX1 using sgRNA1 compared to non-targeting control (sgLUC) over the course of 15 days. **I** Flow-cytometry-based cell-cycle analysis in MOLM-13 cells after genetic inactivation of YBX1 using the BrdU assay. Left panel: representative FACS plots. Right panel: bar graphs showing quantitative analysis of cells detected in S- and G0/G1 phase. Unpaired t test, $**p < 0.01$, $***p < 0.001$. **J** Flow cytometry-based assessment of CD11b surface expression of MOLM-13 and OCI-AML3 cells after knockout of YBX1 using 2 different sgRNAs. Unpaired t test, $*p < 0.05$, $***p < 0.001$. **K** Representative cytological pictures showing cell morphology of MOLM-13 cells after YBX1 knockout compared to control (empty; Quick-Dip staining kit, JORVET, Loveland, CO, USA). **L** Apoptosis assay using Annexin V (Biolegend, San Diego, CA, USA) in MOLM-13 and OCI-AML3 cells after knockout of YBX1 using 2 different sgRNAs (day 7 and 14 after YBX1 knockout).

RNA sequencing

RNA was isolated from cultured cells using the Qiagen RNeasy Mini kit or from polysomal fractions using TRIZOL as previously described [4]. Subsequently, mRNAs were purified using the “NEBNext® Poly(A) mRNA Magnetic Isolation Module” followed by RNAseq library preparation using the “NEBNext® Ultra™ RNA Library Prep Kit for Illumina™” according to the manufacturer’s instruction. Sequencing was performed at Dana-Farber Cancer Institute (NexSeq, 37 bp, paired end) or at Genewiz (HiSeq, 150 bp, paired end) (Illumina, South Plainfield, NJ, USA).

Mass spectrometry

MOLM13 cell pellets from growing cultures were washed in PBS and lysed as previously described [20] before trypsin digest. A nanoflow HPLC (EASY-nLC1000, Thermo Fisher Scientific) coupled to an Orbitrap Exploris 480 Mass Spectrometer (Thermo Fischer Scientific) via a nano electrospray ion source was utilized for the sample analysis. Peptide calling and quantification was performed as previously established [21–23]. A detailed description of the procedure is provided in the Supplementary Methods section.

CRISPR-Cas9 screening

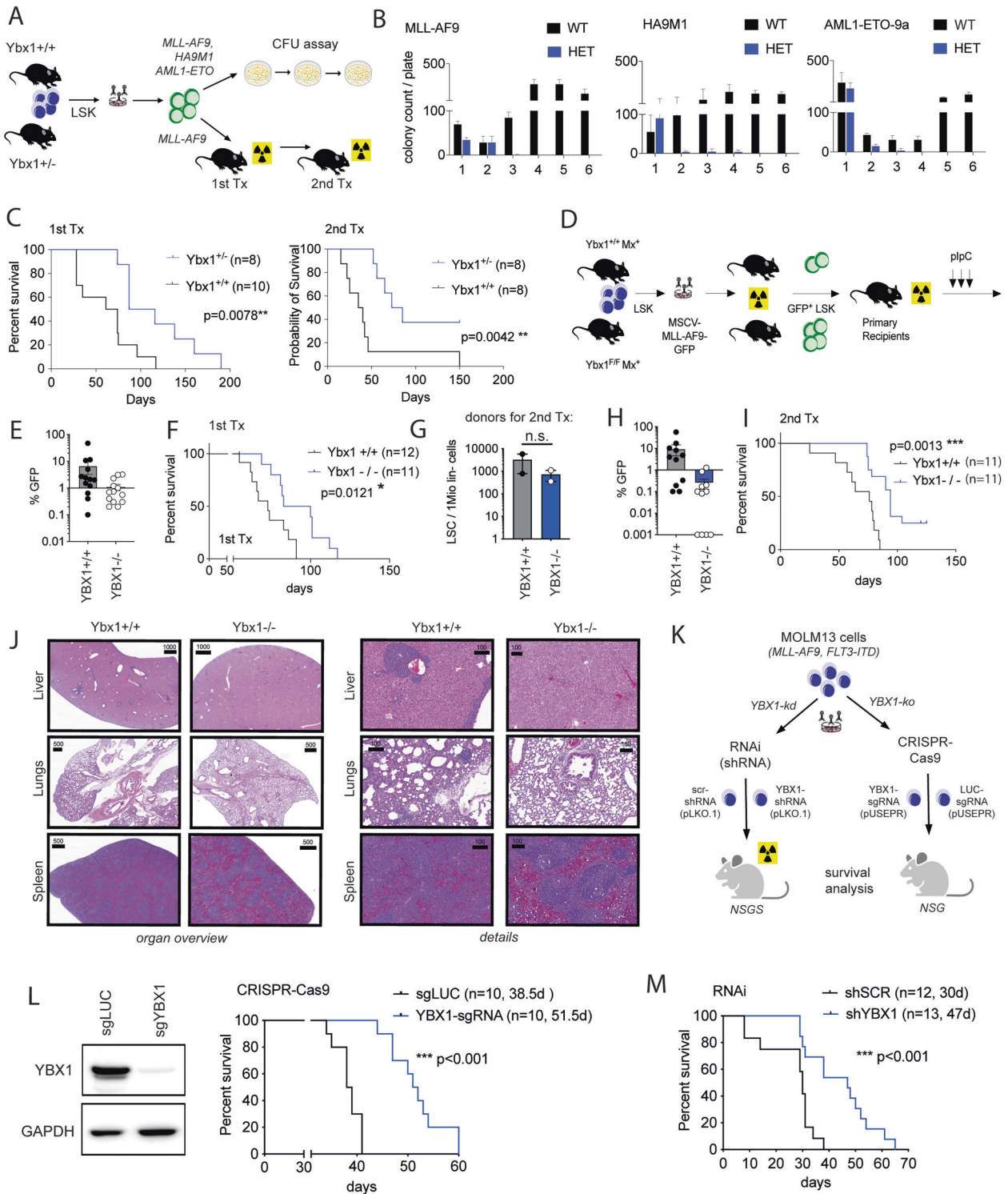
Paired human genome-scale CRISPR-Cas9 screening libraries (H1/H2) were a gift from Dr. Xiaole Shirley Liu (Addgene #1000000132). The H1 and H2 libraries cover protein coding genes of the genome with a total of 10 guide RNAs per gene. Lentivirus was produced using each separate library pool and used to transduce each 4×10^8 MOLM13 cells harboring a knockout of YBX1 (YBX1-sgRNA1, pLKO5.GFP) or non-targeting control at low MOI. 48 h after library transduction cells were selected with puromycin. After 3 d of puromycin selection a baseline sample was collected, and cells were cultured in duplicates for 12 d (splitting and counting every 3 d) before harvest of the terminal samples. Subsequently, genomic DNA was isolated using phenol-chloroform extraction. Guide-RNA amplicon libraries were prepared and data analysis using MAGeCK MLE was performed as previously described [24–26].

RESULTS

YBX1 is a pan-cancer dependency and drives cell proliferation in human and murine models of AML

Given the fact that RNA-binding proteins may exert different functions depending on the cellular context, we employed functional and descriptive screening methods to investigate mechanisms by which CSPs may influence cellular homeostasis in AML.

To generate insights into functional properties of different CSPs on a pan-cancer scale we utilized publicly available functional genomic datasets. Gene-dependency data from genome-wide CRISPR-Cas9 screens in over 700 cancer cell lines [27] indicated a pan-cancer dependency only for YBX1 (Fig. 1A). Of note, AML cell lines were particularly sensitive to its inactivation (Fig. 1C). In order to validate these observations, we defined CSP-specific dependencies in AML cells using an arrayed CRISPR-Cas9 based negative selection screen (Supplementary Fig. 1A). Consistent with the public pan-cancer screening data, murine MLL-AF9 transformed AML cells [28] showed a relevant gene-dependency only on Ybx1 (Fig. 1B). Analysis of a recently published large-scale proteome dataset covering 375 cell lines of the Cancer Cell Line Encyclopedia [29] for CSP-family expression showed that YBX1 and CARHSP1 are specifically overexpressed in hematologic malignancies (Fig. 1D; Supplementary Fig. 1B). Similarly, gene-expression of YBX1, CARHSP1 and YBX2 was shown to be elevated in a set of primary AML patient samples [30] (Supplementary Fig. 1C). Since YBX1 was particularly upregulated and functionally relevant we aimed to validate our findings by immunohistochemistry in bone marrow (BM) biopsies from patients. Compared to healthy donors (HD), patients with myelodysplastic syndrome (MDS) or AML showed increased expression during disease progression with the highest scores documented in the AML specimens (Fig. 1E). We further validated these findings in two different human AML cell lines (MOLM13, OCI-AML3) using 3 sgRNAs targeting YBX1 that potentially reduced protein expression (Fig. 1F). YBX1-inactivation led to gradual out-competition of guide infected cells (Fig. 1G). Loss of cell competition could be attributed to impaired proliferative capacity and delayed S-phase entry of YBX1-deficient AML cells (Fig. 1H, I). Furthermore, AML cell lines showed discrete immunophenotypic and morphological signs of differentiation (Fig. 1J, K) while induction of apoptosis was not observed (Fig. 1L). To validate our findings, we used RNAi to genetically inactivate YBX1 in a larger panel of AML cell lines. For both YBX1 shRNAs 6/8 AML cell lines showed >70% reduction in cell proliferation (Supplementary Fig. 2A) but no consistent increase in apoptosis. Signs of myeloid differentiation could also be detected but appeared rather inconsistent and not clearly associated with cellular responses (Supplementary Fig. 2B).



YBX1 is essential for development and maintenance of AML in vivo

Reduction of YBX1 expression by RNAi in primary MLL-AF9 (MA9) transformed murine leukemic cells resulted in decreased colony formation capacity and a significant delay of disease development in vivo ($p = 0.0446$ *; Supplementary Fig. 3A, B). In order to determine the relevance of YBX1 for AML development in a more sophisticated genetic system, we used a retroviral model of leukemic transformation in a conventional YBX1 knockout mouse

model [17] in which exon 3 is genetically deleted leading to loss of a functional protein. As homozygous deletion of Ybx1 is embryonically lethal, we compared heterozygous animals to wildtype controls. Bone marrow (BM) cells of the respective donor animals were isolated as published before [19, 31] and Ybx1 +/+ or Ybx1 +/- Lin⁻Kit⁺Sca1⁺ (LSK) cells were transduced with MLL-AF9 (MA9), HoxA9-Meis1a or AML1-ETO. Transformed cells were investigated by serial re-plating in methylcellulose to assess colony formation and self-renewal capacity in vitro (Fig. 2A). As

Fig. 2 YBX1 is essential for development and maintenance of AML in vivo. **A** Flow-scheme depicting the experimental procedures performed using the Ybx1 straight knockout mouse model for assessment of Ybx1 function in development of AML. **B** Bar graphs showing the number of AML colonies in a methylcellulose-based colony-formation assay in Ybx1 +/+ and Ybx1 +/- AML cells after retrovirally mediated leukemic transformation with MLL-AF9, HOXA9-MEIS1a (HA9M1) or AML1-ETO9a. The numbers on the X axis correspond to the rounds of plating. **C** Survival-curves of primary (left) and secondary (right) recipient animals after transplantation of MLL-AF9 transformed AML cells harboring a heterozygous deletion of Ybx1 (YBX1 +/-) or WT (Ybx1 +/+). **D** Scheme depicting the experimental procedures for assessment of Ybx1 function in maintenance of AML. **E** Bar graphs showing the % of GFP + cells (MLL-AF9 expressing leukemia cells) in the peripheral blood of Ybx1 +/+ and Ybx1 +/- primary recipient animals 4 weeks after transplantation. **F** Survival of primary recipient animals transplanted with Ybx1 +/+ and Ybx1 +/- MLL-AF9 driven AML. **G** Bar graphs showing the LSC frequency (number of GFP + Kit + cells per 1 Mio lin- viable bone marrow cells) in primary recipient animals that were used as donors for secondary recipients. **H** Bar graphs showing the % of GFP + cells (MLL-AF9 expressing leukemia cells) in the peripheral blood of Ybx1 +/+ and Ybx1 +/- secondary recipient animals 2 weeks after transplantation. **I** Survival of secondary recipient animals transplanted with Ybx1 +/+ and Ybx1 +/- MLL-AF9 driven AML. **J** Histological pictures (H&E staining) of liver, lung and spleen of representative secondary recipient animals that were transplanted with a Ybx1 +/+ and Ybx1 +/- AML. On the left side is the organ overview, the right side shows the same sections in higher magnification for the visualization of microscopic structures. The numbers on the scale bars show the respective scale in μm . **K** Scheme depicting the experimental procedures for CRISPR-Cas9-mediated knockout and RNAi mediated knockdown of YBX1 in human MOLM-13 cells before transplantation into xenograft mice. **L** Left side: Western blot showing knockout efficiency before transplantation. Right side: survival curve for xenograft mice injected with MOLM13 cells after CRISPR-Cas9 mediated knockout of YBX1. **M** Survival curve of mice transplanted with MOLM13 after RNAi mediated knockdown of YBX1 (shYBX1) or non-targeting control.

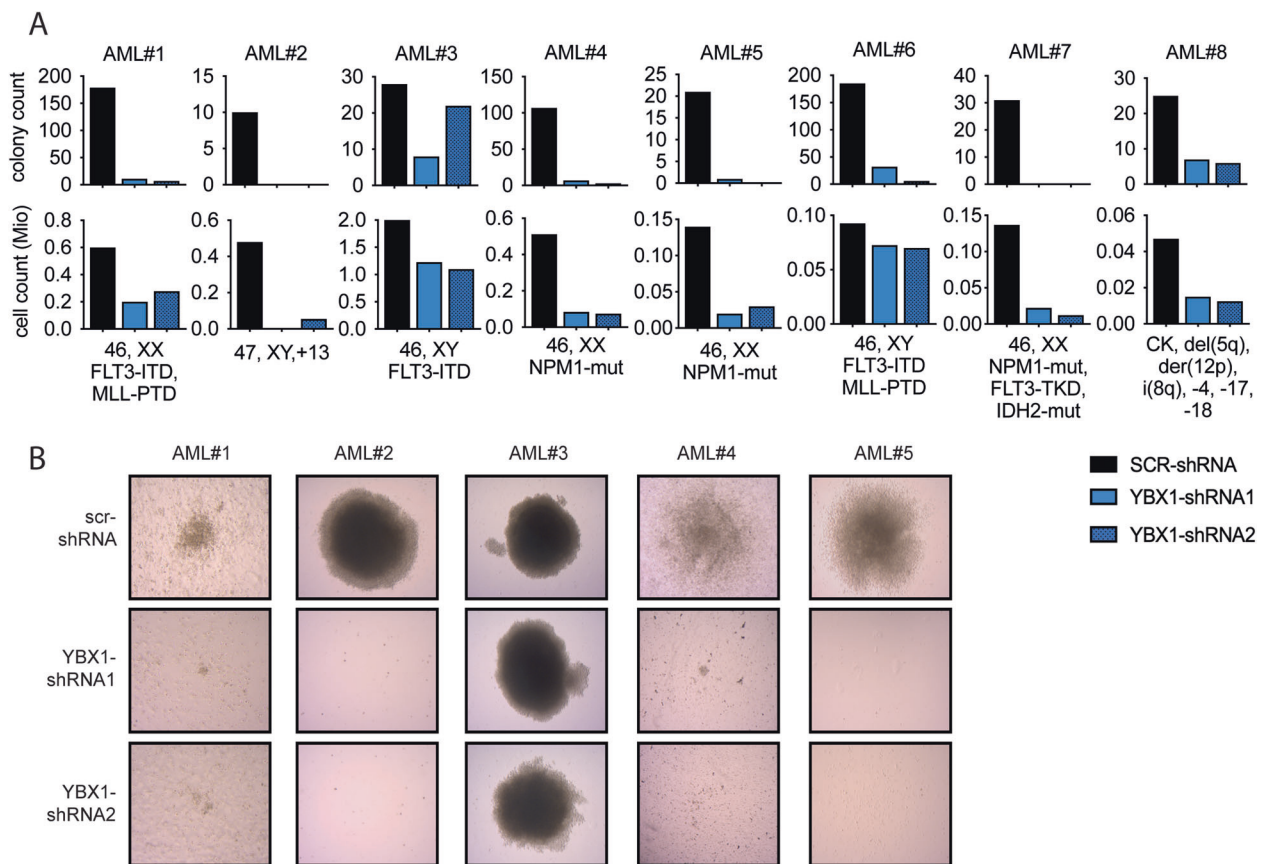
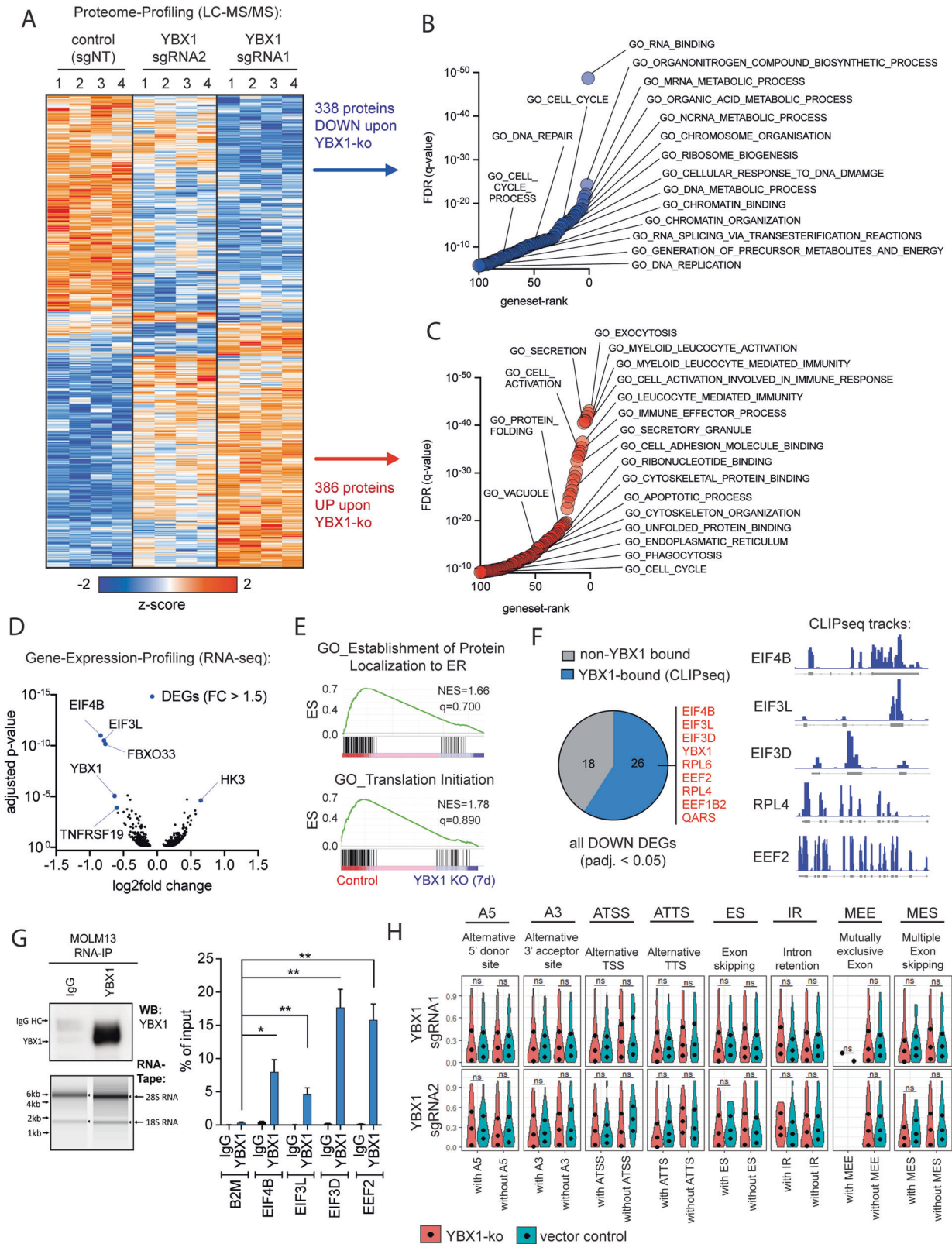


Fig. 3 YBX1 is a dependency in primary human AML patient samples. **A** Bar graphs showing the colony counts (top panel) and cell counts (bottom panel) of primary human AML patient samples after genetic inactivation of YBX1 (YBX1-shRNA1/2) or control (SCR-shRNA). After lentiviral transduction cells were plated in methylcellulose (MethoCult™ H4034 Optimum, Stemcell Technologies, Vancouver, Canada) supplemented with 1 $\mu\text{g}/\text{ml}$ puromycin at a density of 100,000 cells/4 ml of methylcellulose in a 6-well plate. Colonies were counted and analyzed at 10-14d after plating. **B** Representative pictures of colonies from 5 primary AML patients after YBX1 inactivation and plating in methylcellulose.

expected, Ybx1 +/+ cells showed increased self-renewal. In contrast, Ybx1 +/- cells failed to sustain colony growth beyond 3 rounds of serial re-plating for all oncogenes investigated (Fig. 2B). To investigate whether Ybx1 is required for leukemia development in vivo, Ybx1 +/+ and Ybx1 +/- LSK cells were transduced with the MA9 fusion oncogene and a total of 7×10^4 GFP + cells were injected into primary recipient hosts (Fig. 2A). Recipients of Ybx1 +/- cells showed delayed disease onset and

significantly prolonged survival (median survival of MA9-Ybx1 +/+ 67 days; MA9-Ybx1 +/- 101 days; $p = 0.0078^{**}$) (Fig. 2C, left panel). Likewise, secondary recipients of Ybx1 +/- cells showed prolonged survival (median survival of MA9-Ybx1 +/+ 37 days; MA9-Ybx1 +/- 90 days; $p = 0.0042^{**}$) and 3/8 (37.5%) of animals failed to establish leukemia within 150 days (Fig. 2C, right panel). To assess for a potential therapeutic index and for the role of Ybx1 in normal HSPC function, Ybx1 +/- and Ybx1 +/+ cells were



transplanted into primary recipient hosts in a competitive manner. We found no loss of function in heterozygous *Ybx1* cells when competing against wildtype controls as indicated by stable peripheral blood (PB) chimerism over 16 weeks in primary and secondary recipient hosts (Supplementary Fig. 3C). Furthermore,

the composition of hematopoietic stem- and progenitor cells (HSPCs) in the BM of *Ybx1* $+/-$ mice was not altered compared to *Ybx1* $+/+$ animals (Supplementary Fig. 3D). These findings indicate that heterozygous deletion of *Ybx1* impairs leukemia development in vivo while it does not affect normal HSPC function

Fig. 4 YBX1 maintains an oncogenic protein network in AML at the post-transcriptional level. **A** Heatmap derived from hierarchical clustering of proteins that were detected as being differentially abundant in mass-spectrometry based whole proteome analysis. *YBX1* was inactivated in MOLM-13 cells using CRISPR-Cas9 mediated knockout (2 different sgRNAs). Lentiviral transductions were performed in quadruplicates and 2×10^6 cells per replicate were FACS-sorted 14 days after transduction for the strongest guide-expressing cells (RFP-high) before cell lysis, trypsin digest and analysis via mass-spectrometry. Proteins significantly up- or down-regulated with both guide RNAs (ANOVA $p < 0.05$) were considered. **B** Gene-set enrichment analysis for Gene-ontology terms on proteins that were significantly down-regulated in the whole proteome analysis. Selected terms are annotated. **C** Gene-set enrichment analysis for Gene-ontology terms on proteins that were significantly up-regulated in the whole proteome analysis. Selected terms are annotated. **D** Volcano-plot of differentially expressed genes in RNAseq at day 7 after knockout of *YBX1* by CRISPR-Cas9 (2 different guide RNAs). Every dot represents a gene with a p value below 0.05. The dots highlighted in blue are genes among those that show a fold change above 1.5. **E** Two of the top Gene-ontology terms that were found to be lost in GSEA of RNAseq data in MOLM-13 cells with knockout of *YBX1*. **F** Depiction of differentially expressed genes from RNAseq in *YBX1*-deficient MOLM-13 cells that were previously identified as RNA-binding targets of *YBX1* [2]. Left: Pie chart showing the proportion of DEGs that are known binding partners of *YBX1* (blue) in relation to genes that have not been shown to bind to *YBX1* (gray). Right: iCLIP-seq IGV-tracks of selected DEGs, that are established binding partners of *YBX1* [2]. **G** RIP-qPCR of *YBX1* from MOLM-13 cells. Left: Western-blot and RNA-tape bands as a quality control of the *YBX1*-enrichment during immunoprecipitation and RNA integrity post IP. Right: results of RIP-qPCR shown as % of enrichment over input validating the binding of EIF4B, EIF3L, EIF3D and EEF2 to *YBX1* in MOLM-13 cells. **H** Analysis of differential splicing in *YBX1*-deficient cells (sgRNA1/sgRNA2) compared to vector control. The computational analysis to call alternative splicing events was performed using the “IsoformSwitchAnalyzeR”-package [33].

to a major extent. To confirm the role of *Ybx1* in leukemia maintenance, we used a conditional knockout mouse model that was recently published by our group [16] and allows for conditional deletion of *Ybx1* after leukemia onset. Here, exon 3 of *Ybx1*, that encodes for a part of the conserved cold shock domain was genetically deleted through activation of *Mx1-Cre*-recombinase (Fig. 2D). Inactivation of *Ybx1* by *plpC* injections after engraftment of leukemic cells in primary recipient mice resulted in a delay of leukemia onset (Fig. 2E, Supplementary Fig. 3E) and prolongation of survival (median survival of MA9-*Ybx1* +/+ 73 days; MA9-*Ybx1* -/- 91.5 days; $p = 0.0121^*$) (Fig. 2F). Of note, the frequency of leukemic stem cells was not significantly decreased in the primary recipient hosts transplanted with *Ybx1* -/- leukemia cells (Fig. 2G) compared to WT controls. This finding indicates a competitive disadvantage rather than exhaustion of AML-LSCs. In secondary recipient hosts, *Ybx1* +/- leukemias showed reduced proliferation (Fig. 2H, Supplementary Fig. 3F), failed to re-establish leukemia in 3/10 recipients (Fig. 2H, I) and significantly prolonged survival compared to *Ybx1* +/+ controls (median survival of MA9-*Ybx1* +/+ 76 days; MA9-*Ybx1* +/- 94 days; $p = 0.0013^{**}$) (Fig. 2I). Histopathological analysis of internal organs of *Ybx* +/+ recipients showed expected infiltration in liver, spleen and lungs (Fig. 2J, left panel). In contrast, in *Ybx1* -/- mice sacrificed without clinical signs of leukemia at day 150, no relevant leukemic organ infiltration could be observed (Fig. 2J, right panel).

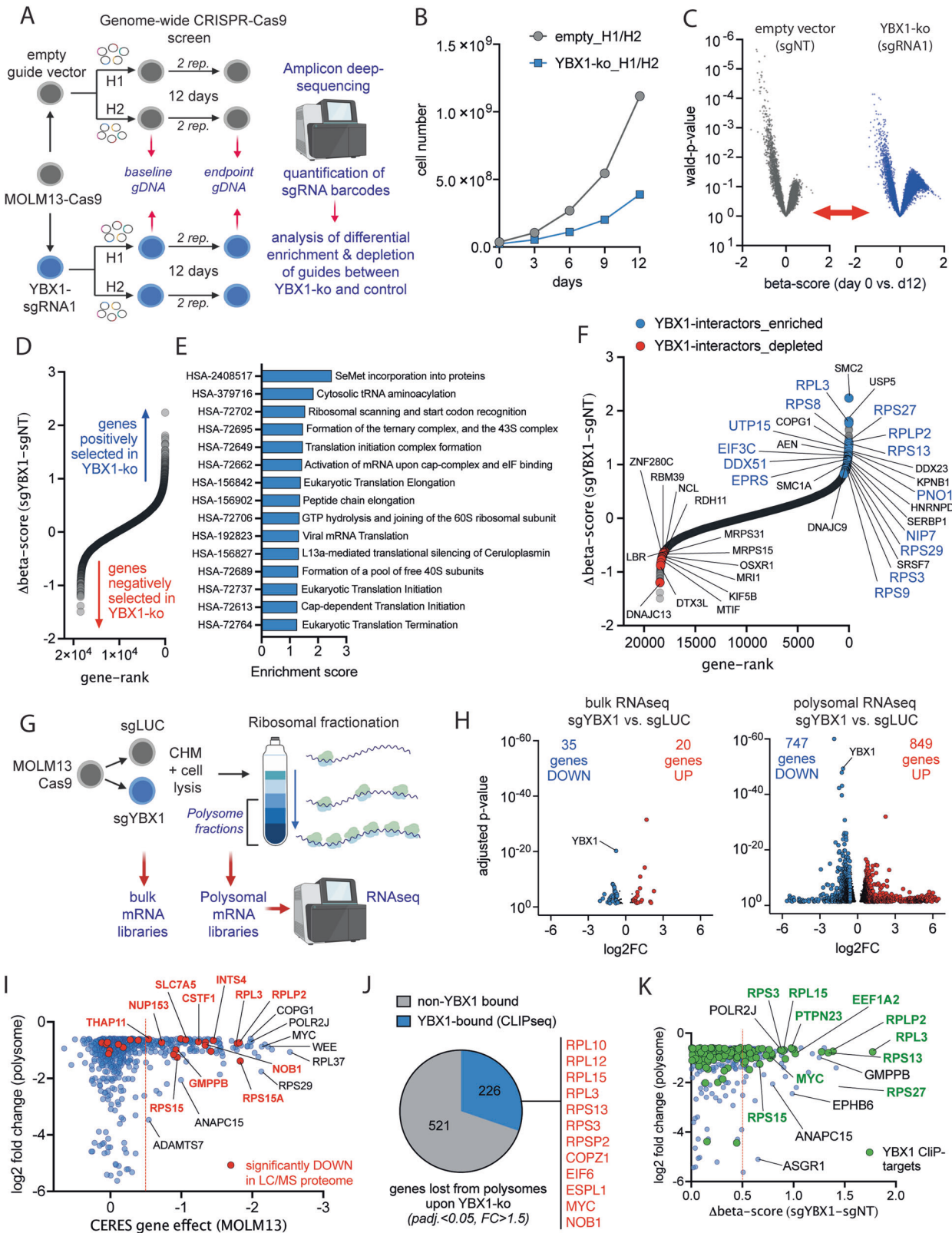
To validate the functional impact of *YBX1* depletion in human AML *in vivo*, we performed a CRISPR-Cas9 mediated knockout as well as shRNA-mediated knockdown of *YBX1* in MOLM13 cells and assessed leukemia dynamics after transplantation in humanized mice (Fig. 2K). Inactivation of *YBX1* delayed disease progression in both models and led to a significantly improved overall survival (CRISPR: median survival of sgLUC: 38 days; sgYBX1 51 days; $p < 0.001^{***}$; RNAi: median survival of shSCR: 30 days; shYBX1: 47 days; $p < 0.001^{***}$) (Fig. 2L, M). To further assess the effects of *YBX1*-depletion in primary AML-specimens, we used BM aspirates from 8 AML patients reflecting a diverse spectrum of molecular- and cytogenetic aberrations. Depletion of *YBX1* led to decreased cell numbers and colony formation *in vitro* (Fig. 3A, B). Together, these findings confirm a functional requirement of *YBX1* for the development and maintenance of murine and human AML *in vitro* and *in vivo*.

YBX1 maintains an oncogenic protein network in AML cells at the post-transcriptional level

For an unbiased assessment of protein networks that are regulated by *YBX1*, we performed whole proteome profiling using mass-spectrometry. Statistical analysis revealed a total of

386 significantly up- and 338 downregulated proteins (Fig. 4A). Gene-ontology analysis showed that *YBX1* inactivation led to reduced abundance of proteins associated with cellular homeostasis of proliferating cells, including RNA- and DNA-metabolism, splicing, chromatin- and protein-homeostasis and cell division (Fig. 4B). Conversely, signatures associated with proteins upregulated in response to *YBX1* deletion were associated with myeloid differentiation and innate immunity, reflecting cell cycle arrest and loss of immaturity (Fig. 4C).

To determine how *YBX1* is regulating the abundance of these proteins, we performed RNA-sequencing 7 days after knockout. Interestingly, the number of differentially expressed genes (DEGs, fold-change > 1.5 , adjusted $p < 0.05$) appeared rather small, with only 6 genes meeting the criteria for significance (Fig. 4D). When considering all genes with an adjusted p value below 0.05 irrespective of the fold-change, 75 genes reached statistical significance (Supplementary Fig. 4A). Gene-set-enrichment analysis (GSEA) revealed signatures associated with translation-initiation (Fig. 4E). The ability of *YBX1* to impact gene expression by binding and stabilizing mRNAs has been previously demonstrated [2, 5]. Therefore, we aimed to assess if the transcripts that are regulated by *YBX1* on the RNA level may be targets of *YBX1*-mRNA binding. Utilizing a previously published iCLIPseq dataset [2] we confirmed that the majority of transcriptionally downregulated genes are substrates of *YBX1*-binding (Fig. 4F). Using RNA-immunoprecipitation followed by quantitative real-time PCR (RIP-qPCR) *YBX1*-binding to 4 of those transcripts encoding for proteins involved in translation initiation and elongation could be validated (Fig. 4G). Our group had previously demonstrated, that *YBX1* is safeguarding splicing in MPN and that deletion of *YBX1* led to a global increase in miss-splicing affecting specific transcripts that are required for disease persistence [16]. Therefore, we assessed for differential splicing and miss-splicing events in our RNAseq dataset. In contrast to our previous findings in *JAK2*-mutated cells, no global alterations in alternative splicing events could be detected after *YBX1* deletion in human AML cells (Fig. 4H). Furthermore, we aimed to assess for DNA-binding of *YBX1* and its postulated potential to act as a transcription factor. In order to determine localization and distribution of *YBX1* over the genome, ChIP-sequencing was performed. Approximately 50% of *YBX1*-specific peaks were localized at regions mapping to genes, with the majority of peaks localized at intronic regions (Supplementary Fig. 4B). However, genes that were differentially expressed following *YBX1* deletion did not show relevant *YBX1* binding. Notably, *YBX1*-DNA binding to a specific gene may be associated with a repressive function, since we detected a trend for *YBX1*-bound genes to show increased expression following *YBX1* deletion (Supplementary Fig. 4C).



YBX1 mediates translation in a transcript-dependent manner

In order to generate a global view on the functional properties of YBX1 in AML, we performed a genome-wide CRISPR-Cas9 screen in MOLM13 cells comparing the genetic vulnerabilities of YBX1-knockout and control cells (Fig. 5A). This functional genomics

approach enabled us to screen in an unbiased manner for cellular networks that are specifically affected by YBX1 loss. As expected, genetic deletion of YBX1 reduced cellular proliferation thus providing the required selective pressure to conduct the screen (Fig. 5B). Following Next-Generation Sequencing, alignment and

Fig. 5 **YBX1 modulates translation in a transcript-dependent manner.** **A** Schematic depicting the experimental procedure to conduct the genome-wide CRISPR-Cas9 screen. MOLM13 cells were transduced YBX1-sgRNA1 or non-targeting control in the p.LKO5-GFP vector system. Cells were subsequently sorted for GFP^{high} expressing cells and expanded to facilitate genome-wide screening. Lentiviral transductions with 2 paired human whole genome-libraries (H1/H2) [25] were performed at low multiplicity of infection (MOI) and cells were selected with puromycin for 3 days. The screen was carried out for 12 days after puromycin selection was completed and the baseline DNA sample was harvested. **B** Growth curve of MOLM-13 cells with a YBX1-KO (blue line) or empty vector control (gray line) during the CRISPR-Cas9 screen for the estimation of the selective pressure applied during the screen. **C** Volcano-plots showing the distribution of genes being enriched (positive beta-scores) or depleted (negative beta-scores) in the genome-wide CRISPR-Cas9 screen in cells harboring a YBX1-KO compared to control. **D** Dot-plot of ranked differential CRISPR-Cas9 screening hits between the YBX1-KO and control condition. The X axis shows the gene-rank, on the Y axis the differential beta scores (Δ beta-scores) are plotted. **E** Top15 REACTOME-terms showing differential enrichment in the CRISPR-Cas9 screening dataset between the YBX1-KO and the control condition. **F** Dot-plot of ranked differential CRISPR-Cas9 screening hits between the YBX1-KO and control condition. Highlighted as red or blue dots are the genes among the top 500 differentially enriched or depleted genes in the YBX1-KO condition, that have previously been identified as binding partners of YBX1 in IP-Mass spec [16]. **G** Schematic depicting the experimental procedure underlying the polysomal RNA profiling in MOLM-13 harboring a YBX1-KO or non-targeting control (sgLUC). MOLM13 cells were transduced with YBX1-sgRNA (or NT-control), selected with puromycin and expanded for 14 days prior to polysomal fractionation followed by RNA-sequencing. **H** Volcano-plot of differentially expressed genes in RNAseq 14 days after knockout of *YBX1* by CRISPR-Cas9 (YBX1-sgRNA1). Left: DEGs in YBX1-KO cells compared to control when sequencing the total cellular mRNA content. Right: DEGs in YBX1-KO cells when sequencing mRNAs that are bound to polysomal chains. **I** Correlation between the magnitude of gene-loss from the polysomal fractions (Y axis: log2FC) upon YBX1-KO and the dependency of the respective genes from the cancer dependency map portal (X axis: CERES gene effect, depmap.org). The red dotted line marks the arbitrary cutoff of genes that are generally considered functional dependencies. Genes that are labeled in red are genes that have been identified as differentially expressed hits in proteome screening. **J** Pie chart showing the proportion of genes that were found to be lost from polysomes and are known binding partners of YBX1 (blue) in relation to genes that have not been shown to bind to YBX1 (gray). **K** Correlation between the magnitude of gene-loss from the polysomal fractions (Y axis: log2FC) upon YBX1-KO and the differential dependency of the respective genes in our CRISPR-Cas9 screen in YBX1-KO vs. control cells. Genes that are labeled in green are genes that have been identified as RNA-targets of YBX1 in iCLIPseq [2].

quantification of each guide-RNA barcode to the respective guide library, *p* values and corresponding beta-scores were calculated for each gene (Fig. 5C). Positive beta scores represent an enrichment of guides targeting a certain gene over time, typically being interpreted as a tumor-suppressor-like function, while negative beta-scores represent selective dependencies resulting in out-competition. The beta score of each gene in the non-targeting (NT) control condition was then subtracted from the respective score in the *YBX1*-knockout condition to generate a Δ beta-score that reflects differential dependency (Fig. 5D). When performing GSEA for REACTOME-terms on the ranked list of Δ beta-scores, the top 15 enriched terms reflected pathways and functions associated with translational initiation and elongation (Fig. 5E). Most genes associated with these terms represent functional dependencies in the NT-control condition, since translation mediators and ribosomal subunits are important housekeeping genes but lose this specific gene-dependency in the *YBX1*-knockout setting (Supplementary Fig. 5A). This finding suggests that *YBX1* exerts its function via these molecules. Of note, among the top differential dependencies, several targets had previously been identified as protein binding partners of *YBX1* [16], highlighting the power of functional genomic screening for the identification of functional molecular networks (Fig. 5F).

In order to assess for the ability of *YBX1* to influence translation of mRNAs, we performed transcriptomic profiling from purified ribosomal fractions (Fig. 5G, Supplementary Fig. 5G, 6). Recruitment of mRNAs to polysomal chains is a major mechanism to increase the output of protein synthesis per mRNA molecule and is therefore considered a crucial determinant of translation efficiency. Consistent with our observations from RNA-sequencing (day 7), the number of DEGs in the bulk RNAseq-sample appeared rather limited (Fig. 5H, left panel). Genes showing reduced expression were predominantly translation initiation factors with *EIF4B* showing the strongest reduction on the protein level (Supplementary Fig. 5B–D). In contrast, we observed a large number of genes being differentially expressed within the polysomal fractions (Fig. 5H, right panel). The number of DEGs detected after polysomal fractionation was about 20-fold increased, compared to bulk mRNA and some genes showed a high magnitude of change. Of note, forced expression of *EIF4B* as the single initiation factor that was consistently and strongly affected by *YBX1*-ko on the total RNA and protein level was not

sufficient to rescue the competitive disadvantage of *YBX1*-inactivation (Supplementary Figure 5E,F), suggesting a direct impact of *YBX1* on polysomal transcript recruitment. Relevant *YBX1*-targets on polysomes were validated on the protein level by Western blot (Supplementary Fig. 5H). To identify candidates that are lost from polysomes and represent relevant functional dependencies, we integrated the magnitude of loss from the polysomes of each significantly down-regulated gene (adjusted *p* < 0.05, fold change >1.5) with the CERES gene effect score from genome-wide CRISPR-Cas9 screens (Broad-Institute, Achilles-portal). 153/747 (20.5%) of genes lost from the polysomes were shown to be functional dependencies identified by CRISPR-Cas9 editing (CERES-score < -0.5) (Fig. 5I). Importantly, a number of those genes, including cell cycle mediators and ribosome subunits showed decreased expression in global proteome analysis (Fig. 5I, highlighted in red). Furthermore, 30% (*n* = 226) of genes that were lost from the polysomes represent RNA-binding targets of *YBX1* in iCLIP-sequencing analyses (Fig. 5J) [2]. Finally, we aimed to understand how genes that are lost from polysomes are associated with *YBX1*-dependent functional pathways. Therefore, we integrated the magnitude of loss from polysomes with the respective functional dependencies (Δ beta-scores; Fig. 5K). Here, relevant targets could be identified that were differentially recruited to polysomes and also enriched following CRISPR-Cas9 editing. Several of these targets, including *MYC*, were also CLIP-targets of *YBX1*. GSEA showed significant loss of the *MYC* target gene signature (Fig. 6A). Using iCLIP-sequencing it had been demonstrated, that *YBX1* is consistently bound to *MYC*-transcripts, establishing *MYC* as a high confidence mRNA-binding partner of *YBX1* (Fig. 6B). Importantly, genetic inactivation of *YBX1* did not affect *MYC*-transcript abundance in bulk RNA-sequencing (Fig. 6C). In contrast, *MYC* mRNA was significantly lost from the polysomal mRNA fraction upon *YBX1*-deletion demonstrating an involvement of *YBX1* in the recruitment of *MYC* transcripts to polysome chains (Fig. 6C). Consequently, using two different sgRNAs that reduce *YBX1* expression to a different extent, gene-dose dependent reduction in *MYC* expression could be confirmed (Fig. 6D). Likewise, *MYC* was a prominent dependency in MOLM13 cells, an effect that was significantly reduced following genetic deletion of *YBX1* (Fig. 6E). The fact that *MYC* was identified as a relevant driver of *YBX1* dependent gene expression and *YBX1* is binding to *MYC* mRNA, indicates its role as a direct downstream

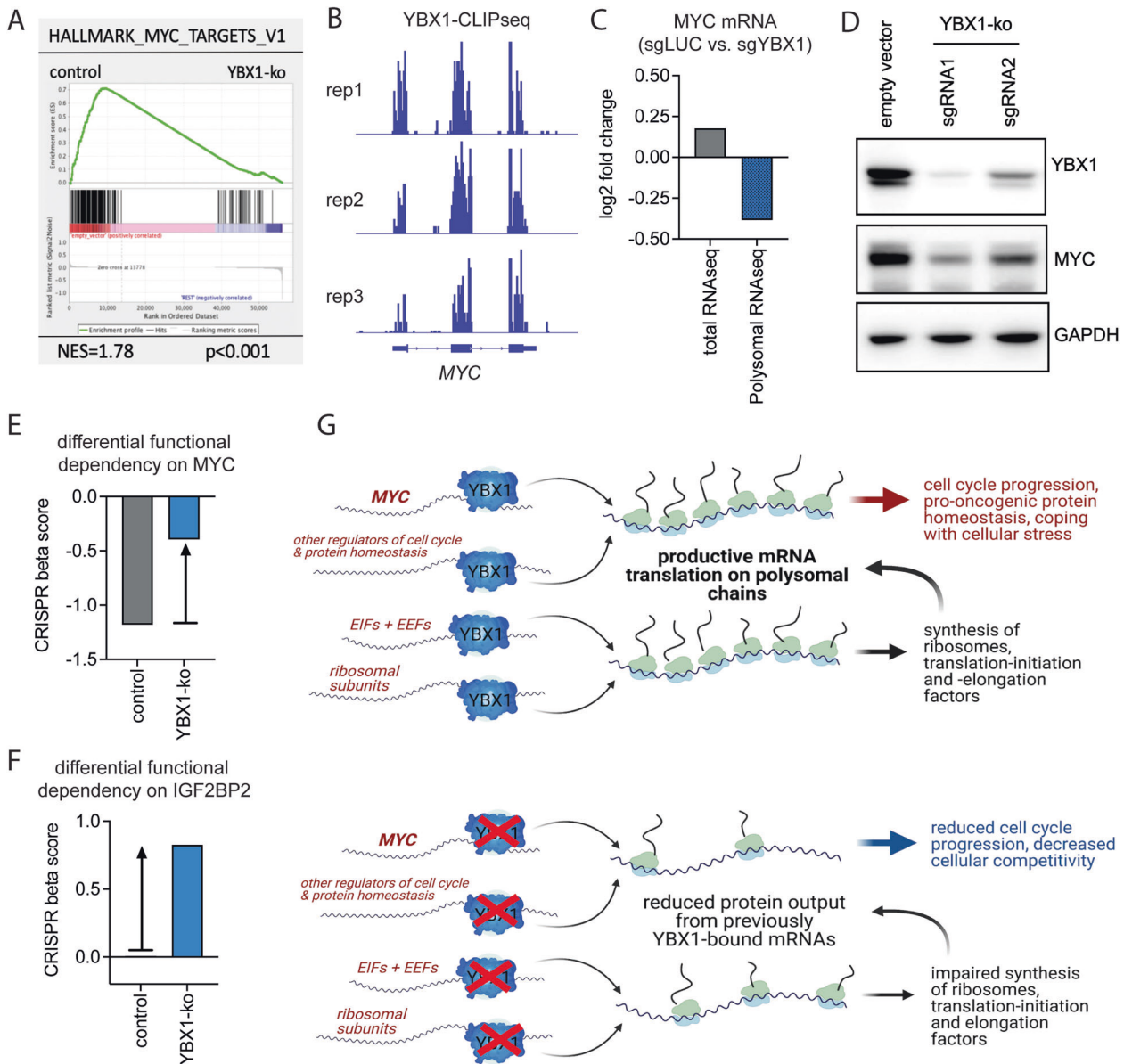


Fig. 6 YBX1 regulates MYC by modulating polysomal recruitment. **A** Geneset enrichment analysis showing a loss of a MYC target gene signature in MOLM-13 cells harboring a knockout of YBX1 (sgRNA1/2, day 7 after lentiviral transduction). **B** Representative iCLIPseq tracks over the MYC gene from 3 independent replicates, showing binding of YBX1 to MYC in breast cancer [2]. **C** Bar graph depicting gene expression changes of MYC in total RNAseq (gray) and polysomal RNAseq, showing that a reduction in MYC-expression appears to be restricted to the polysomal fractions rather than to the unfractionated total RNA. **D** Western Blot showing the protein expression of MYC in relation to the knockout efficiency of YBX1 using 2 different sgRNAs in MOLM-13-Cas9 cells. **E** Bar graph visualizing the beta scores of MYC in control MOLM-13 cells compared to YBX1-KO cells. **F** Bar graph visualizing the beta scores of IGF2BP2 in control MOLM-13 cells compared to YBX1-KO cells. **G** Schematic showing the proposed model of YBX1-action in AML by binding to its target RNAs and mediating their recruitment to polysomal chains to drive productive translational output.

effector. In line with a recent report demonstrating IGF2BP-family proteins as being critical for YBX1-binding to its target mRNAs [5], IGF2BP2-knockout was shown to mediate resistance to YBX1-inactivation (Fig. 6F).

Taken together, we propose, that YBX1 associates with target mRNAs, including MYC, and thereby modulates translational output by recruitment of relevant mRNAs to polysomal chains (Fig. 6G). Protein expression of MYC (among other mediators of cell cycle progression and cellular homeostasis) appears to be stabilized through YBX1 due to its preferential recruitment to polysomes. Furthermore, YBX1 may indirectly influence translation by regulating the availability of ribosomal building blocks and translation mediators (Fig. 6G). Therefore, genetic inactivation of

YBX1 impacts the translational output of transcripts on the protein level and thereby selectively modulates protein abundance of oncogenic drivers and influences proliferative capacity and cell competition in AML.

DISCUSSION

Identification of therapeutic targets that are tractable vulnerabilities and selective dependencies in cancer while being dispensable for normal tissues represent the ideal prerequisite for the development of cancer therapies. Cold shock protein YBX1 has been identified as a pan-cancer dependency in publicly available CRISPR-Cas9-screens and several studies in different tumor entities

[1–5, 15]. Conversely, genetic inactivation of *YBX1* had no deleterious effects on normal hematopoiesis [16], making it a potentially interesting therapeutic target for cancer therapy. Consistent with recent reports [5], we have shown, that *YBX1* is required for development and maintenance of human and murine AML *in vitro* and *in vivo*. Even though the cold shock domain as a common structural component of the CSPs is conserved among the family members, only *YBX1* showed a potent phenotype in leukemia as well as in other cancers.

Mechanistically, we demonstrate that deletion of *YBX1* in AML shows minor impact on mRNA abundance, while having significant effects on the cellular proteome. Moreover, no relevant increase in mis-spliced isoforms could be found in AML cells after deleting *YBX1*, clearly distinguishing the apparent mechanisms in AML from our previous findings in MPN, where *YBX1* was acting as a relevant splicing factor [16]. Using an unbiased multi-omics screening approach, we found that *YBX1* mediates translation of specific transcripts in AML, which is in line with previous reports [1, 4, 15]. To the best of our knowledge this is the first report describing a global CSP regulatory network using functional genomics. Taken together, our data provide strong evidence for *YBX1* acting as a cancer-specific modulator of translation in AML, while leaving total mRNA levels largely unaffected.

A recent report published by Feng and colleagues [5] complements our findings by providing novel insights into how *YBX1* binds its target mRNAs in leukemia cells. *YBX1* appears to bind to methylated (m⁶A) transcripts via IGF2BP-family of proteins to facilitate RNA binding and stabilization. In line with this claim, we find that deletion of *IGF2BP2* confers resistance to *YBX1*-inactivation in our CRISPR-Cas9 screen. Structurally, the cold-shock domain seems to be required for both IGF2BP- and mRNA-binding of *YBX1*. Consistent with our findings, Feng et al. report an impact of *YBX1* on *MYC* expression and show that its expression can rescue the phenotype evoked by inactivation of *YBX1*.

In contrast to our findings the authors assume that regulation of RNA stability represents a major mechanism of *YBX1*-action in AML, similar to findings described in breast cancer [2]. This assessment is based on experimental data showing that shRNA-mediated knockdown of *YBX1* can affect RNA abundance [5]. However, when we conducted parallel RNA-sequencing comparing RNAi- and CRISPR-mediated genetic inactivation of *YBX1* (to rule out a potential bias) we found regulation of RNA-stability exclusively in RNAi- but not CRISPR-treated AML cells. In RNAi-treated samples, we observed high numbers of DEGs, including *MYC*, *BCL2* and *MCL1*, consistent with findings described by Feng and colleagues (Supplementary Fig. 5). Absence of these findings in cells treated with CRISPR-Cas9 technology indicate that an intracellular defense and stress response when using RNAi may influence gene expression changes. Therefore, we assume that the mechanism of action and kinetics of *YBX1* inactivation substantially influence experimental results.

Taken together, our data and the findings presented by Feng et al. establish *YBX1* as a selective genetic vulnerability in leukemia without major restrictions towards specific genetic subtypes.

Of note, a novel small molecule, SU056, was recently reported to directly bind and inhibit *YBX1* [32]. SU056 demonstrated activity in ovarian cancer models *in vitro* and *in vivo* and showed favorable biochemical and pharmacologic properties. The availability of this compound will allow direct targeting of *YBX1* in pre-clinical models and may facilitate translation into early clinical trials in AML.

DATA AVAILABILITY

Raw and processed sequencing data have been made publicly available via the Gene-Expression-Omnibus platform (GEO) under the Accession numbers: GSE175713 (RNAseq), GSE175714 (Polysomal RNAseq), GSE175712 (ChIPseq). The proteomic dataset has been made available via ProteomeXchange under the identifier PXD026329.

REFERENCES

- El-Naggar AM, Veinotte CJ, Cheng H, Grunewald TG, Negri GL, Somasekharan SP, et al. Translational activation of HIF1alpha by YB-1 promotes sarcoma metastasis. *Cancer Cell*. 2015;27:682–97.
- Goodarzi H, Liu X, Nguyen HC, Zhang S, Fish L, Tavazoie SF. Endogenous tRNA-Derived fragments suppress breast cancer progression via YBX1 displacement. *Cell*. 2015;161:790–802.
- Evdokimova V, Tognon C, Ng T, Ruzanov P, Melnyk N, Fink D, et al. Translational activation of snail1 and other developmentally regulated transcription factors by YB-1 promotes an epithelial-mesenchymal transition. *Cancer Cell*. 2009;15:402–15.
- Kwon E, Todorova K, Wang J, Horos R, Lee KK, Neel VA, et al. The RNA-binding protein YBX1 regulates epidermal progenitors at a posttranscriptional level. *Nat Commun*. 2018;9:1734.
- Feng M, Xie X, Han G, Zhang T, Li Y, Li Y, et al. YBX1 is required for maintaining myeloid leukemia cell survival by regulating BCL2 stability in an m6A-dependent manner. *Blood*. 2021;138:71–85.
- Lindquist JA, Mertens PR. Cold shock proteins: from cellular mechanisms to pathophysiology and disease. *Cell Commun Signal*. 2018;16:63.
- Lindquist JA, Brandt S, Bernhardt A, Zhu C, Mertens PR. The role of cold shock domain proteins in inflammatory diseases. *J Mol Med (Berl)*. 2014;92:207–16.
- Raffetseder U, Frye B, Rauen T, Jurchott K, Royer HD, Jansen PL, et al. Splicing factor SRp30c interaction with Y-box protein-1 confers nuclear YB-1 shuttling and alternative splice site selection. *J Biol Chem*. 2003;278:18241–8.
- Stickeler E, Fraser SD, Honig A, Chen AL, Berget SM, Cooper TA. The RNA binding protein YB-1 binds A/C-rich exon enhancers and stimulates splicing of the CD44 alternative exon v4. *EMBO J*. 2001;20:3821–30.
- Wei WJ, Mu SR, Heiner M, Fu X, Cao LJ, Gong XF, et al. YB-1 binds to CAUC motifs and stimulates exon inclusion by enhancing the recruitment of U2AF to weak polypyrimidine tracts. *Nucleic Acids Res*. 2012;40:8622–36.
- Viswanathan SR, Powers JT, Einhorn W, Hoshida Y, Ng TL, Toffanin S, et al. Lin28 promotes transformation and is associated with advanced human malignancies. *Nat Genet*. 2009;41:843–8.
- Horn G, Hofweber R, Kremer W, Kalbitzer HR. Structure and function of bacterial cold shock proteins. *Cell Mol Life Sci*. 2007;64:1457–70.
- Gottesman S. Chilled in translation: adapting to bacterial climate change. *Mol Cell*. 2018;70:193–4.
- Zhang Y, Burkhardt DH, Rouskin S, Li GW, Weissman JS, Gross CA. A stress response that monitors and regulates mRNA structure is central to cold shock adaptation. *Mol Cell*. 2018;70:274–86 e7.
- El-Naggar AM, Somasekharan SP, Wang Y, Cheng H, Negri GL, Pan M, et al. Class I HDAC inhibitors enhance YB-1 acetylation and oxidative stress to block sarcoma metastasis. *EMBO Rep*. 2019;20:e48375.
- Jayavelu AK, Schnoder TM, Perner F, Herzog C, Meiler A, Krishnamoorthy G, et al. Splicing factor YBX1 mediates persistence of JAK2-mutated neoplasms. *Nature*. 2020;588:157–63.
- Lu ZH, Books JT, Ley TJ. YB-1 is important for late-stage embryonic development, optimal cellular stress responses, and the prevention of premature senescence. *Mol Cell Biol*. 2005;25:4625–37.
- Heidel FH, Bullinger L, Feng Z, Wang Z, Neff TA, Stein L, et al. Genetic and pharmacologic inhibition of β -catenin targets imatinib-resistant leukemia stem cells in CML. *Cell Stem Cell*. 2012;10:412–24.
- Mohr J, Dash BP, Schnoeder TM, Wolleschak D, Herzog C, Tubio Santamaria N, et al. The cell fate determinant Scribble is required for maintenance of hematopoietic stem cell function. *Leukemia*. 2018;32:1211–21.
- Kulak NA, Pichler G, Paron I, Nagaraj N, Mann M. Minimal, encapsulated proteomic-sample processing applied to copy-number estimation in eukaryotic cells. *Nat Methods*. 2014;11:319–24.
- Tyanova S, Temu T, Sinitcyn P, Carlson A, Hein MY, Geiger T, et al. The Perseus computational platform for comprehensive analysis of (prote)omics data. *Nat Methods*. 2016;13:731–40.
- Cox J, Hein MY, Luber CA, Paron I, Nagaraj N, Mann M. Accurate proteome-wide label-free quantification by delayed normalization and maximal peptide ratio extraction, termed MaxLFQ. *Mol Cell Proteom*. 2014;13:2513–26.
- Cox J, Mann M. MaxQuant enables high peptide identification rates, individualized p.b.-range mass accuracies and proteome-wide protein quantification. *Nat Biotechnol*. 2008;26:1367–72.
- Wang B, Wang M, Zhang W, Xiao T, Chen CH, Wu A, et al. Integrative analysis of pooled CRISPR genetic screens using MAGeCKFlute. *Nat Protoc*. 2019;14:756–80.
- Chen CH, Xiao T, Xu H, Jiang P, Meyer CA, Li W, et al. Improved design and analysis of CRISPR knockout screens. *Bioinformatics*. 2018;34:4095–101.
- Li W, Xu H, Xiao T, Cong L, Love MI, Zhang F, et al. MAGeCK enables robust identification of essential genes from genome-scale CRISPR/Cas9 knockout screens. *Genome Biol*. 2014;15:554.
- Broad D DepMap 20Q2 Public2020.

28. Krivtsov AV, Twomey D, Feng Z, Stubbs MC, Wang Y, Faber J. et al. Transformation from committed progenitor to leukaemia stem cell initiated by MLL-AF9. *Nature*. 2006;442:818–22.
29. Nusinow DP, Szpyt J, Ghandi M, Rose CM, McDonald ER,3rd, Kalocsay M. et al. Quantitative proteomics of the cancer cell line encyclopedia. *Cell*. 2020;180:387–402.e16.
30. Bagger FO, Kinalis S, Rapin N. BloodSpot: a database of healthy and malignant haematopoiesis updated with purified and single cell mRNA sequencing profiles. *Nucleic Acids Res*. 2018;47:D881–D5.
31. Heideel FH, Bullinger L, Arreba-Tutusaus P, Wang Z, Gaebel J, Hirt C, et al. The cell fate determinant Lgl1 influences HSC fitness and prognosis in AML. *J Exp Med*. 2013;210:15–22.
32. Tailor D, Resendez A, Garcia-Marques FJ, Pandrala M, Going CC, Bermudez A, et al. Y box binding protein 1 inhibition as a targeted therapy for ovarian cancer. *Cell Chem Biol*. 2021;28:1206–1220.e6.
33. Vitting-Seerup K, Sandelin A. IsoformSwitchAnalyzeR: analysis of changes in genome-wide patterns of alternative splicing and its functional consequences. *Bioinformatics*. 2019;35:4469–71.

ACKNOWLEDGEMENTS

The authors thank A. Fenske (Central Animal Facility, OvGU Magdeburg) and M. v.d. Wall (Animal Facility UK Jena) for their support with animal care, R. Hartig (Flow Facility, OvGU Magdeburg), M. Locke and K. Schubert (Flow Facility, FLI, Jena) for their support with cell sorting, L. Rothenburger (Core Service Histology, FLI, Jena) for support with histopathology and S. Frey and C. Kathner-Schaffert for technical assistance. This work was supported by grants of the German Research Council (DFG) (HE6233/4-2 and HE6233/9-1 to F.H.H. and Project-ID 97850925/SFB854, ME-1365/7-2, ME-1365/9-2 to P.R.M.) and the Thuringian state program ProExzellenz (RegenerAging - FSU-I-03/14) of the Thuringian Ministry for Research (to FHH). FP was supported by a grant from the German Research Foundation (DFG, PE 3217/1-1) and a Momentum Fellowship award by the Mark Foundation for Cancer Research. AKJ and MM were supported by the Max Planck Society and by the German Research Foundation (DFG/Gottfried Wilhelm Leibniz Prize). SAA is supported by NIH grants CA176745, CA206963, CA204639 and CA066996.

AUTHOR CONTRIBUTIONS

Conceptualization: FHH; Methodology: FP, FHH; Investigation: FP, YX, NTS, NH, MH, TMS, NM, CM, KT, AKJ, BP, TE; Resources: FP, SAA, AKJ, MM, PRM, AM, FHH; Data Curation: AKJ, SB, NS, NH, CH, AM; Writing-original Draft: FHH; Writing-Review & Editing: FP, PRM, AM, AH, SAA, FHH; Supervision: FHH.

FUNDING

Open Access funding enabled and organized by Projekt DEAL.

COMPETING INTERESTS

SAA has been a consultant and/or shareholder for Epizyme Inc, Vitae/Allergan Pharmaceuticals, Imago Biosciences, Cyteir Therapeutics, C4 Therapeutics, OxStem Oncology, Accent Therapeutics, Neomorph Inc, and Mana Therapeutics. SAA has received research support from Janssen, Novartis, and AstraZeneca. All other authors have no competing financial interests to declare.

ADDITIONAL INFORMATION

Supplementary information The online version contains supplementary material available at <https://doi.org/10.1038/s41375-021-01393-0>.

Correspondence and requests for materials should be addressed to F.P. or F.H.H.

Reprints and permission information is available at <http://www.nature.com/reprints>

Publisher's note Springer Nature remains neutral with regard to jurisdictional claims in published maps and institutional affiliations.



Open Access This article is licensed under a Creative Commons Attribution 4.0 International License, which permits use, sharing, adaptation, distribution and reproduction in any medium or format, as long as you give appropriate credit to the original author(s) and the source, provide a link to the Creative Commons license, and indicate if changes were made. The images or other third party material in this article are included in the article's Creative Commons license, unless indicated otherwise in a credit line to the material. If material is not included in the article's Creative Commons license and your intended use is not permitted by statutory regulation or exceeds the permitted use, you will need to obtain permission directly from the copyright holder. To view a copy of this license, visit <http://creativecommons.org/licenses/by/4.0/>.

© The Author(s) 2021

RESEARCH

Open Access



Immunoproteasome function maintains oncogenic gene expression in KMT2A-complex driven leukemia

Nuria Tubío-Santamaría^{2,1}, Ashok Kumar Jayavelu^{3,4}, Tina M. Schnoeder^{2,1}, Theresa Eifert^{2,1}, Chen-Jen Hsu^{2,1}, Florian Perner¹, Qirui Zhang¹, Daniela V. Wenge⁵, Fynn M. Hansen³, Joanna M. Kirkpatrick⁶, Nidhi Jyotsana⁷, Steven W. Lane⁸, Björn von Eyss², Aniruddha J. Deshpande⁹, Michael W. M. Kühn¹⁰, Juerg Schwaller¹¹, Clemens Cammann¹², Ulrike Seifert¹², Frédéric Ebstein¹³, Elke Krüger¹³, Andreas Hochhaus¹⁴, Michael Heuser¹⁵, Alessandro Ori², Matthias Mann³, Scott A. Armstrong⁵ and Florian H. Heidel^{2,1,15*}

Abstract

Pharmacologic targeting of chromatin-associated protein complexes has shown significant responses in *KMT2A*-rearranged (*KMT2A-r*) acute myeloid leukemia (AML) but resistance frequently develops to single agents. This points to a need for therapeutic combinations that target multiple mechanisms. To enhance our understanding of functional dependencies in *KMT2A-r* AML, we have used a proteomic approach to identify the catalytic immunoproteasome subunit PSMB8 as a specific vulnerability. Genetic and pharmacologic inactivation of *PSMB8* results in impaired proliferation of murine and human leukemic cells while normal hematopoietic cells remain unaffected. Disruption of immunoproteasome function drives an increase in transcription factor BASP1 which in turn represses *KMT2A*-fusion protein target genes. Pharmacologic targeting of PSMB8 improves efficacy of Menin-inhibitors, synergistically reduces leukemia in human xenografts and shows preserved activity against Menin-inhibitor resistance mutations. This identifies and validates a cell-intrinsic mechanism whereby selective disruption of proteostasis results in altered transcription factor abundance and repression of oncogene-specific transcriptional networks. These data demonstrate that the immunoproteasome is a relevant therapeutic target in AML and that targeting the immunoproteasome in combination with Menin-inhibition could be a novel approach for treatment of *KMT2A-r* AML.

*Correspondence:

Florian H. Heidel

heidel.florian@mh-hannover.de

Full list of author information is available at the end of the article



© The Author(s) 2023. **Open Access** This article is licensed under a Creative Commons Attribution 4.0 International License, which permits use, sharing, adaptation, distribution and reproduction in any medium or format, as long as you give appropriate credit to the original author(s) and the source, provide a link to the Creative Commons licence, and indicate if changes were made. The images or other third party material in this article are included in the article's Creative Commons licence, unless indicated otherwise in a credit line to the material. If material is not included in the article's Creative Commons licence and your intended use is not permitted by statutory regulation or exceeds the permitted use, you will need to obtain permission directly from the copyright holder. To view a copy of this licence, visit <http://creativecommons.org/licenses/by/4.0/>. The Creative Commons Public Domain Dedication waiver (<http://creativecommons.org/publicdomain/zero/1.0/>) applies to the data made available in this article, unless otherwise stated in a credit line to the data.

Statement of significance

Resistance to targeted epigenetic therapies evolves as a clinical challenge. Identification and validation of immunoproteasome function for the first time as a cell intrinsic target across KMT2A-complex dependent leukemias creates a unique functional KMT2A-r and NPM1c AML specific dependency, limiting LSC self-renewal. This facilitates therapeutic targeting with preserved efficacy against Menin-inhibitor resistant clones.

Introduction

Leukemias harboring translocations involving chromosome 11q23 are characterized by rearrangements of the Mixed-Lineage-Leukemia-gene (*MLL1*, *KMT2A*) and result in aberrant regulation of the epigenetic landscape [1]. These rearrangements involve several potential translocation partners and confer a particularly poor prognosis [2]. KMT2A-fusion proteins generated by *KMT2A*-rearrangements are part of a large multi-protein complex that is associated with chromatin and drives leukemia through deregulation of transcriptional networks. While direct targeting of the KMT2A-fusions has not been successful, recent reports indicate that indirect targeting of KMT2A-associated protein-chromatin-complexes is feasible and effective [1]. Here, pharmacologic inactivation of KMT2A-complex proteins Dot1L and Menin (*MEN1*) resulted in loss of self-renewal and out-competition of leukemic cells [3–7]. Interestingly, gene expression programs driven by oncogenic KMT2A-fusions are also relevant for other subtypes of leukemia, especially *NPM1*-mutant (*NPM1c*) AML [6, 8]. Translation of these findings into early clinical trials have demonstrated impressive responses but also show development of clinical resistance [9, 10]. These results emphasize the need to prevent therapy resistance and to develop drug combinations that target dysregulated transcriptional networks to improve efficacy. As oncogenes can generate secondary dependencies, targeting of these vulnerabilities may result in synthetic lethality that is oncogene specific. Our studies uncover a selective dependency of *KMT2A*-rearranged (*KMT2A-r*) leukemias on proteostasis and specifically immunoproteasome function. This interferon-induced version of the proteasome with high efficacy for basic proteins is most abundantly expressed in hematopoietic and immune cells [11–14]. Differential expression of immunoproteasome (and proteasome) subunits has been correlated with therapeutic response and sensitivity to proteasome inhibitors in leukemia [15, 16]. Recently, morphologically defined subsets of AML (FABM5) and those with KMT2A rearrangements have been shown to upregulate immunoproteasome genes in a cell-intrinsic manner in order to resist cell stress

[17]. Consistent with this finding, activity of immunoproteasome inhibitors was described in two acute lymphoblastic leukemia (ALL) cell lines harboring KMT2A::AFF1 (*MLL-AF4*) fusions [18].

Our studies uncover a selective dependency of all *KMT2A*-complex dependent (*KMT2A-r* and *NPM1c*) leukemias, across phenotypic subtypes, on immunoproteasome function. We describe immunoproteasome function—as executed by its catalytic subunit PSMB8—as a tractable target that is required to maintain homeostasis of transcription factor abundance. We identify Brain Abundant Membrane Attached Signal Protein 1 (*BASP1*) as a transcriptional repressor of KMT2A- and *NPM1c*-target genes that increases in abundance upon inhibition of immunoproteasome function. Combined targeting of PSMB8 and Menin leads to synergistic anti-proliferative effects, eradicates *KMT2A-r* leukemia in patient-derived xenografts and prevents development of Menin-inhibitor resistance in AML.

Results

Proteostasis is a unique vulnerability in KMT2A-r leukemia

To assess for specific cellular functions required for fusion-oncogene driven AML and to identify oncogenic cellular functions with relevance for *KMT2A-r* leukemia, we performed global proteome profiling on either KMT2A::MLLT3 (*MLL-AF9*; MA9) or AML1-ETO9a (AE) AMLs generated by expression of the fusion oncogenes in murine HSPCs (Lineage⁻ Sca1⁺ c-Kit⁺, LSK). MA9 and AE induce leukemic self-renewal but have different dependency profiles as a result of different mechanisms of transformation. Cells isolated from 4 different primary recipient hosts were analyzed by in-depth quantitative proteomic analysis using high-resolution mass spectrometry (MS) [19]. The analysis determined that 868 proteins (FDR < 0.05) have differential abundance between AE- and MA9 LSC-enriched (GFP⁺ c-Kit⁺) populations. Gene set enrichment analyses (GSEA) revealed a significant enrichment of cellular functions related to proteostasis such as protein degradation and proteasome function (Fig. 1A) in the MA9 AML cells. Expression of proteasome subunits is highly heterogeneous between different cell types [12] and may also be influenced by the underlying oncogene. To investigate the expression of relevant catalytic proteasome subunits, we analyzed transcriptional regulation in published datasets. Here, catalytic subunits of the standard proteasome (PSMB5) and immunoproteasome (IP) PSMB8, PSMB9 and PSMB10 (corresponding to murine LMP7, LMP2 and LMP10) showed significantly higher expression in *KMT2A-r* AML (Fig. 1B) compared to non-*KMT2A-r* -AMLs. Likewise,

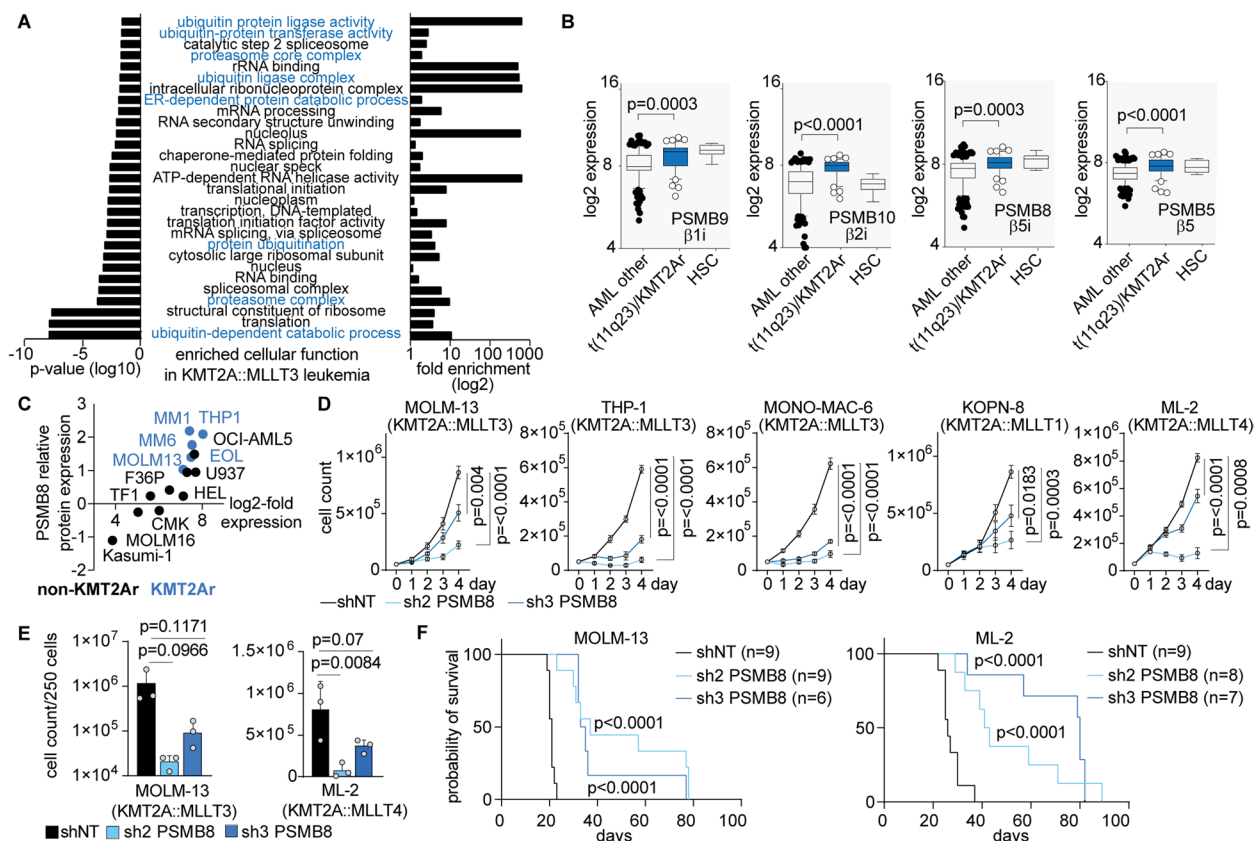


Fig. 1 Immunoproteasome function is a vulnerability in KMT2A-r AML. **A** GO enrichment analysis on MS-based global proteome analysis on murine LSC-enriched GFP⁺ c-Kit⁺ cells of KMT2A::MLLT3-induced leukemia compared to AML1-ETO9a (n=4). Displayed are the Top 30 GO-terms (“molecular function”) sorted by p-value. **B** Gene expression of catalytic proteasome subunits in hematopoietic stem cells (HSC), KMT2A-r leukemia (AML t(11q23)/KMT2A) or non-KMT2A-r AML (AML other) (<https://servers.binf.ku.dk/bloodspot/>). The box-and-whisker plots display the 90/10 percentiles at the whiskers, the 75/25 percentiles at the boxes, and the median. Mann-Whitney U test was performed. **C** Protein abundance of catalytic immunoproteasome subunit PSMB8 in KMT2A-r (blue) or non-KMT2A-r (black) AML cell lines (<https://depmap.org/portal/>). **D** Growth curves depicting cell counting after trypan blue exclusion of MOLM-13, THP-1, MONO-MAC-6, KOPN-8 and ML-2 cells transduced with shRNAs targeting PSMB8 or a non-targeting control (shNT). n=3–5 independent experiments, in triplicate; mean with Standard Error of Mean (SEM); 2-way ANOVA. **E** Cell numbers on day 10; plating of 2.5 × 10² MOLM-13 or ML-2 cells in methylcellulose. n=3 independent experiments; mean with Standard Deviation (SD); paired Student t test. **F** Kaplan–Meier survival curves of NSGS recipient mice transplanted with 1 × 10⁵ MOLM-13 or ML-2 cells, expressing PSMB8-shRNA2 (n=9 for MOLM-13; n=8 for ML-2) and -shRNA3 (n=6; n=7) or non-targeting control (shNT: n=9; n=9); two independent cohorts; Mantel-Cox test

KMT2A-r cells showed increased protein abundance of PSMB8 (Fig. 1C, Supplementary Figure S1A-B). In order to assess the functional relevance of catalytic immunoproteasome components in human AML, we performed a CRISPR-Cas9 based negative selection screen. Here, *KMT2A-r* cells showed a relevant gene-dependency specifically on PSMB8 (Supplementary Figure S1C). To validate these findings, we performed genetic suppression by RNAi with two independent shRNAs against PSMB8 (sh2- and sh3-PSMB8) compared to non-targeting control (shNT) in *KMT2A-r* cell lines. Cell counts assessed on days 1–4 revealed attenuated cell growth in *PSMB8*-suppressed cells (Fig. 1D) with variable degree of apoptosis induction contributing to this phenotype (Supplementary Figure S1D).

Of note, lentiviral re-expression of codon-optimized PSMB8 blunted the response and confirmed specificity of PSMB8-dependencies (Supplementary Figure S1E). Consistently, colony forming capacity of MOLM-13 and ML-2 cells in methylcellulose was impaired following suppression of *PSMB8* (Fig. 1E, Supplementary Figure S1F). To corroborate our findings and to confirm the functional relevance of PSMB8 in vivo, we injected equal numbers of *PSMB8* depleted human AML cells into pre-conditioned (2 Gy, single dose irradiation) immuno-compromised mice (Fig. 1F, Supplementary Figure S1G). Recipients of *PSMB8* deficient cells revealed a delay in disease development and prolonged survival (median survival MOLM-13 for sh2-PSMB8: 37 days and sh3-PSMB8: 34 days; ML-2 for sh2-PSMB8:

42 days and sh3-PSMB8: 80 days) compared to NT-control (median survival MOLM-13: 21 days, $p < 0.0001$ and ML-2: 26 days; $p < 0.0001$).

Recently, pharmacologic targeting of specific immunoproteasome subunits has been reported [20]. The cell permeable and PSMB8 (b5i) specific compound PR-957 (ONX-0914) selectively inhibits murine and human immunoproteasome function. At nanomolar concentrations, the inhibitor does not target other standard- or immunoproteasome subunits [20, 21]. To test whether the observed dependency on PSMB8 is attributed to the loss of protein expression or rather its function, we used PR-957 on an extended panel of *KMT2A-r* versus non-*KMT2A-r* cell lines (Fig. 2A). Pharmacologic inactivation of PSMB8 resulted in dose-dependent reduction of cell growth in *KMT2A-r* cell lines with a rather subtle increase in dead cells (Fig. 2A), while leaving non-*KMT2A-r* cell lines largely unaffected. The only non-*KMT2A-r* cell line responding in a dose-dependent manner was the *NPM1*-mutated OCI-AML3 line with dependency on a shared oncogenic gene expression program. Cell cycle progression was also affected by pharmacologic inactivation of PSMB8 in *KMT2A-r* cell lines (Supplemental Figure S2A-B).

To confirm this selective vulnerability on primary human AML in vivo, we transplanted patient-derived xenografts (PDXs) harboring an *KMT2A::MLL3* (MLL-AF9) or *KMT2A::AFF1* (MLL-AF4) fusion, into NOD.*Cg*^{KitW-41J}*Prkdc*^{scid}*Il2rg*^{tm1Wjl} (NSGW41) animals. The

relative abundance of human AML cells in the recipients' peripheral blood was measured over time by flow cytometry, and PR-957 treatment was initiated once hCD45⁺ AML cells constituted 0.05%–0.9% of peripheral blood (PB) cells (Supplementary Figure S2C). PR-957 treatment was initiated at 3 mg/kg i.v. for 5 consecutive days and continued every 2 weeks with dose escalation to 6 mg/kg. While *KMT2A-r* leukemic cells engrafted at equal numbers, they failed to expand and outcompete murine hematopoiesis when exposed to PR-957, resulting in improved survival of animals receiving *KMT2A::MLL3* ($p = 0.0004$) or *KMT2A::AFF1* ($p < 0.0001$) xenograft cells (Fig. 2B, Supplementary Figure S2D). Flow cytometric analysis of bone marrow (BM) and spleen compartments showed immunophenotypic eradication of leukemic cells in 2/7 animals transplanted with *KMT2A::MLL3* and 6/8 animals transplanted with *KMT2A::AFF1* leukemia after PR-957 treatment (Supplementary Figure S2E). Together, these results suggest a critical requirement of PSMB8 function for proliferation and clonogenicity of human *KMT2A-r* AML cells.

KMT2A-r leukemia initiation depends on PSMB8/LMP7

To assess for the requirement of immunoproteasome function for leukemia initiation, we used a retroviral model of leukemic transformation. Transformation of murine stem and progenitor cells with oncogenic *KMT2A*-fusions results in aberrant self-renewal, unlimited re-plating capacity in methylcellulose and rapid

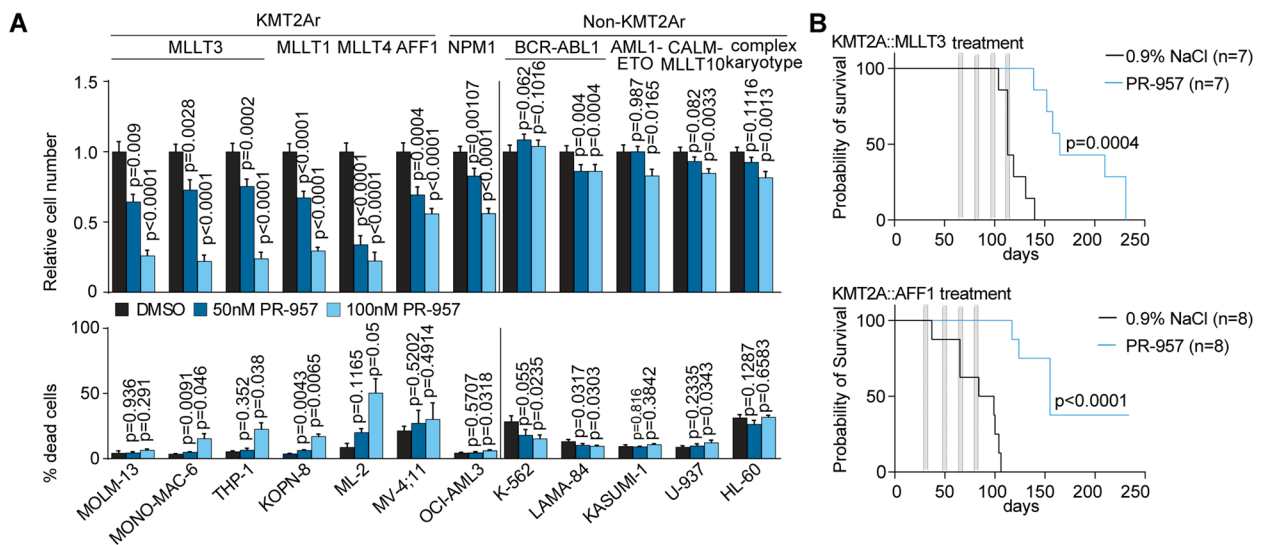


Fig. 2 Pharmacologic targeting of PSMB8 confirms immunoproteasome requirement in *KMT2A-r* AML. **A** Relative cell number and percentage of dead cells (SYTOX[®]Blue⁺) of human leukemic cell lines as indicated after treatment with PR-957 (50 nM, 100 nM) for 96 h or DMSO as diluent control. $n = 4$ independent experiments, in triplicate; mean with SEM; paired Student t test. **B** Kaplan–Meier survival curves for two patient derived xenografts (PDX) using $1-5 \times 10^4$ cells from patient samples containing an *KMT2A::MLL3* (upper) or *KMT2A::AFF1* (lower) translocation injected into NSGW41 recipient mice. Recipients treated in vivo with 3–6 mg/kg PR-957 for 5 days/week or NaCl 0.9% as diluent control on 4 alternate weeks ($n = 7$ per group for *KMT2A::MLL3*; $n = 8$ for *KMT2A::AFF1*). Two independent cohorts; Mantel-Cox test

leukemia onset in vivo following transplantation into irradiated recipient hosts [22, 23]. We used murine Lineage⁻ Sca1⁺ c-Kit⁺ (LSK) progenitor cells derived from a conventional PSMB8 (murine: LMP7) knockout mouse model [24], where exons 1–5, encoding the first 247 amino acids of the protein, are genetically deleted and lead to loss of a functional protein. Cells were isolated from the bone marrow (BM) of the respective donor animals as published before [25, 26]. LMP7^{+/+} or LMP7^{-/-} LSK cells were then transduced with KMT2A-oncogenes (KMT2A::MLLT3 or KMT2A::MLLT1) followed by serial re-plating in methylcellulose to assess colony forming capacity and self-renewal capacity in vitro. While LMP7^{+/+} cells showed unlimited re-plating capacity, LMP7^{-/-} cells failed to sustain colony growth beyond 3 rounds of serial re-plating (Supplementary Figure S3A). To investigate whether immunoproteasome function is required for leukemia development in vivo, LMP7^{+/+} and LMP7^{-/-} LSK cells were transduced with the KMT2A::MLLT3 oncogene (MSCV-KMT2A::MLLT3-GFP) and a total of 7 × 10⁴ transduced (GFP⁺) cells were injected into sublethally (7 Gy) irradiated recipient hosts (Supplementary Figure S3B). When followed over time, recipients of LMP7-deficient cells showed delayed onset of leukocytosis and delayed increase of GFP⁺ cells in the PB (Fig. 3A). This delay in disease development resulted in significantly prolonged

survival (median survival of MA9-LMP7^{+/+}: 63.0 days; MA9-LMP7^{-/-}: 92.5 days; *p* = 0.0387) and 6/12 (50%) of animals failed to establish leukemia within 100 days of observation (Fig. 3B). To validate the requirement of immunoproteasome function for leukemia development, we used a Doxycycline (DOX) inducible mouse model of KMT2A::MLLT1 (i-KMT2A::MLLT1). BM cells of i-KMT2A::MLLT1 (treated for 2 weeks with DOX) were transduced with two independent shRNAs against LMP7 (sh1- and sh4-LMP7) or a non-targeting control (shNT). 1 × 10⁶ transduced cells were transplanted into CD45.1 recipient mice (kept in food supplement with 0.545 g/kg of DOX) (Supplementary Figure S3C). Recipients of LMP7-deficient cells had a delay in disease development and significant prolonged survival (median survival of sh1-LMP7 i-KMT2A::MLLT1: not reached, *p* = 0.1108; sh4-LMP7 i-KMT2A::MLLT1: 123 days, *p* = 0.0029; shNT i-KMT2A::MLLT1: 71 days) (Supplementary Figure S3D-E). These findings indicate a requirement of LMP7 for development and propagation of KMT2A-r induced leukemia in vitro and in vivo. To assess for the role of LMP7 in non-leukemic, normal HSPC function, we monitored peripheral blood (PB) counts and distribution of immune cell subsets of LMP7 knockout mice compared to wildtype littermate controls over 4 months but failed to detect abnormalities in white blood count, hemoglobin or platelet count (Fig. 3C). Consistently,

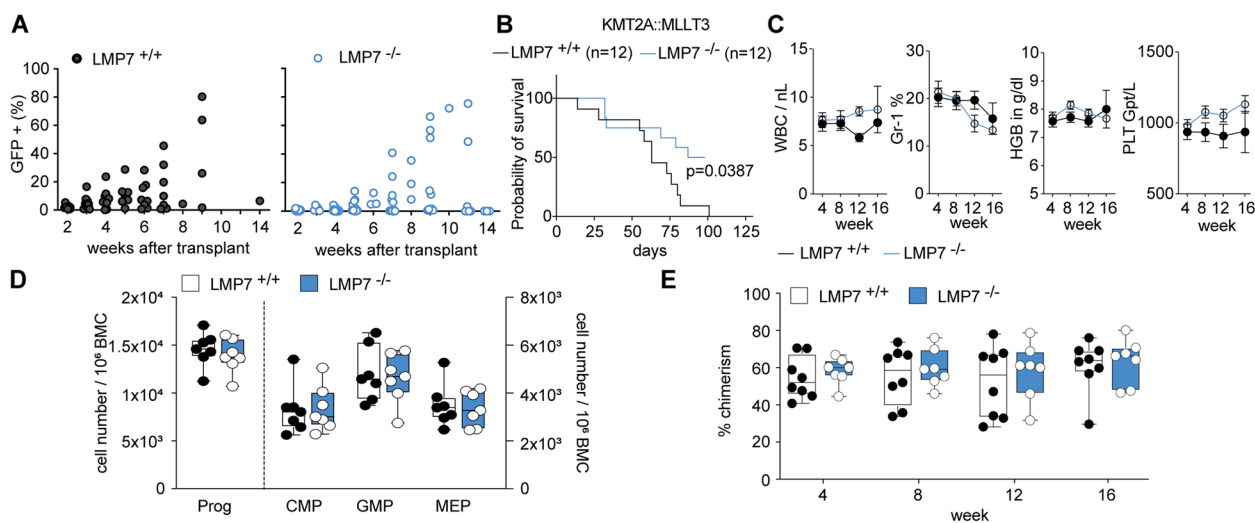


Fig. 3 LMP7/PSMB8 is essential for KMT2A-r AML development but dispensable for normal hematopoiesis. **A** Dot plots depicting % of GFP⁺ cells in peripheral blood of recipient mice transplanted with 7 × 10⁴ KMT2A::MLLT3 transformed LSKs from LMP7^{+/+} (*n* = 12) or LMP7^{-/-} (*n* = 12) mice over 14 weeks. Two independent cohorts. **B** Kaplan–Meier survival curves of recipient mice (KMT2A::MLLT3 transformed LSKs from LMP7^{+/+} (*n* = 12) or LMP7^{-/-} (*n* = 12) mice). Two independent cohorts; Mantel–Cox test. **C** White blood counts (WBC), hemoglobin (HGB) and platelets (PLT) in the peripheral blood of LMP7^{-/-} (*n* = 7) for 16 weeks of steady-state hematopoiesis, compared with LMP7^{+/+} controls (*n* = 7). **D** Immunophenotypic quantification of progenitor cell abundance (Prog: Lin⁻ Sca1⁺ c-Kit⁺), common myeloid progenitors (CMP: Lin⁻ Sca1⁻ c-Kit⁺ CD34⁺ Fcgr⁻), granulocyte–macrophage progenitors (GMP: Lin⁻ Sca1⁻ c-Kit⁺ CD34⁺ Fcgr⁺) and megakaryocyte–erythroid progenitors (MEP: Lin⁻ Sca1⁻ c-Kit⁺ CD34⁻ Fcgr⁺) in the bone marrow. **E** Peripheral blood chimerism over 16 weeks; competitive repopulation assay using BM cells from LMP7^{-/-} (*n* = 8) or LMP7^{+/+} (*n* = 8) donors

immunophenotypic analysis of BM at 4 months of age revealed no significant quantitative changes in all HSPC subsets (Fig. 3D). To dissect the functional influence of LMP7 deletion on long-term (LT)-HSC versus more differentiated progenitors (short-term (ST)-HSC/multipotent progenitors—MPP), we investigated short-term colony formation in vivo. Colony forming unit spleen cells repopulate irradiated recipients for 1–3 weeks but fail long-term engraftment [27]. Injection of 100 sorted LMP7^{-/-} LSK cells resulted in pronounced spleen colony formation (Supplementary Figure S3F), which was comparable to the colony numbers generated by LMP7^{+/+} littermate controls. These findings indicate that LMP7 is dispensable for short-term repopulation and multipotent progenitor function. To test for the function of LMP7 deficient HSC, we performed competitive transplantation into irradiated recipient hosts (Supplementary Figure S3G). When LMP7^{-/-} cells or LMP7^{+/+} controls of 6–8 week old donor mice were transplanted into primary recipient hosts in a competitive manner at a ratio of 1:1 we found no loss of function in LMP7 deficient cells as they competed against wildtype controls as indicated by stable PB chimerism over 16 weeks (Fig. 3E). Taken together, inactivation of LMP7 does not impair normal HSCP function in vivo.

Pharmacologic inhibition of PSMB8/LMP7 impairs murine KMT2A-r leukemia stem cell (LSC) self-renewal

Gene expression programs induced by KMT2A-fusion proteins confer stemness and aberrant self-renewal capacity to committed progenitors [1]. To study the effects of *PSMB8* (murine: LMP7) inactivation on LSC self-renewal, we used established models of murine, KMT2A-fusion driven leukemia. Exposure of KMT2A::MLLT3/KRAS or KMT2A::MLLT4 induced

murine leukemic cells to PR-957 at nanomolar concentrations resulted in profound dose dependent reduction of clonogenic potential, which was not detectable when treating non-KMT2A fusion oncogenes such as AML1-ETO/KRAS (Fig. 4A). Moreover, treatment with PR-957 resulted in reduction of colony size and changes in colony shape, specifically in *KMT2A-r* leukemia (Supplementary Figure S4A).

As leukemic cells are highly heterogeneous, we also aimed to assess the LSC pool that frequently persists after treatment and is a source of clinical relapse. Murine HSPCs were transduced with KMT2A::MLLT3 (MA9) to induce leukemia in sublethally irradiated primary recipient mice (Supplementary Figure S4B). Primary recipients were treated with 10 mg/kg PR-957 i.v. QD for 3 weeks (5 days/week) and PB and BM were investigated 3 days after treatment discontinuation. Leukemic cells in the PB, spleen, lung and liver of PR-957 treated animals were reduced compared to diluent treated controls (Fig. 4B–C; Supplementary Figure S4C). Consistently, we found significant decrease in the abundance of leukemic cells in the BM of PR-957 treated mice (42.9% versus 69.8%; $p < 0.0001$; Fig. 4D). Next, we assessed the frequency of L-GMPs (Lin⁻ Sca1⁻ c-Kit⁺ CD34⁺ FcgR⁺) by flow cytometry, which have been described as the functionally relevant LSC population in MA9 driven leukemia [29]. Of note, PR-957 treated animals showed significant reduction of L-GMPs compared to diluent treated controls (2.25 ± 0.8% and 3.57 ± 0.52%, respectively, $p = 0.032$; Fig. 4E). Injection of 1 × 10⁶ total BM cells into sublethally irradiated secondary recipient mice resulted in decreased numbers of leukemic cells in the peripheral blood two weeks after transplantation (17.2 vs. 1.6 Gpt/L GFP⁺ WBC; $p < 0.0001$; Fig. 4F) and significant delay in disease development for recipients of

(See figure on next page.)

Fig. 4 Pharmacologic inhibition of LMP7/PSMB8 impairs KMT2A-r leukemia stem cell function without affecting normal hematopoietic stem cells. **A** Serial re-plating to assess for colony formation in methylcellulose using murine LSK cells transformed with KMT2A::MLLT3/KRAS, KMT2A::MLLT4 or AML1-ETO/KRAS. Cells were treated with DMSO as diluent control or PR-957 (100 nM, 200 nM). $n = 3–4$ independent experiments; mean with SD; paired Student t test. **B–D** 3 × 10⁵ KMT2A::MLLT3 murine BM cells transplanted into sublethally irradiated recipient mice. Mice were treated for 5 days/week for 3 cycles with 10 mg/kg PR-957 ($n = 10$) or NaCl 0.9% as diluent control ($n = 11$). Relative abundance of leukemic cells after 3 weeks of treatment in primary recipient mice in **(B)** peripheral blood, **(C)** spleen and **(D)** bone marrow. Two independent cohorts; mean with SD; Mann–Whitney U test. **E** Relative abundance of L-GMP (Lin-Kit + Sca1-CD34 + FcgR + GFP +) in diluent or PR-957 treated mice. Two independent cohorts; mean with SD; Mann–Whitney U test. **F** 2 × 10⁶ whole bone marrow cells from the PR-957 or NaCl in vivo treated KMT2A::MLLT3 mice were transplanted into secondary recipients ($n = 14$ recipients of PR-957 treated mice; $n = 15$ recipients of NaCl treated mice). Abundance of leukemic cells in the peripheral blood, 2 weeks after transplantation. Two independent cohorts; Mann–Whitney U test. **G** Survival of secondary recipient mice. Mantel–Cox test. **H–I** Limiting dilution (LD) assay using murine KMT2A::MLLT3 BM cells treated for 48 h with diluent or 200 nM PR-957. **H** Reduction of leukemia initiating cells and **(I)** Cell dose, animal numbers, LSC-frequency and confidence intervals (CI) following diluent or PR-957 exposure. $n = 4$ mice per dilution and treatment, analysis performed using ELDA (Extreme Limiting Dilution Assay) software [28]. **J** Schematic depicting competitive repopulation assay to investigate effects of PR-957 treatment on normal HSPCs. **K–M** Relative abundance of hematopoietic cells in CD45.1 mice after 3 weeks of treatment with 10 mg/kg PR-957 ($n = 6$) or NaCl 0.9% ($n = 6$), specifically in **(K)** Peripheral blood, **(L–M)** Bone marrow. **L** HSC abundance (HSC: Lin⁻ Sca1⁺ cKit⁺ CD48⁻ CD150⁺); **(M)** Progenitor cell abundance; **(N)** Peripheral blood chimerism of recipient animals using BM cells from in vivo treated mice with PR-957 or diluent control. **O–Q** Abundance of hematopoietic cells in the BM of recipient mice at week 16. **O** mature cell compartments; **(P)** progenitor cells; **(Q)** HSCs (HSC: Lin⁻ Sca1⁺ cKit⁺ CD34⁻)

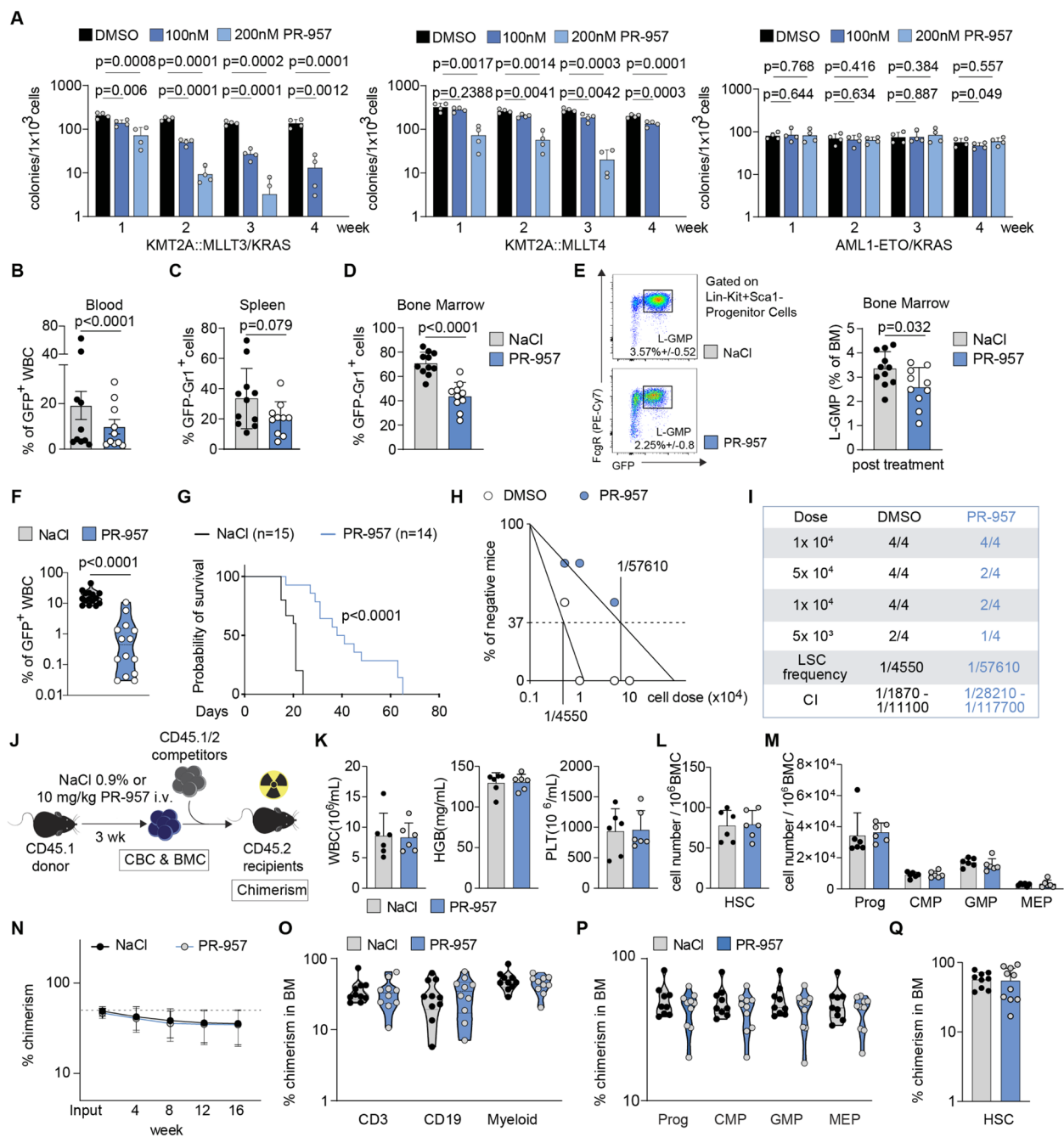


Fig. 4 (See legend on previous page.)

PR-957 treated cells (median survival 39.5 vs. 21 days; $p < 0.0001$; Fig. 4G). To determine the functional abundance of LSCs and the leukemia initiating potential, we performed limiting dilution assays by injecting sublethally irradiated recipient mice (7 Gy) with limiting numbers (1×10^5 , 5×10^4 , 1×10^4 , 5×10^3) of GFP⁺ leukemic BM cells. PR-957 treated cells showed profound, more than log-fold reduction in LSC frequency compared to

diluent treated controls ($1/57610$, CI $1/1870-1/11100$ versus $1/4550$, CI $1/28210-1/117700$; Fig. 4H-I). Taken together, pharmacologic immunoproteasome inhibition using the specific PSMB8/LMP7 inhibitor PR-957 attenuated the leukemia initiating potential of *KMT2A-r* AML cells in vivo. This effect was even more pronounced in the LSC (L-GMP) population, indicating reduced fitness and decreased LSC numbers as potential causes. To examine

for potential toxicity to normal hematopoietic stem- and progenitor cells (HSPCs), 6–8 week old C57BL/6 animals were treated with 10 mg/kg PR-957 i.v. QD for 3 weeks (5 days/week) (Fig. 4J). In contrast to our findings in *KMT2A-r* leukemic cells PSMB8/LMP7 function appeared to be dispensable for steady state hematopoiesis regarding PB counts (Fig. 4K) and immunophenotypic abundance of BM HSPCs (Fig. 4L–M). Likewise, normal murine HSC function was not impaired during competitive transplantation (Fig. 4J) as indicated by PB chimerism of primary recipient hosts (Fig. 4N) and abundance of BM HSPCs at week 16 (Fig. 4O–Q, Supplementary Figure S4D).

PSMB8 inhibition increases BASP1 which represses *KMT2A*-fusion target gene expression

To determine to what extent the inhibition of PSMB8 modulates oncogenic gene expression programs, we sought to investigate transcriptional regulation in *KMT2A-r* cells. Global transcriptome analysis by RNA-sequencing performed in MOLM-13 cells revealed differential regulation of 973 down- and 991 upregulated genes upon PR-957 treatment (Supplementary Figure S5A). Among the significantly induced genes we found compensatory up-regulation of proteasome subunits (Fig. 5A). Unexpectedly, down-regulated genes included several bona fide *KMT2A*-target genes such as *HOX*-genes (*HOXA*-cluster, *PBX3*, *MEIS1*, *VENTX*), cell cycle regulators (*CDK6*, *CDK9*), transcription factors (*MEF2C*, *RUNX2*) and signaling molecules (*FLT3*, *AXL*, *GNAS*), among others (Fig. 5A). Consistently, genes deregulated by epigenetic inhibitors of the *KMT2A*-complex (Dot1L- or Menin-inhibitors) were enriched in the gene sets regulated by pharmacologic PSMB8 inhibition (Fig. 5B). To assess for changes on chromatin as consequence of PSMB8 inhibition, we performed Cut&Tag-sequencing for *KMT2A*-related histone tail modifications and

ATAC-sequencing to assess for early changes in chromatin conformation (Supplementary Figure S5B–E).

Of note, neither changes in *KMT2A*-complex associated histone tail modifications nor changes in chromatin accessibility could be detected. These findings suggest an inhibitory effect of PSMB8 inactivation on expression of *KMT2A*-target genes that is not mediated by modulation of epigenetic complexes, including *KMT2A*-function. To identify functional effectors of PSMB8 activity, we applied a genome-wide CRISPR/Cas9 screen in the human *KMT2A-r* cell line MOLM-13. This cell line was selected for its sensitivity to PR-957 (Fig. 2A) and ability to be efficiently transduced among the *KMT2A-r* cell lines evaluated above. For the screen, MOLM-13 cells were infected with the human Liu lentiviral library, containing 92,817 single guide RNAs targeting against 18436 genes and treated with PR-957 (or DMSO, as control) for 12 days (Supplementary Figure S5F–G). Use of the MAGeCK-MLE and FluteMLE algorithms [30] offered the opportunity to specifically identify synthetic lethal hits and resistance mediators, as well as genes that are potential downstream effectors of the drug target. While deletion of molecules functionally related to the ubiquitin–proteasome system (UPS) could be identified as sensitizers to PR-957 treatment, several transcriptional regulators, such as CEBPD, RPAP3, POLR3B, AF4, BASP1 and TP53 (Fig. 5C) scored as resistance mediators. To assess whether disrupting homeostasis of transcriptional regulators by immunoproteasome inhibition could account for the observed repression of *KMT2A*-target genes, we performed in-depth proteome analysis on MOLM-13 cells with or without exposure to PR-957 (Fig. 5D). Overall, 1329 proteins (500 up and 829 down) showed differential abundance in response to PR-957 treatment. Consistent with transcriptomic changes, compensatory upregulation of UPS-related proteins was detectable. Among the transcriptional regulators

(See figure on next page.)

Fig. 5 Enrichment of BASP1 by PSMB8 inhibition inhibits *KMT2A* target gene expression. **A** Heatmap of differentially expressed genes in MOLM-13 cells: 100 nM PR-957 vs. DMSO (72 h). Upregulated (red; fold-change (FC) > 2, $p < 0.05$) and downregulated (blue; FC < -2, $p < 0.05$) genes. **B** Gene Set Enrichment Analysis (GSEA) of PR-957 treated MOLM-13 cells compared to EPZ5676- or VTP-50469-treatment; NES (normalized enrichment score). **C** Hockey-stick-plot of ranked genes found to be differentially enriched/depleted in genome wide CRISPR/Cas9 screening in MOLM-13 cells. **D** Heatmap depicting unsupervised hierarchical clustering of differentially abundant proteins detected by mass-spectrometry. 100 nM PR-957 vs. DMSO, 72 h, MOLM-13. Upregulated (red; FC > 2, $p < 0.05$) and downregulated (blue; FC < -2, $p < 0.05$) proteins. **E** Correlation between the magnitude of differential protein abundance ($-\log_{10}$ Padj) as determined by proteome analysis and the functional dependencies obtained by CRISPR/Cas9 screening (Δ beta-scores PR-957 vs. DMSO) in MOLM-13 cells. **F** Western Blotting showing expression of BASP1 in nuclear (N) and cytoplasmic (C) fractions of MOLM-13, KOPN-8, ML-2 and MV4;11 cells. PR-957 (100 nM, 200 nM) vs. DMSO, 72 h. **G** Heatmaps displaying IgG and BASP1 Cut&Run signal mapping to a 2-kb window around the TSS (Transcription Start Site). 100 nM PR-957 vs. DMSO, 48 h, MOLM-13 cells; 1 (out of $n = 3$) representative replicate. **H** Stacked bar plot depicting genomic distribution of BASP1 Cut&Run peaks. MOLM-13 cells; $n = 3$ independent replicates. **I** Dot-plot of ranked BASP1-bound TSS according to their abundance; 1 representative replicate. **J** Growth curves of *KMT2A-r* cells (MOLM-13, MV-4;11, ML-2, KOPN-8) transduced with pLEX-BASP1-HA-Tag (BASP1-HA) or pLEX-HA-Tag (EV-HA). $n = 4$ independent experiments, in triplicate; mean with SEM; 2-way ANOVA. **K** Survival curves of NXG recipient mice transplanted with 1×10^5 MOLM-13 or MV-4;11 cells expressing pLEX-BASP1 (BASP1) or pLEX-EV (EV) ($n = 10$ per construct and cell line). Two independent cohorts; Mantel-Cox test

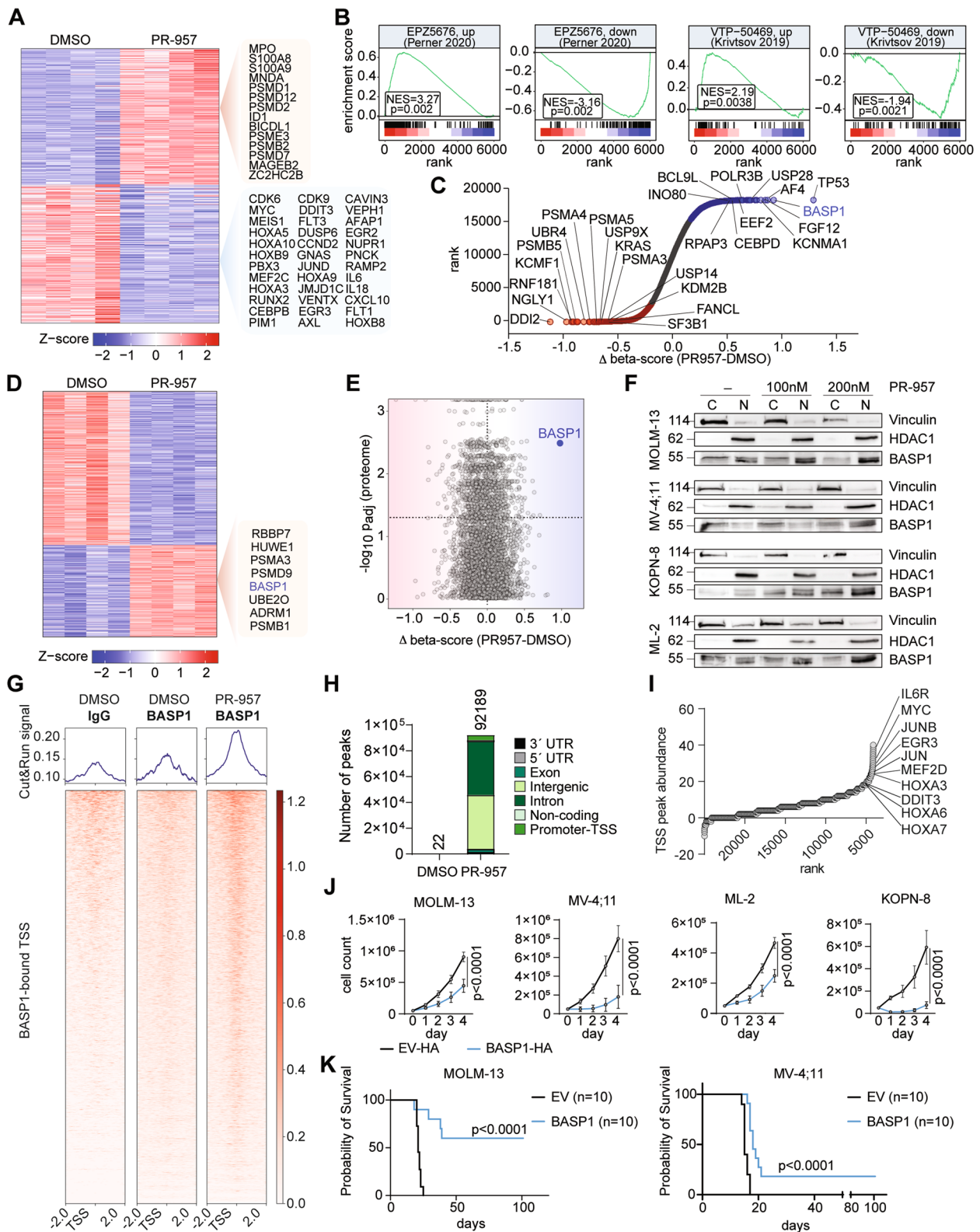


Fig. 5 (See legend on previous page.)

classified as resistance mediators by functional CRISPR/Cas9 screening, protein abundance of BASP1 was significantly increased in global proteome analysis (Figs. 5D-E). As also seen by Western Blotting, abundance of BASP1 protein levels increased in a dose dependent manner and specifically in the nuclear fraction of PR-957 (Fig. 5F) as well as Bortezomib (BTZ) and Carfilzomib (CFZ) (Supplementary Figure S5H-I) treated MOLM-13, MV-4;11, KOPN-8 and ML-2 cells. Therefore, we sought to confirm DNA-binding of BASP1 by Cut&Run sequencing. Here, we found that pharmacologic inhibition of PSMB8 by PR-957 treatment increased BASP1 binding, including at active transcriptional start sites (TSS) (Fig. 5G-H). Notably, specifically TSS of KMT2A-target genes appeared occupied by BASP1 upon PSMB8-inhibition (Figs. 5I, Supplementary Figure S5J). To assess for the functional consequences of increased BASP1 expression and to confirm its repressive role, we conducted (lentiviral and CRISPRa-induced) overexpression studies in KMT2A-r cell lines. Increased abundance of BASP1 attenuated growth of KMT2A-r AML cells in vitro and reduced leukemia formation in humanized recipient mice (Fig. 5J-K, Supplementary Figure S6). Together, these findings indicate a functional role of BASP1 as a transcriptional repressor of KMT2A-target genes that may be independent from the epigenetic functions of the oncogenic KMT2A-fusion protein.

Combined targeting of oncogenic gene expression through pharmacologic inactivation of Menin and PSMB8

These results prompted us to assess for enhanced efficacy when combining inhibitors of the KMT2A-complex with immunoproteasome inhibitors. Combinatorial use of Menin-inhibitor MI-503 (1 μ M, 72 h) with immunoproteasome inhibitor PR-957 at nanomolar concentrations (100 nM, 72 h) resulted in enhanced repression of the KMT2A-related gene expression program (Fig. 6A).

Consistently, abundance of relevant transcriptional effectors such as MEF2C, FLT3 or PBX3 (and partially c-MYC) was more efficiently reduced by combined targeting compared to monotherapy (Fig. 6B, Supplementary Figure S7A). Combinatorial treatment efficiently attenuated proliferative capacity of KMT2A-r or NPM1-mutated cell lines in vitro (Fig. 6C) without induction of apoptosis (Supplementary Figure S7B). These findings could be recapitulated when using other specific (M3258; Fig. 6D) or non-specific (Bortezomib, BTZ; Carfilzomib, CFZ; Figs. 6E-F) inhibitors of the immunoproteasome or second-generation clinical grade Menin-inhibitors (Revenenib (SNDX-5613); Fig. 6G), confirming a class-effect.

Combinatorial treatment of MI-503 (2.5 μ M, 96 h) with PR-957 (100 nM, 48 h) in MOLM-13 cells resulted in prolonged survival of recipient NXG mice as compared to MI-503 and PR-957 monotherapy (MI-503: 30 days; PR-957: 20 vs. comb: not reached; $p < 0.0001$) and reduced disease penetrance by 83.3% (Fig. 6H). We sought to validate these findings by in vivo treatment of patient derived xenograft (PDX) models and assess for quantitative reduction of leukemia initiating cells by limiting dilution assays (Fig. 6I). Assessment of leukemic bone marrow infiltration in treated primary recipients revealed pronounced reduction of human CD45⁺ leukemic cells (MI-503: median 57%, Combination: 100%) compared to diluent control (DMSO/NaCl0.9%; Fig. 6J). When injected into secondary recipient mice at limiting numbers (2×10^6 , 2×10^5 , 2×10^4) recipients of MI-503 + PR957 treated bone marrow cells showed profound reduction in LSC frequency compared to MI-503 or diluent treated controls (0 versus 1/553030, CI 1/170979–1/1788772; 0 versus 1/2154382, CI 1/49956–1/477049, respectively; Fig. 6K-L). Moreover, combinatorial treatment prolonged survival (median survival not reached) compared to MI-503 (median survival 2×10^6 : 114.5 days; for 2×10^5 : not reached, 2×10^4 : not

(See figure on next page.)

Fig. 6 Synergistic targeting of oncogenic gene expression through pharmacologic inactivation of Menin and PSMB8. **A** Heatmap of differentially expressed genes in MOLM-13 cells. 1 μ M MI-503 treatment, 1 μ M MI-503 and 100 nM PR-957 treatment or DMSO for 72 h. Upregulated (red; FC > 2, $p < 0.05$) and downregulated (blue; FC < -2, $p < 0.05$) genes. **B** Representative plots (out of $n = 3-4$) showing protein expression of c-Myc, MEF2C, FLT3 and PBX3 upon treatment with DMSO, 100 nM PR-957, 1 μ M MI-503 or 1 μ M MI-503 + 100 nM PR-957 for 72 h in MOLM-13 cells. **C** Bar plots depicting cell counts in MOLM-13, MV-4;11, ML-2, KOPN-8 and OCI-AML3 cells after treatment with 20 nM PR-957, 200 nM MI-503, a combination of both or DMSO for 6 days. $n = 4-5$ independent experiments; mean with SD; paired Student t test. **D-G** Bar plots representing proliferation of MOLM-13 cells after treatment with indicated monotherapies, combinations or DMSO for 6 days. $n = 3$ independent experiments; mean with SD; paired Student t test. **H** Xenograft of human MOLM-13 cells: Survival curve of NXG recipient mice transplanted with 1×10^5 MOLM-13 cells pre-treated ex vivo with either 100 nM PR-957 ($n = 5$) for 48 h, 2.5 μ M MI-503 ($n = 15$) for 96 h or a combination of 2.5 μ M MI-503 for 96 h and 100 nM PR-957 for 48 h ($n = 14$). Four independent cohorts; Mantel-Cox test. **I** Patient derived xenograft (PDX): Schematic representation of the in vivo MI-503 (50 mg/kg, $\times 7$), MI-503 + PR-957 (6 mg/kg, i.v., 5 days/week for 3 weeks) or 30% DMSO-70% NaCl0.9% ($\times 7$) treatment of NXG mice ($n = 5$ /treatment) injected with 2×10^4 KMT2A::AFF1 PDX-cells. BM cells were subsequently transplanted at limiting numbers (2×10^6 , 2×10^5 , 2×10^4) into NXG recipient mice. **J** Immunophenotyping of human CD45⁺ (hCD45⁺) cells in the BM of NXG mice after in vivo treatment with MI-503, MI-503 + PR-957 or DMSO/NaCl0.9%. $n = 5$ mice per treatment; Mann-Whitney U test. **K-L** Limiting dilution (LD) assay. **K** Reduction of leukemia initiating cells. **L** Cell dose, animal numbers, LSC-frequency and CI following diluent, MI-503 or PR-957 + MI-503 exposure. $n = 4$ per dilution and treatment; analysis was performed using ELDA software [28]

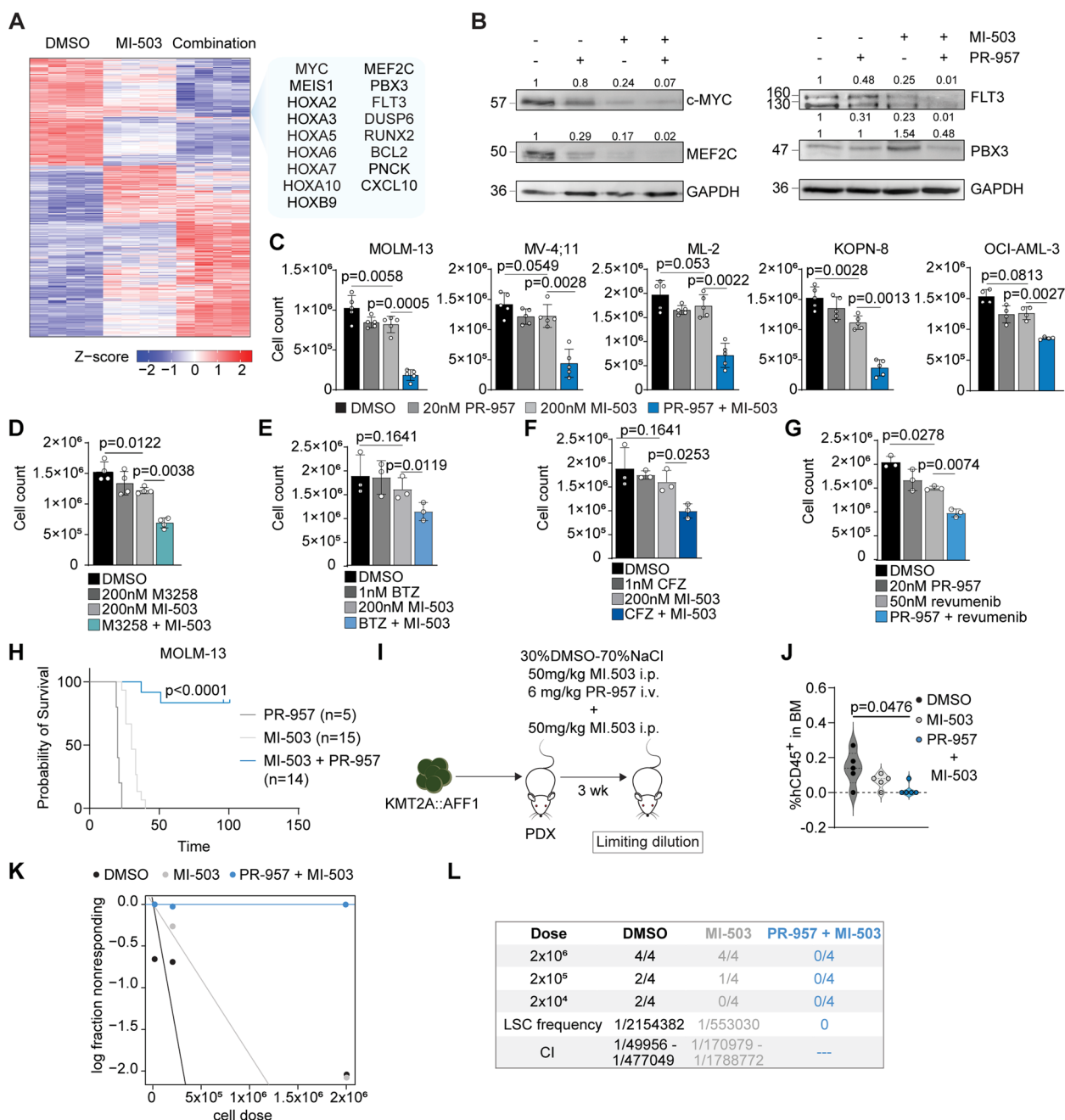


Fig. 6 (See legend on previous page.)

reached; $p < 0.0001$) or diluent controls (median survival 2×10^6 : 114 days; 2×10^5 : 225 days; 2×10^4 : 211.5 days; $p < 0.0001$) and reduced hCD45+ leukemic cells in recipient BM (Supplementary Figure S7C-D). Recently, Menin-inhibitors have shown promising clinical responses in patients with relapsed/refractory KMT2A-r or NPM1c AML [31]. However, more than one third of patients on prolonged inhibitor treatment acquired resistance to Menin-inhibition through somatic mutations in *MEN1*

[32]. As these findings indicate evolution of escape mutants upon chromatin-complex-inhibitors, we sought to assess for the efficacy of immunoproteasome inhibition in the context of resistance mediating mutations. KMT2A-r cell lines MV-4;11 harboring the M327I- and T349M-resistance mutations were exposed to increasing concentrations of PR-957 (50 nM, 100 nM). Notably, immunoproteasome inhibition efficiently attenuated cell growth in MV-4;11-WT and MV-4;11-M327I or

MV-4;11-T349M mutants to a similar extent, indicating preserved sensitivity (Fig. 7A) while both cell lines showed preserved resistance against Menin-inhibitors (MI-503 and Revumenib; Supplementary Figure S8). To assess for the effects of combined targeting on cell competition in vivo, we injected MV-4;11 wildtype (-BFP) and MV-4;11-M327I (-RFP) in a 20:1 ratio sequentially into immunocompromised NXG animals and treated them over 3 weeks either with diluent/chow control, 0.05% diet

of the Menin-inhibitor Revumenib or a combination of Revumenib with 6 mg/KG PR-957 i.v. (overlapping for 2 out of 3 weeks) (Fig. 7B). As previously published, treatment with Revumenib efficiently eradicates KMT2A-r MV-4;11-WT cells in NXG mice, while there was rapid leukemia development in diluent/control chow treated controls (Fig. 7C). Outgrowth of MV-4;11-M327I resistant clones could be observed in 10% of recipient animals upon Revumenib monotherapy. In contrast, combination

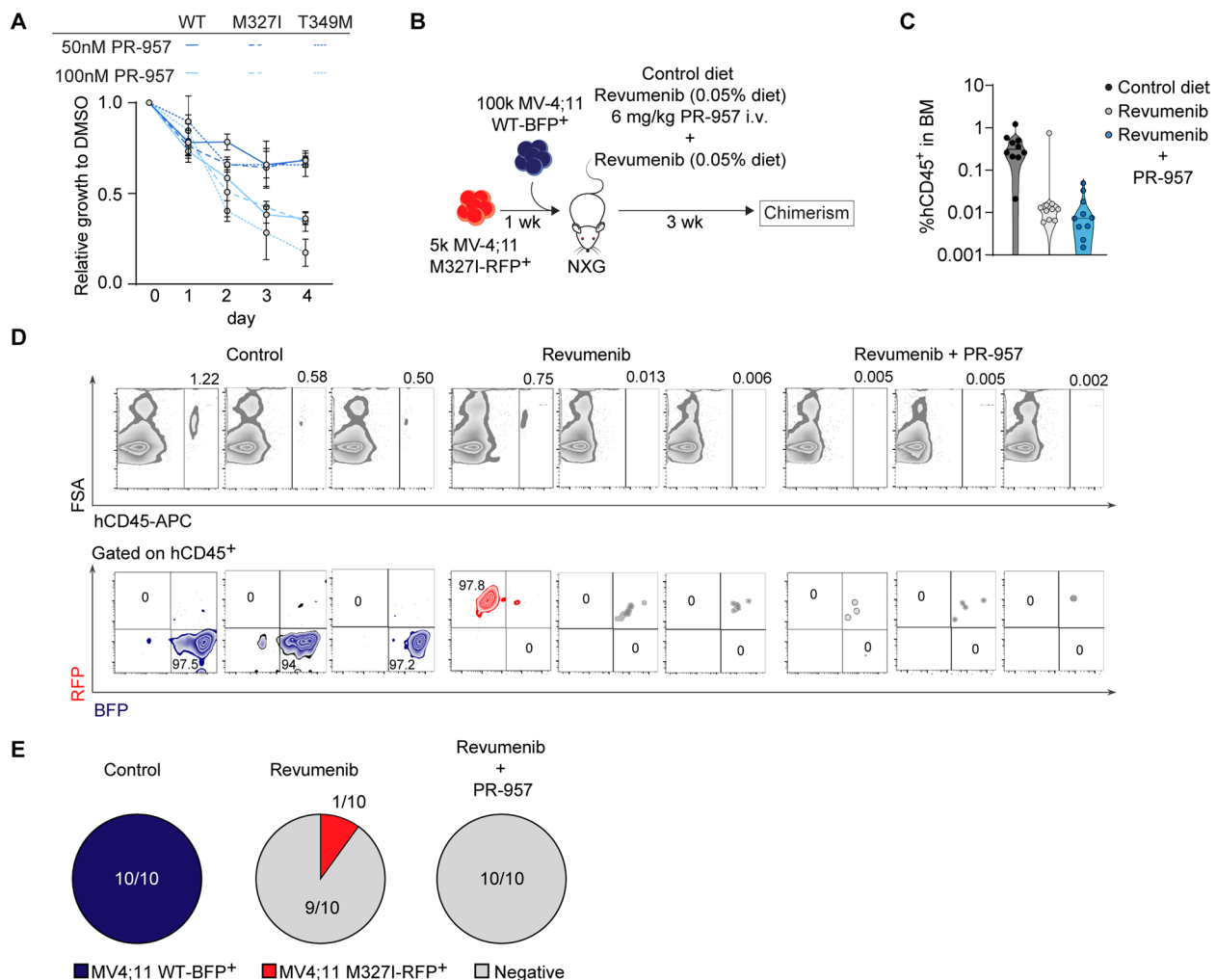


Fig. 7 Menin mutated cells with acquired resistance to Menin-inhibition retain sensitivity to immunoproteasome inhibition and preserved activity of combinatorial treatment strategies against MEN1-mutated clones may blunt outgrowth of resistant cells. **A** Relative growth to DMSO of wild-type MV-4;11 (MV-4;11 WT) and two MV-4;11 cell lines containing mutations in MEN1 (MV-4;11 M327I, methionine to isoleucine change at position 327; MV-4;11 T349M, threonine to methionine at position 349) after treatment with PR-957 (50 nM, 100 nM). *n* = 4 independent experiments; mean with SD. **B** Schematic representation of the competitive transplantation of 5×10^4 MV-4;11 M327I-RFP+ cells and 1×10^5 MV-4;11 WT-BFP+ cells (transplanted one week later) into NXG mice. Recipient mice were treated for 3 weeks with food supplemented with 0.05% Revumenib, Revumenib + PR-957 (6 mg/kg, 5 days/week, at week 1 and week 3) or control diet. **C** Immunophenotyping of human CD45+ (hCD45+) cells in the BM of NXG mice after in vivo treatment with Revumenib, Revumenib + PR-957 or control diet. *n* = 10 mice per treatment. **D** Representative flow cytometry plots (3 per cohort) showing the percentage of hCD45+ and percentage of RFP+ hCD45+ and BFP+ hCD45+ bone marrow cells in the control, Revumenib-treated and Revumenib + PR-957 treated mice. **E** Pie charts depicting the number of mice expressing MV-4;11 WT-BFP+ cells (blue), MV-4;11 M327I-RFP+ cells (red) or no RFP+ / BFP+ cells (negative, grey), respectively

of Revumenib with PR-957 resulted in complete eradication of human CD45+ leukemic cells and prevented outgrowth of Menin-inhibitor resistant mutants in vivo (Fig. 7C-E). These results indicate a potential therapeutic window to combine clinically relevant doses of Menin- and immunoproteasome-inhibitors to increase therapeutic efficacy and potentially prevent outgrowth of Menin-inhibitor resistant clones.

Discussion

Leukemic cells show aberrant regulation of the epigenetic machinery to activate and maintain transcriptional programs required for cell competition, proliferation and self-renewal. Leukemias that harbor balanced translocations involving the KMT2A-gene locus show a unique disease biology and particularly poor prognosis [1, 32] due to molecular persistence and a high relapse rate. Direct targeting of the oncogenic fusion has not been successful so far [1]. Most recently, inhibitors of the KMT2A-complex members Dot1L and Menin have shown promising activity in pre-clinical studies [3, 5, 6]. However, clinical use of the chromatin complex inhibitors has been hampered by their bioavailability, limited efficacy [10] and emergence of resistance mediating mutations [33].

As the presence of the KMT2A-fusion may create secondary dependencies, we aimed to explore the proteomic landscape of KMT2A-r leukemia. Proteostasis appeared as an important cellular function enriched in KMT2A::MLL3 driven murine AML. Moreover, catalytic proteasome subunits were highly expressed in human KMT2A-r AML, a finding that had been reported by others before [17] without providing functional or mechanistic explanation. Here, we provide first evidence, that inactivation of catalytic immunoproteasome subunit PSMB8 results in impaired cellular proliferation of KMT2A-r leukemia.

The immunoproteasome is a specialized version of the proteasomal catalytic core particle [12, 34], where catalytic subunits of the standard proteasome can be rapidly substituted by their immunoproteasome counterparts PSMB8 (LMP7, beta5i), PSMB9 (LMP2, beta1i) and PSMB10 (MECL-1, beta2i) to increase specificity and efficacy in a context dependent manner. Use of the covalent and specific PSMB8-inhibitor PR-957 (ONX-0914) prevented disease progression in models of autoimmune disorders, without evidence of significant toxicity [20, 35]. Immunoproteasome inhibitors have demonstrated their efficacy and safety against inflammatory and autoimmune diseases, even though their development for the treatment of hematologic malignancies is still in the early phases. Recently, M3258 was synthesized using the

α -aminoboronic acid scaffold as a starting point to optimize selectivity for PSMB8 (>500fold over PSMB5) and has entered early clinical trials for multiple myeloma [14, 36, 37]. In contrast, approved compounds such as bortezomib or carfilzomib inhibit standard- and immunoproteasome subunits in a rather non-specific manner leading to increased hematologic toxicity [14]. While effects of immunoproteasome inactivation on antigen presentation and T-cell activation have been investigated in very detail (reviewed in [12]), our data describes a so far unidentified cell-intrinsic mechanism of immunoproteasome inhibition in the context of KMT2A-r AML: pharmacologic inactivation of its catalytic subunit PSMB8 results in increased abundance of the transcription factor BASP1 and leads to repression of KMT2A-target genes (Fig. 8). BASP1 has been described as a repressive transcriptional co-factor in conjunction with several transcriptional regulators such as WT, Prohibitin, MYC or ERalpha [38–40] that may modulate chromatin accessibility [41] and also exerts cytoplasmatic functions [42, 43]. Depending on the cellular context, both, oncogenic and tumor suppressor functions of BASP1 have been described. Exploiting this alternative mechanism of targeting transcriptional oncogenic networks, we demonstrate that combination of pharmacologic PSMB8- and Menin-inhibition results in synergistic abrogation of human leukemic cells in vivo and improved elimination of leukemia initiating cells in pre-clinical PDX-models when compared to Menin-inhibitor treatment alone. The enhanced effect by inhibiting both molecules is preserved across the class of (immuno-) proteasome inhibitors irrespective of their specificity and for second-generation clinical grade Menin-inhibitors. Although both types of inhibitors reduce proliferative capacity and self-renewal capacity of leukemic stem cells (rather than induction of apoptosis), combination of both classes may facilitate eradication of residual leukemic clones through mechanisms of cell competition and induction of differentiation.

While identified as a selective functional vulnerability in KMT2A-r cells, inactivation of PSMB8 attenuated growth of NPM1-mutated cells, suggesting activity in this frequent subtype of AML. This finding is consistent with recent findings that mutated NPM1 binds to KMT2A co-occupied targets, which explains its sensitivity to Menin-inhibitor treatment [44]. Most recently, a phase 1 trial investigating the Menin-inhibitor Revumenib (SNDX-5613) in KMT2A-r and NPM1c AML reported on emergence of MEN1 mutations mediating resistance in 38.7% of patients [33]. While this report emphasizes the evolution of resistance mutants against a chromatin-targeting therapy, the non-epigenetic mechanism of inhibiting oncogenic gene expression through repression

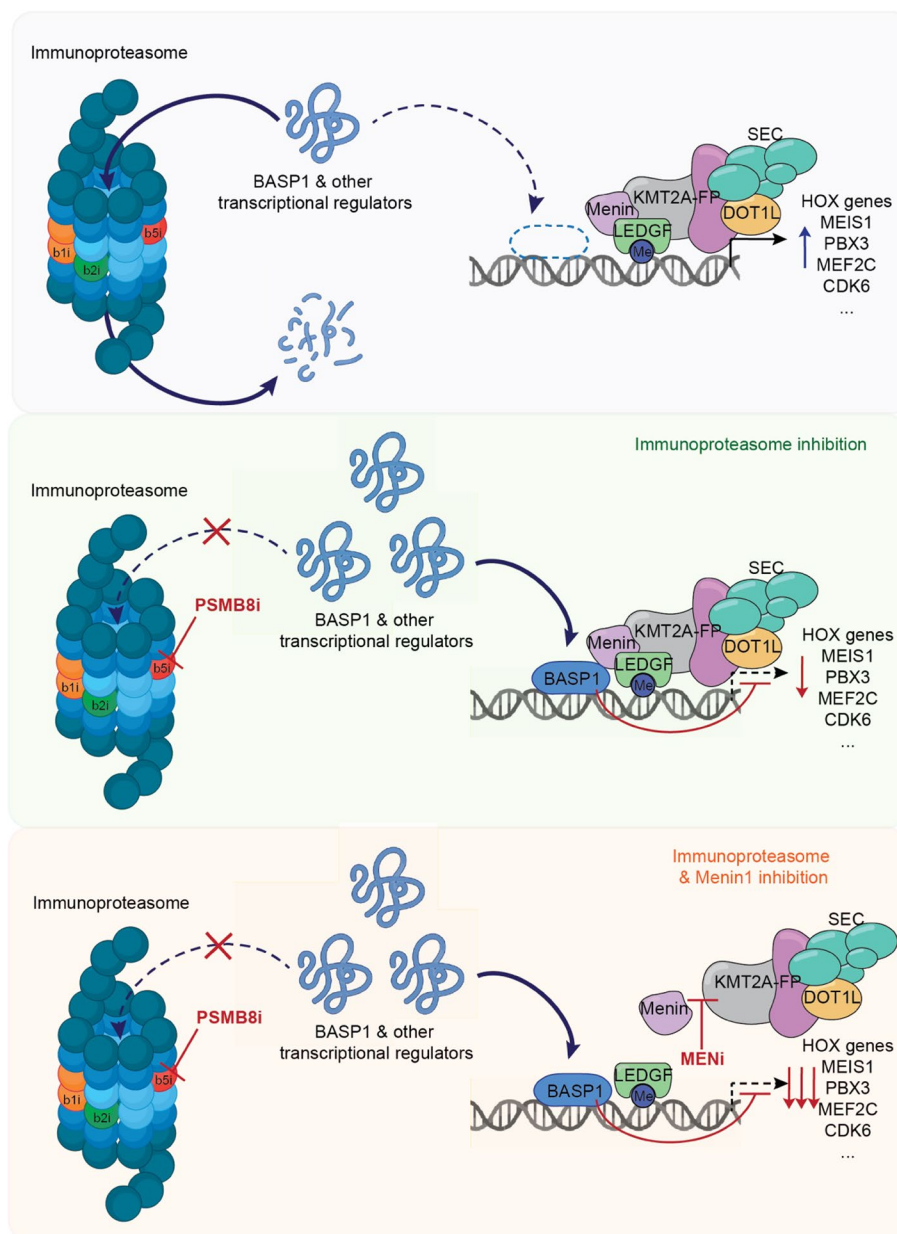


Fig. 8 Schematic depicting the relevant mechanisms of PSMB8 inhibition as a functional vulnerability in KMT2A-r leukemia through repressive nuclear functions of BASP1 in conjunction with Menin-inhibitor treatment

of KMT2A-target genes described here is still effective in KMT2A-r, MEN1-mut cells.

Conclusion

Thus, combined use of immunoproteasome- and Menin-inhibitors facilitates efficient drug targeting of oncogenic transcriptional networks in AML (Fig. 8) and provides the opportunity for improved reduction of disease burden and preserved activity against MEN1-mutated clones to prevent resistance to targeted epigenetic therapies.

Material & methods

Cell lines

Human AML cell lines were purchased from DSMZ (Braunschweig, Germany). Cas9-Blast or deadCas9-Blast (dCas9) cell lines are subclones of the respective cell lines and stably transduced with lentiCas9-Blast (Addgene #52962) or dCas9-VP64-Blast (Addgene #61425) and MS2-P65-HSF1-Hygro (Addgene #61426). MV-4;11 M327I and MV-4;11 T349M have been previously described [33]. Cells were cultured in RPMI 1640 medium (Thermo Fisher Scientific, Waltham, USA)

supplemented with 10-20% FBS (Thermo Fisher Scientific) in 5% CO₂ at 37°C.

Animal studies

All mice were housed under pathogen-free conditions in the Animal Research Facility of the Otto-von-Guericke University Medical Faculty Magdeburg, the ZET (University Hospital Jena) and ZTL (University Medicine Greifswald). All experiments were conducted after approval by the respective authorities of Sachsen-Anhalt (42502-2-1279 UniMD), Thüringen (02-030/2016) and Mecklenburg-Vorpommern (7221.3-1-019/22). Conventional LMP7^{-/-} and i-KMT2A::MLLT1 mouse models have been previously published [24, 45]. For induction of KMT2A::MLLT1 expression in the i-KMT2A::MLLT1 model, mice were treated for 2 weeks with food supplemented with Doxycycline (DOX; 0.545 g/kg). For induction of KMT2A::MLLT3 driven leukemia we used established retroviral MSCV-GFP-based vectors to express KMT2A::MLLT3 in hematopoietic stem- and progenitor cells (Lineage⁻Scal⁺c-Kit⁺, LSK cells) as described before. For competitive repopulation assays of normal hematopoiesis, 2x10⁶ BM cells of 6-8-weeks old B6.SJL-PtprcaPepcb/BoyCrl (CD45.1) or C57BL/6Jrj (CD45.2) animals (Janvier Labs) and 2x10⁶ (CD45.1/2) competitor cells (derived from intercrossing B6.SJL-PtprcaPepcb/BoyCrl (Charles River) with C57BL/6Jrj (CD45.2) animals) were transplanted via lateral tail vein injection into lethally irradiated (13 Gy, single-dose) 6-8-weeks old C57BL/6Jrj (CD45.2) recipient mice or B6.SJL-PtprcaPepcb/BoyCrl (CD45.1) (females), respectively.

Primary patient samples

Primary AML patient samples and healthy donor controls were obtained after informed consent and according to the Helsinki declaration within the AML-trials of the German-Austrian AMLSG study group and from the Hematology Tumor Bank Jena and Magdeburg, approved by the respective local ethics committee (Ethics Committee of the Medical Faculty, University Hospital Jena #4753/04-16 or University Hospital Magdeburg #115/08). Human bone marrow aspirates were separated with Ficoll-Paque Plus (GE Healthcare, Chicago, IL, USA) following the manufacturer's instruction and cryopreserved in 1x freezing medium (80% FBS + 10% DMSO + 10% IMDM medium).

Mouse xenotransplantation

NOD.Cg-Prkdc^{scid} Il2rg^{tm1Wjl} Tg(CMV-IL3, CSF2, KITLG) 1Eav/MloySzJ (NSGS) mice were obtained from The Jackson Laboratory (Bar Harbor, ME, USA). NOD.Cg-Prkdc^{scid} Il2rg^{tm1Wjl}/RJ (NXG) mice were obtained from Janvier (Le Genest-Saint-Isle, France). 8-12-weeks old adult mice (male and female) were irradiated with 2

Gy (single dose) before transplantation. 1x10⁵ MOLM-13, ML-2 or MV-4;11 cells transduced with either of two PSMB8 shRNAs or non-targeting control; with a pLEX vector containing the sequence of BASP1 or an empty vector; or treated *ex vivo* with the indicated inhibitors were injected intravenously via the tail vein. For patient derived xenograft experiments (PDX) of human KMT2A leukemia, 1-5x10⁴ cells from patient samples containing an KMT2A::MLLT3 or KMT2A::AFF1 translocation were injected into NOD.Cg-Kit^{W-41}Prkdc^{scid}Il2rg^{tm1Wjl}/WaskJ (NSGW41) [46]. Human myeloid engraftment (hCD45+) was analyzed by flow cytometry.

In vivo drug treatment

PR-957 (MedChemExpress, Monmouth Junction, NJ, USA) was solved in DMSO and diluted in CAPTISOL[®] from a sterile stock solution and administered by i.v. injections (3mg/kg, 6mg/kg or 10mg/kg as indicated) once daily as published before [20]. NaCl0.9% was injected as diluent control. MI-503 (Selleckchem, Houston, TX, USA) was dissolved in 25%DMSO/25%PEG-400/50%NaCl0.9% or a diluted solution of DMSO in CAPTISOL[®] and administered i.p. at 50mg/kg versus NaCl0.9% or 30%DMSO-70%NaCl0.9% as diluent control.

Methylcellulose colony-forming assays

Primary mouse bone marrow (BM) cells (transduced with MA9/KRAS, MA6 or AML1-ETO/KRAS) were seeded in MethoCult GF M3434 (Stemcell Technologies, Vancouver, Canada) at a concentration of 1x10³ cells/replicate. LSK cells isolated from LMP7^{-/-} or LMP7^{+/+} mice (transduced with KMT2A::MLLT3 or KMT2A::MLLT1) were seeded at 500 cells/replicate. Colonies propagated in culture were scored on day 7 and replated for 4 weeks. For re-plating of BM cells, colonies were harvested from the methylcellulose medium, washed with PBS/1%FBS and re-seeded at the same concentration. Human AML cell lines infected with either NT or PSMB8-specific shRNAs were plated at 250 cells/replicate in MethoCult H4230 (Stemcell Technologies) supplemented with 10% FBS. Colony numbers were counted on day 10-14.

Immunohistochemistry

Spleen, liver and lung were fixed in 4% paraformaldehyde for 24 hours followed by incubation in 30% ethanol for 30 min and 50% ethanol for 24 hours. Organs were embedded in paraffin and paraffin sections were cut on a rotary microtome (Microm HM 355S, Thermo Fisher Scientific), mounted on microscope slides and air-dried in an oven at 37°C overnight. Tissue section slides were then processed automatically for H&E staining (Leica AutoStainer XL, Leica Biosystems, Wetzlar, Germany). Images were acquired at 10x magnification on an Axiolmager A.2 (Carl

Zeiss Microscopy, Jena, Germany). Images were processed using the ImageJ software (NIH, Bethesda, MD, USA).

Flow cytometry and antibody staining

Immunophenotyping of immature and mature cell compartments and of leukemic cells was performed as described before [19]. The antibodies used for cell surface staining are provided in Table S1. Cells were stained in PBS/1% FBS for 1.5 hours at 4°C. SYTOX[®]Blue Dead Cell Stain (Life Technologies, Darmstadt, Germany) was used to exclude dead cells. Flow cytometry was performed on a LSRFortessa or FACS Canto II cytometer (BD Biosciences, Franklin Lakes, NJ, USA). Cell cycle analysis was performed using the Click-iT[™] EdU Alexa Fluor[™] 647 Assay Kit (Thermo Fisher Scientific) as per the manufacturer's instructions.

Genetic inactivation by RNAi

The pLKO.1-vector system with puromycin resistance gene was used. HEK293T cells were transfected using FUGENE[®]HD Transfection Reagent (Promega, Madison, WI, USA) to generate lentiviral particles as described before [19]. Target cells were infected twice (8 hours gap) by spinfection (872g, 1.5 h, 33°C). Puromycin selection (1 µg/ml) was started at 48h. shRNA sequences are provided in Table S2.

CRISPR activation

Guide RNAs were designed using the CRISPick tool (Broad Institute, <https://portals.broadinstitute.org/gppx/crispick/public>). sgRNA sequences: Luciferase_sgRNA (GATTCTAAAACGGAT-TACCA), sgRNA3a BASP1 (CGGGGAGCGCGGGAGGAGGG), sgRNA5a BASP1 (GGGCGGGGAGCGCGG-GAGGA). For cloning sgRNA sequences, the improved-scaffold-pU6-sgRNA-EF1A1- α -PURO-T2A-RFP (ipUSEPR) vector system was used. HEK293T cells were transfected using FUGENE[®]HD Transfection Reagent (Promega, Madison, WI, USA) to generate lentiviral particles as described before [19]. Cell lines stably expressing Cas9 were infected twice (8 hours gap in between) by spinfection (872xg, 1.5 hours, 33°C). The cells expressing sgRNAs were selected with 1 µg/ml puromycin starting on day 2 post-infection. Cells were collected for RT-qPCR on day 8 post-infection

Cellular proliferation & apoptosis

Cellular proliferation was assessed by cell counting using Trypan Blue exclusion. Apoptosis was measured by flow cytometry using Annexin V/ SYTOX[®]Blue staining.

Genome-wide CRISPR/Cas9 screening

6x10⁸ MOLM-13 cells were transfected (872 g, 37C, 2h) with lentiviral particles containing the human lentiviral

CRISPR/Cas9 library (developed and kindly provided by Dr. X. S. Liu (Addgene, #1000000132)). Cells were treated for 12 days with increasing concentrations of PR-957 (50-200nM) or DMSO as a control. Genomic DNA was extracted, and library amplification performed according to standard protocols (<https://www.addgene.org/pooled-library/liu-crispr-knockout/>).

Quantitative real-time PCR

1µg of total RNA were extracted using TRIzol Reagent (Thermo Fisher Scientific,) or the RNeasy Mini Kit (Qiagen, Hilden, Germany). RNA was reverse-transcribed using Omniscript RT Kit (Qiagen, Hilden, Germany) as per the manufacturer's instructions and complementary DNA samples were analyzed by RT-qPCR using SYBR[®] Premix Ex TaqII[™] (Clontech Laboratories, Mountain View, CA, USA) following the manufacturer's instruction. Gene-specific primers were designed to span exon-exon boundaries. All expression values were normalized and standardized using the Bio-Rad CFX Manager software (Munich, Germany) and presented as fold changes of gene expression in the test sample compared to the control. Primer sequences are listed in Table S4.

Protein extraction and immunoblotting

Cells were washed twice with ice-cold PBS and lysed in lysis buffer (50 mM HEPES pH7.4, Glycerol 10%, NaCl 150 mM, TritonX-100 1%, MgCl 1.5 mM, EGTA 5mM) for 1 hour on ice. For nuclear extraction, NE-PER[™] Nuclear and Cytoplasmic Extraction Kit (Thermo Fisher Scientific) was used following the manufacturer's instructions. Protein concentration was calculated using the Protein Assay Dye Reagent Concentrate (Bio-Rad Laboratories, Inc., Hercules, CA, USA) following the manufacturer's instruction. HRP-conjugated anti-rabbit or anti-mouse secondary antibodies were purchased from Cell Signaling (Denvers, MA, USA). Primary antibodies used included: anti-BASP1 (Thermo Fisher Scientific, 703692), anti-c-Myc (Abcam, Cambridge, UK; ab32072), anti-FLT3 (Cell Signaling, CS3462), anti-GAPDH (Meridian Life Sciences, Cincinnati, OH, USA; H68504M), anti-HA-Tag (Cell Signaling, CS3724), anti-HDAC1 (Cell Signaling, CS5356), anti-MEF2C (Cell Signaling, CS5030S), anti-PBX3 (Abcam, ab109173), anti-PSMB5 (Santa Cruz Biotechnology, Dallas, TX, USA; sc393931), anti-PSMB8/LMP7 (Abcam, ab3329 / Santa Cruz Biotechnology, sc365699), anti-PSMB9/LMP2 [47], anti-PSMB10/MECL1 (Thermo Fisher Scientific, PA5-19146), anti-Vinculin (Sigma Aldrich, St Louis, MO, USA; V9131), anti- β -actin (Santa Cruz Biotechnology, sc47778).

Global proteome analysis

For global proteome profiling, leukemia development was initiated with KMT2A::MLLT3 (or AML1-ETO as control) containing MSCV-GFP constructs. Murine stem and progenitor cells (LSK cells: Lin⁻Sca⁺c-Kit⁺) from 6-8 weeks-old C57BL/6J donors (females) were sorted and infected by co-localization of virus supernatant (containing one of the oncogenes) on retronectin-coated plates. 72 hours after infection equal numbers of GFP⁺ cells were injected into sublethally irradiated recipient hosts (7Gy). 2x 10⁵ LSC-enriched (GFP⁺ c-Kit⁺) cells (4 replicates per oncogene) were sorted directly into 2x lysis buffer (for a final concentration: 1% SDS, 50 mM HEPES, pH 8.5, 10 mM DTT; volume of lysis buffer added to collection tube was estimated to be equal to the volume of the sheath buffer). For global proteome profiling of human AML cell lines, 2x10⁶ cells treated with 100nM PR-957 or DMSO, 72h (4 replicates per treatment). Sample processing was performed as described previously [48].

ATAC-sequencing

5x10⁴ MOLM-13 cells were used for nuclear extraction. Nuclear fractions were tagmented using Illumina Tagment DNA TDE1 Enzyme and Buffer Kit (New England Biolabs® (NEB), Ipswich, MA, USA). Subsequently, DNA was extracted using the DNA Clean & Concentrator-5 (Zymo Research, Irvine, CA, USA). DNA was mixed with a universal i5 and uniquely barcoded i7 primer and amplified using NEB-Ultra II Q5 master mix (New England Biolabs, M0544S) in a thermocycler using the following conditions: 98°C for 30 seconds; 7 cycles of 98°C for 10 seconds, 63°C for 30 seconds; and 72°C for 1 minute. Post amplification libraries were size selected at >250bp in length using SPRI-select beads (Beckman Coulter, Brea, CA, USA). Library fragment length was checked by HSD5000 Tape (Agilent, Santa Clara, CA, USA) and DNA concentration was determined by the Qubit dsDNA HS Assay Kit (Thermo Fisher Scientific).

Cut & Tag-sequencing

Protein A fused to Tn5-transposase was expressed and purified using a publicly available construct (Addgene #124601). In brief, 1x10⁵ MOLM-13 cells were washed in Wash Buffer (20 mmol/L HEPES pH 7.5, 150 mmol/L NaCl, 0.5 mmol/L Spermidine, protease inhibitor cocktail) and bound to Concanavalin A beads (Bangs Laboratories, Fishers, NC, USA; BP531). Cells were resuspended in 50µL Digitonin Wash Buffer (20 mmol/L HEPES pH 7.5, 150 mmol/L NaCl, 0.5 mmol/L Spermidine, protease inhibitor cocktail, 2 mmol/L EDTA, 0.05% Digitonin) and incubated with anti-H3K4me3, -H3K4me1, -H3K27ac, -and H3K27me3 antibody at a 1:100 dilution overnight at 4°C. Beads were resuspended in 100µL

Digitonin Wash Buffer with a secondary antibody diluted 1:100 and incubated for 30min at room temperature. Cells were washed three times in Digitonin Wash Buffer and resuspended in Digitonin-300 Buffer (0.05% Digitonin, 20 mmol/L HEPES, pH 7.5, 300 mmol/L NaCl, 0.5 mmol/L Spermidine, protease inhibitor cocktail) containing 1:250 pA-Tn5 transposase and incubated at room temperature for 1 hour. Subsequently, cells were washed three times in Digitonin-300 Buffer and resuspended in 100 µL Tagmentation Buffer (10 mmol/L MgCl₂ in Digitonin-300 Buffer) and incubated at 37°C for 1 hour. Tagmentation was stopped by adding 10µL of 0.5 M EDTA, 3µL of 10% SDS, and 2.5 µL of 20 mg/mL Proteinase K (Thermo Fisher Scientific, 25530049), and samples were incubated 37°C overnight. Tagmented DNA was purified using AMPureXP-beads (Beckman Coulter). For each sample, 21µL DNA was mixed with a universal i5 and uniquely barcoded i7 primer and amplified using NEB-Next High Fidelity 2x PCR Master Mix (New England Biolabs, M0541S) in a thermocycler using the following conditions: 98°C for 30 seconds; 14 cycles of 98°C for 10 seconds, 63°C for 10 seconds; and 72°C for 2 minutes. DNA was purified with AMPureXP beads and quality was assessed by the Qubit dsDNA HS Assay Kit and HSD5000 Tape.

Cut & Run-sequencing

6x10⁵ MOLM-13 cells were harvested per reaction. Preparation of the samples was performed using CUTANA™ ChIC/CUT&RUN Kit (EpiCypher, Chapel Hill, NC, USA) following the manufacturer's instructions. Antibodies used: anti-BASP1 (Thermo Fisher Scientific, 703692), IgG Control (EpiCypher, 13-0042k) and H3K4me3 (positive control) (EpiCypher, 13-0041k). Library amplification was done using the NEBNext® Ultra™ II DNA Library Prep Kit for Illumina® (NEB) using 6ng of sample. Post amplification libraries were size selected at 150-250bp in length using AMPure beads (Beckman Coulter). Library fragment length was checked by HSD1000 Tape and DNA concentration was determined by Qubit.

Statistics and analysis of sequencing and proteome data

Statistical analyses were performed using Student's *t* test or 2-way ANOVA (normal distribution) or Mann-Whitney U test (when normal distribution was not given). *p* less than 0.05 was considered statistically significant. mRNA expression data of the catalytic (immuno-) proteasome subunits in different genetic AML subtypes was downloaded from BloodSpot data base [49] (<http://servers.binf.ku.dk/bloodspot/>) and protein expression data from depmap.org. Detailed information on the analyses of proteome, RNA-, ATAC-, Cut&Tag-, Cut&Run-sequencing data is provided in the Supplementary Material and Methods.

Abbreviations

AE	AML1-ETO9a
ALL	Acute Lymphoblastic Leukemia
AML	Acute myeloid leukemia
BASP1	Brain Abundant Membrane Attached Signal Protein 1
BM	Bone marrow
BTZ	Bortezomib
C	Cytoplasmic
CFZ	Carfilzomib
CI	Confidence intervals
CMP	Common myeloid progenitors
DOX	Doxycycline
ELDA	Extreme Limiting Dilution Assay
FC	Fold change
GMP	Granulocyte–macrophage progenitors
GSEA	Gene set enrichment analysis
HGB	Hemoglobin
hCD45 ⁺	Human CD45 ⁺
HSC	Hematopoietic stem cell
HSPCs	Hematopoietic stem- and progenitor cell
IP	Immunoproteasome
KMT2A-r	KMT2A-rearranged
LD	Limiting dilution
LSC	Leukemic stem cell
LSK	Lineage [−] Sca1 ⁺ c-Kit ⁺
LT-HSC	Long-term HSC
MA9	MLL-AF9
MEN1	Menin
MEP	Megakaryocyte-erythroid progenitors
MLL	Mixed-Lineage-Leukemia
MPP	Multipotent progenitor
MS	Mass spectrometry
N	Nuclear
NES	Normalized enrichment score
NPM1c	NPM1-mutant
NSGW41	NOD.Cg ^{KitW-41} .Prkdc ^{scid} Il2rg ^{tm1Wjl}
NXG	NOD.Cg-Prkdc ^{scid} Il2rg ^{tm1Wjl} /RJ
PB	Peripheral blood
PDX	Patient derived xenografts
PLT	Platelets
Prog	Progenitor cell abundance
SD	Standard Deviation
SEM	Standard Error of Mean
shNT	Non-targeting control
ST-HSC	Short-term HSC
TSS	Transcription Start Site
UPS	Ubiquitin–proteasome system
WBC	White blood counts
WT	Wild-type

Supplementary Information

The online version contains supplementary material available at <https://doi.org/10.1186/s12943-023-01907-7>.

Additional file 1: Fig. S1. (A) Western Blotting showing expression of PSMB8, PSMB9 and PSMB10 in KMT2A-r (ML-2, THP-1, MV-4;11, KOPN-8, MOLM-13) and non-KMT2A-r (HL-60, K-562) cell lines. HeLa cells were used as a negative control, since they do not express immunoproteasome, and T cells as a positive control. (B) Violin plots displaying log₂-fold protein expression as assessed by proteome analysis (Jayavelu et al., Cancer Cell, 2022; PXD022894) of PSMB8, PSMB9 and PSMB10 in different KMT2A-r and non-KMT2A-r cell lines. Mann-Whitney U test. (C) CRISPR-Cas9 cell competition assay showing the effect of deletion of each catalytic immunoproteasome subunit over time. Catalytic immunoproteasome subunits were knocked out using different single guide RNAs (5 specific for PSMB8; 3 specific for PSMB9 and PSMB10, respectively) in human KMT2A-r AML cells (MOLM-13) and the chimerism of knockout and wildtype cells over time is visualized in the graphs. Each blue line represents the chimerism at day 0, 3, 6, 9, and 12. A decrease in the % of

RFP⁺ cells (shown on the Y axis) over time, as seen most pronounced for PSMB8, reflects a competitive disadvantage of cells that harbor the respective knockout. Single guide RNAs (red lines) against the essential gene RPA3 were used as a positive control and non-targeting guide against Luciferase as a negative control (black line). (D) Percentage of Annexin⁺ cells (containing Annexin⁺-SYTOX^{Blue} and Annexin⁺-SYTOX^{Blue} populations measured by flow cytometry) in KMT2A-r cell lines (MOLM-13, THP-1, MONO-MAC-6, KOPN-8, ML-2) transduced with shRNAs targeting PSMB8 or a non-targeting control (shNT) at day 6 post-infection. *n*=3-5 independent experiments; mean with SD; paired Student t test. (E) Growth curves depicting cell counting after trypan blue exclusion of MOLM-13 cells and MOLM-13 PSMB8 overexpressing cells (+PSMB8) transduced with shRNAs targeting PSMB8 or a non-targeting control (shNT). *n*=3 independent experiments; mean with SD. (F) Representative pictures of colonies from MOLM-13 and ML-2 cells transduced with PSMB8 shRNAs or shNT. Scale bars, 200 μm. Representative Western Blotting plots of MOLM-13 and ML-2 cells confirming PSMB8 deletion at day 4 post-infection before transplantation into NSGS recipient mice. (G) Representative Western Blotting plots of MOLM-13 and ML-2 cells confirming PSMB8 deletion at day 4 post-infection before transplantation into NSGS recipient mice. **Fig. S2.** (A) Violin plots showing the percentage of cells detected in S phase in MOLM-13, ML-2, KOPN-8 and MV-4;11, cells after treatment with 100nM PR-957 or DMSO for 24 hours. Samples were labeled for flow cytometry-based analysis of cell cycle using the Click-iT[®] EdU assay. *n*=3 independent experiments; paired Student t test. (B) Representative flow cytometry plots from Click-iT[®] EdU assay. (C) Schematic representation of patient derived xenografts (PDX). (D) Violin plots depicting % of hCD45⁺ cells in peripheral blood in PDX models of KMT2A::MLL3 and KMT2A::AFF1. 2-way ANOVA. (E) Violin plots of hCD45⁺ cells in spleen and bone marrow at the time of sacrifice. Mann-Whitney U test. **Fig. S3.** (A) Serial re-plating to assess colony formation in methylcellulose using murine LSK (Lin[−] Sca1⁺ c-Kit⁺) cells isolated from LMP7^{+/+} or LMP7^{−/−} mice and transformed with KMT2A::MLL3 or KMT2A::MLL1. *n*=4 independent experiments; mean with SD; paired Student t test. (B) Schematic representation showing the transplantation of KMT2A::MLL3 retrovirally transformed LSKs from LMP7^{+/+} or LMP7^{−/−} mice. (C) Schematic representation describing the transplantation of i-KMT2A::MLL1 BM cells lentivirally transduced with shRNA1 or shRNA4 against LMP7 or a non-targeting control (shNT) into CD45.1 recipient mice. Diet of the donor mice was supplemented with Doxycycline (DOX; 0,545 g/kg) for 2 weeks to induce KMT2A::MLL1 expression. Recipient mice were also kept with DOX supplemented food. (D) Violin plots depicting percentage of CD45.2⁺ cells in peripheral blood of CD45.1 recipient mice from sh1 LMP7 (*n*=4), sh4 LMP7 (*n*=4) or shNT (*n*=4) transformed i-KMT2A::MLL1. One cohort; 2-way ANOVA. (E) Kaplan-Meier survival curves of CD45.1 recipient mice transplanted with 1x10⁶ cells as shown in S3C. One cohort; Mantel-Cox test. (F) Spleen Colony Formation Assay *in vivo* (CFU-S12): Spleen colony numbers 12 days after injection of 100 LSK cells isolated from LMP7^{+/+} (*n*=10) or LMP7^{−/−} (*n*=10) mice. Two independent cohorts; Mann-Whitney U test (G) Schematic representation depicting competitive repopulation assay to investigate the effects of LMP7 depletion on normal hematopoietic stem- and progenitor cells (HSPCs). **Fig. S4.** (A) Representative pictures of colonies from murine LSK cells transformed with KMT2A::MLL3/KRAS, KMT2A::MLL4 or AML1-ETO/KRAS at week 2. Scale bars, 200 μm. (B) Schematic representation of *in vivo* PR-957 vs NaCl 0.9% treatment in C57BL/6 mice transplanted with KMT2A::MLL3 leukemic cells. Subsequent secondary transplantation of whole bone marrow cells into secondary recipients. (C) Pictures of tissue sections from liver, lung and spleen of *in vivo* PR-957 vs NaCl treated mice at the time of sacrifice. (D) Representative flow cytometry plots with the gating strategy for the analysis of granulocyte-macrophage progenitors (GMPs), megakaryocyte-erythroid progenitors (MEPs), common myeloid progenitors (CMPs), hematopoietic stem cells (HSCs) and multipotent progenitors (MPPs) in the competitive repopulation assay. FSA: Forward Scatter Area; SSA: Side Scatter Area; FSH: Forward Scatter Height; FSW: Forward Scatter Width; SSH: Side Scatter Height; SSW: Side Scatter Width; LK: Lineage- cKit⁺; LSK: Lineage- Sca1⁺ cKit⁺. **Fig. S5.** (A) Volcano plot of differentially regulated genes in RNA-sequencing. 100nM PR-957 vs. DMSO, 72h, MOLM-13.

Upregulated (red; $FC > 1.5$, $p < 0.05$) and downregulated (blue; $FC < -1.5$, $p < 0.05$). (B) Heatmaps displaying H3K27ac, H3K27me3, H3K4me1 and H3K4me3 Cut&Tag signal mapping to a 2-kb window around TSS. 100nM PR-957 vs. DMSO, 48h, MOLM-13. (C) Integrative Genomics Viewer (IGV) tracks from Cut&Tag-sequencing data in MOLM-13 cells depicting binding of H3K27ac, H3K27me3, H3K4me1 and H3K4me3 after DMSO or PR-957 treatment at HOXA and MEIS1 loci. (D) Volcano plot of differentially accessible regions in ATAC-seq. 100nM PR-957 vs. DMSO, 72h, MOLM-13. Upregulated (red; $FC > 2$, $p < 0.05$) and downregulated (blue; $FC < -2$, $p < 0.05$). (E) Stacked bar plot depicting genomic distribution of PSMB8 ATAC-seq peaks. 100nM PR-957 vs. DMSO, 72h, MOLM-13. (F) Schematic representation of the genome-wide CRISPR-Cas9 screen. (G) Volcano plots showing the distribution of genes being enriched (positive beta-scores) or depleted (negative beta-scores) in the genome-wide CRISPR-Cas9 screen in PR-957 treated MOLM-13 cells and DMSO diluent control. (H-I) Western Blotting showing expression of BASP1 in nuclear (N) and cytoplasmic (C) fractions of MOLM-13, MV-4;11, KOPN-8 and ML-2 cells. (H) BTZ (4nM) vs. DMSO, 72h. (I) CFZ (4nM) vs. DMSO, 72h. (J) Integrative Genomics Viewer (IGV) tracks from Cut&Run-sequencing data in MOLM-13 cells depicting binding of BASP1 after DMSO or PR-957 treatment and of H3K4me3 after DMSO treatment at the KMT2A, MYC, JUN and GNAS loci. **Fig. S6.** (A) Western Blotting confirming BASP1 overexpression after transduction with a pLEX vector containing the sequence of human BASP1 with an HA tag (BASP1) or an empty vector with the HA tag (EV) as a control in MOLM-13, MV-4;11, ML-2 and KOPN-8 cells. Samples were collected at day 6 post-infection. (B) Percentage of Annexin⁺ cells of KMT2A-r cell lines overexpressing BASP1 or control cells at day 6 post-infection. $n=4$ independent experiments; mean with SD; paired Student t test. (C) Growth curves of MOLM-13-deadCas9 (MOLM-13-dCas9) and MV-4;11-dCas9 cells containing the MS2-P65-HSF1 activator helper complex transduced with sgRNAs designed to target the promoter region of BASP1 (sgRNA3a BASP1 and sgRNA5a BASP1) or sgRNA Luciferase as a negative control. $n=4$ independent experiments; mean with SD; 2-way ANOVA. (D) Relative BASP1 mRNA expression in BASP1-overexpressing cells (MOLM-13-dCas9 and MV-4;11-dCas9) compared to sgRNA Luciferase cells assessed by Real Time Quantitative PCR (RT-qPCR). $n=4$ independent experiments; mean with SD. (E) Western Blotting confirming BASP1 overexpression after transduction with pLEX-BASP1 (BASP1) or pLEX-EV (EV) in MOLM-13 and MV-4;11 cells. Samples were collected 96 hours after transduction and before transplantation into recipient mice. **Fig. S7.** (A) Western Blotting quantification of c-MYC, MEF2C, FLT3 (mature), FLT3 (premature), PBX3, PSMB5 and PSMB8 protein expression in MOLM-13 cells treated with 100nM PR-957, 1 μ M MI-503, a combination of both or DMSO. $n=3-4$ independent experiments; mean with SD; paired Student t test. (B) Percentage of Annexin⁺ cells in MOLM-13, MV-4;11, ML-2, KOPN-8 and OCI-AML3 cells after treatment with 20nM PR-957, 200nM MI-503, a combination of both or DMSO as diluent control at day 8 post-infection. $n=5$ independent experiments; mean with SD; paired Student t test. (C) Kaplan-Meier survival curves of NXG recipient mice transplanted with limiting numbers (2×10^6 , 2×10^5 , 2×10^4) of whole bone marrow cells from *in vivo* treated mice (DMSO, MI-503, MI-503 + PR-957). Two independent cohorts; Mantel-Cox test. (D) Violin plots showing percentage of hCD45⁺ cells in bone marrow (BM) at the time of sacrifice. **Fig. S8.** (A) Negative selection cell competition assay using MV-4;11 Menin-wildtype (BFP⁺) cells and resistant MV4;11 Menin M3271 or T349M (RFP⁺) cells (as published in Perner et al. Nature 2023). Chimerism of RFP⁺ mutant clones over BFP⁺ Menin-wildtype cells is visualized for a total of 9 days upon exposure to PR-957 (100nM), Revumenib (50nM), MI503 (1 μ M) or DMSO as a control. **Table S1.** Flow cytometry and western blot antibodies used in this study. **Table S2.** shRNA sequences used in this study. **Table S3.** sgRNAs for CRISPRs used in this study. **Table S4.** Primer sequences for RT-qPCR used in this study.

Acknowledgements

The authors thank A. Fenske (Central Animal Facility, OvGU Magdeburg) and M. v.d. Wall (Animal Facility UK Jena) for their support with animal care, R. Hartig (Flow Facility, OvGU Magdeburg), M. Locke and K. Schubert (Flow Facility, FLI, Jena) for their support with cell sorting, L. Rothenburger (SF Histology,

FLI, Jena) for support with histopathology, N. Rahnis and P. Riemenschneider (CF Proteomics, FLI, Jena) for support with sample preparation, N. Huber for support with bioinformatic analysis and S. Frey, J. Toensing and C. Kathner-Schaffert for technical assistance.

Authors' contributions

Conceptualization: F.H.H.; Methodology: A.K.J., T.M.S., F.P., J.M.K., B.v.E., M.M., S.A.A., F.H.H.; Investigation: N.T.S., T.E., J.C.H., Q.Z., J.M.K., T.M.S., F.P.; Resources: F.H.H., D.V.W., M.W.M.K., C.C., U.S., J.S., M.H., A.H., A.O., M.M., S.A.A.; Data Curation: N.T.S., T.E., J.C.H., Q.Z., J.M.K., T.M.S., F.P.; Writing-original Draft: F.H.H.; Writing-Review & Editing: T.M.S., A.K.J., S.A.A., F.H.H.; Supervision: F.H.H. All authors reviewed the manuscript.

Funding

Open Access funding enabled and organized by Projekt DEAL. This work was supported by grants of the Wilhelm-Sander-Stiftung (2019.001.01), of the DFG (HE6233/8–1) and by the Thuringian state program ProExzellenz (RegenerAg-ing—FSU-I-03/14) of the Thuringian Ministry for Research (to F.H.H.).

Availability of data and materials

Raw data files for the RNA-sequencing, ATAC-sequencing, Cut&Run and Cut&Tag analysis have been deposited in the NCBI Gene Expression Omnibus (GEO) under accession number GSE225391. The mass spectrometry data have been deposited to the ProteomeXchange Consortium (<http://proteomecentral.proteomexchange.org>) via the PRIDE partner repository with the dataset identifier PXD041245.

Declarations

Ethics approval and consent to participate

Primary AML patient samples and healthy donor controls were obtained after informed consent and according to the Helsinki declaration within the AML-trials of the German-Austrian AMLSG study group and from the Hematology Tumor Bank Jena and Magdeburg, approved by the respective local ethics committee (Ethics Committee of the Medical Faculty, University Hospital Jena #4753/04–16 or University Hospital Magdeburg #115/08).

All mice were housed under pathogen-free conditions in the Animal Research Facility of the Otto-von-Guericke University Medical Faculty Magdeburg, the ZET (University Hospital Jena) and ZTL (University Medicine Greifswald). All experiments were conducted after approval by the respective authorities of Sachsen-Anhalt (42502–2-1279 UniMD), Thüringen (02–030/2016) and Mecklenburg-Vorpommern (7221.3–1-019/22).

Competing interests

S.A.A., M.W.M.K., F.P.: Advisors to Syndax Inc. Otherwise, the authors declare no competing interests.

Author details

¹Innere Medizin C, Universitätsmedizin Greifswald, 17475 Greifswald, Germany. ²Leibniz Institute On Aging, Fritz-Lipman Institute, 07745 Jena, Germany. ³Max-Planck-Institute of Biochemistry, Munich, Germany. ⁴Proteomics and Cancer Cell Signaling Group, DKFZ, Heidelberg, Germany. ⁵Department of Pediatric Oncology, Dana Farber Cancer Institute, Harvard University, Boston, MA 02215, USA. ⁶Independent consultant, London, UK. ⁷Department of Cell and Developmental Biology, Vanderbilt University, Nashville, TN, USA. ⁸Queensland Institute for Medical Research (QIMR), Brisbane, Australia. ⁹Sanford Burnham Research Institute, San Diego, USA. ¹⁰Medizinische Klinik 3, Hämatologie, Onkologie und Pneumologie, Universitätsmedizin Mainz, Mainz, Germany. ¹¹Department of Biomedicine, University Children's Hospital of Basel, Basel, Switzerland. ¹²Friedrich Loeffler-Institut für Medizinische Mikrobiologie - Virologie, Universitätsmedizin Greifswald, 17475 Greifswald, Germany. ¹³Department of Biochemistry, Universitätsmedizin Greifswald, 17475 Greifswald, Germany. ¹⁴Innere Medizin 2, Universitätsklinikum Jena, Jena, Germany. ¹⁵Hematology, Hemostasis, Oncology and Stem Cell Transplantation, Hannover Medical School (MHH), Hannover, Germany.

Received: 17 June 2023 Accepted: 21 November 2023

Published online: 04 December 2023

References

- Brien GL, Stegmaier K, Armstrong SA. Targeting chromatin complexes in fusion protein-driven malignancies. *Nat Rev Cancer*. 2019;19:255–69. <https://doi.org/10.1038/s41568-019-0132-x>.
- Papaemmanuil E, Gerstung M, Bullinger L, Gaidzik VI, Paschka P, Roberts ND, Potter NE, Heuser M, Thol F, Bolli N, et al. Genomic classification and prognosis in acute myeloid leukemia. *N Engl J Med*. 2016;374:2209–21. <https://doi.org/10.1056/NEJMoa1516192>.
- Bernt KM, Zhu N, Sinha AU, Vempati S, Faber J, Krivtsov AV, Feng Z, Punt N, Daigle A, Bullinger L, et al. MLL-rearranged leukemia is dependent on aberrant H3K79 methylation by DOT1L. *Cancer Cell*. 2011;20:66–78. <https://doi.org/10.1016/j.ccr.2011.06.010>.
- Chen CW, Koche RP, Sinha AU, Deshpande AJ, Zhu N, Eng R, Doench JG, Xu H, Chu SH, Qi J, et al. DOT1L inhibits SIRT1-mediated epigenetic silencing to maintain leukemic gene expression in MLL-rearranged leukemia. *Nat Med*. 2015;21:335–43. <https://doi.org/10.1038/nm.3832>.
- Krivtsov AV, Evans K, Gadrey JY, Eschle BK, Hatton C, Uckelmann HJ, Ross KN, Perner F, Olsen SN, Pritchard T, et al. A Menin-MLL inhibitor induces specific chromatin changes and eradicates disease in models of MLL-rearranged leukemia. *Cancer Cell*. 2019;36(660–673): e611. <https://doi.org/10.1016/j.ccell.2019.11.001>.
- Kuhn MW, Song E, Feng Z, Sinha A, Chen CW, Deshpande AJ, Cusan M, Farnoud N, Mupo A, Grove C, et al. Targeting chromatin regulators inhibits leukemogenic gene expression in NPM1 mutant leukemia. *Cancer Discov*. 2016;6:1166–81. <https://doi.org/10.1158/2159-8290.CD-16-0237>.
- Wan L, Wen H, Li Y, Lyu J, Xi Y, Hoshii T, Joseph JK, Wang X, Loh YE, Erb MA, et al. ENL links histone acetylation to oncogenic gene expression in acute myeloid leukaemia. *Nature*. 2017;543:265–9. <https://doi.org/10.1038/nature21687>.
- Uckelmann HJ, Kim SM, Wong EM, Hatton C, Giovinazzo H, Gadrey JY, Krivtsov AV, Rucker FG, Dohner K, McGeehan GM, et al. Therapeutic targeting of preleukemia cells in a mouse model of NPM1 mutant acute myeloid leukemia. *Science*. 2020;367:586–90. <https://doi.org/10.1126/science.aax5863>.
- Issa GC, Aldoss I, DiPersio J, Cuglievan B, Stone R, Arellano M, Thirman MJ, Patel MR, Dickens DS, Shenoy S, et al. The menin inhibitor revumenib in KMT2A-rearranged or NPM1-mutant leukaemia. *Nature*. 2023. <https://doi.org/10.1038/s41586-023-05812-3>.
- Stein EM, Garcia-Manero G, Rizzieri DA, Tibes R, Berdeja JG, Savona MR, Jongen-Lavrenic M, Altman JK, Thomson B, Blakemore SJ, et al. The DOT1L inhibitor pinometostat reduces H3K79 methylation and has modest clinical activity in adult acute leukemia. *Blood*. 2018;131:2661–9. <https://doi.org/10.1182/blood-2017-12-818948>.
- McCarthy MK, Weinberg JB. The immunoproteasome and viral infection: a complex regulator of inflammation. *Front Microbiol*. 2015;6:21. <https://doi.org/10.3389/fmicb.2015.00021>.
- Murata S, Takahama Y, Kasahara M, Tanaka K. The immunoproteasome and thymoproteasome: functions, evolution and human disease. *Nat Immunol*. 2018;19:923–31. <https://doi.org/10.1038/s41590-018-0186-z>.
- Raule M, Cerruti F, Cascio P. Enhanced rate of degradation of basic proteins by 26S immunoproteasomes. *Biochim Biophys Acta*. 2014;1843:1942–7. <https://doi.org/10.1016/j.bbamcr.2014.05.005>.
- Tubio-Santamaria N, Ebstein F, Heidel FH, Kruger E. Immunoproteasome function in normal and malignant hematopoiesis. *Cells*. 2021;10:1577. <https://doi.org/10.3390/cells10071577>.
- Niewerth D, Franke NE, Jansen G, Assaraf YG, van Meerloo J, Kirk CJ, Degenhardt J, Anderl J, Schimmer AD, Zweegman S, et al. Higher ratio immune versus constitutive proteasome level as novel indicator of sensitivity of pediatric acute leukemia cells to proteasome inhibitors. *Haematologica*. 2013;98:1896–904. <https://doi.org/10.3324/haematol.2013.092411>.
- Zhang Y, Xue S, Hao Q, Liu F, Huang W, Wang J. Galectin-9 and PSMB8 overexpression predict unfavorable prognosis in patients with AML. *J Cancer*. 2021;12:4257–63. <https://doi.org/10.7150/jca.53686>.
- Rouette A, Trofimov A, Haberal D, Boucher G, Lavalley VP, D'Angelo G, Hebert J, Sauvageau G, Lemieux S, Perreault C. Expression of immunoproteasome genes is regulated by cell-intrinsic and -extrinsic factors in human cancers. *Sci Rep*. 2016;6:34019. <https://doi.org/10.1038/srep34019>.
- Jenkins TW, Downey-Kopyscinski SL, Fields JL, Rahme GJ, Colley WC, Israel MA, Maksimenko AV, Fiering SN, Kisselev AF. Activity of immunoproteasome inhibitor ONX-0914 in acute lymphoblastic leukemia expressing MLL-AF4 fusion protein. *Sci Rep*. 2021;11:10883. <https://doi.org/10.1038/s41598-021-90451-9>.
- Schnoeder TM, Schwarzer A, Jayavelu AK, Hsu CJ, Kirkpatrick J, Dohner K, Perner F, Eifert T, Huber N, Arriba-Tutusaus P, et al. PLCG1 is required for AML1-ETO leukemia stem cell self-renewal. *Blood*. 2022;139:1080–97. <https://doi.org/10.1182/blood.2021012778>.
- Muchamuel T, Basler M, Aujay MA, Suzuki E, Kalim KW, Lauer C, Sylvain C, Ring ER, Shields J, Jiang J, et al. A selective inhibitor of the immunoproteasome subunit LMP7 blocks cytokine production and attenuates progression of experimental arthritis. *Nat Med*. 2009;15:781–7. <https://doi.org/10.1038/nm.1978>.
- Basler M, Groettrup M. Immunoproteasome-specific inhibitors and their application. *Methods Mol Biol*. 2012;832:391–401. https://doi.org/10.1007/978-1-61779-474-2_27.
- Kuo HP, Wang Z, Lee DF, Muehlestein M, Duque-Afonso J, Wong SH, Lin CH, Figueroa ME, Su J, Lemischka IR, Cleary ML. Epigenetic roles of MLL oncoproteins are dependent on NF-kappaB. *Cancer Cell*. 2013;24:423–37. <https://doi.org/10.1016/j.ccr.2013.08.019>.
- Numata A, Kwok HS, Kawasaki A, Li J, Zhou QL, Kerry J, Benoukraf T, Bararia D, Li F, Ballabio E, et al. The basic helix-loop-helix transcription factor SHARP1 is an oncogenic driver in MLL-AF6 acute myelogenous leukemia. *Nat Commun*. 2018;9:1622. <https://doi.org/10.1038/s41467-018-03854-0>.
- Fehling HJ, Swat W, Laplace C, Kuhn R, Rajewsky K, Muller U, von Boehmer H. MHC class I expression in mice lacking the proteasome subunit LMP-7. *Science*. 1994;265:1234–7. <https://doi.org/10.1126/science.8066463>.
- Heidel FH, Bullinger L, Arriba-Tutusaus P, Wang Z, Gaebel J, Hirt C, Niederwieser D, Lane SW, Dohner K, Vasioukhin V, Fischer T, Armstrong SA. The cell fate determinant Lgl1 influences HSC fitness and prognosis in AML. *J Exp Med*. 2013;210:15–22. <https://doi.org/10.1084/jem.20120596>.
- Mohr J, Dash BP, Schnoeder TM, Wolleschak D, Herzog C, Tubio-Santamaria N, Weinert S, Godavarthy S, Zanetti C, Naumann M, et al. The cell fate determinant Scribble is required for maintenance of hematopoietic stem cell function. *Leukemia*. 2018;32:1211–21. <https://doi.org/10.1038/s41375-018-0025-0>.
- Purton LE, Scadden DT. Limiting factors in murine hematopoietic stem cell assays. *Cell Stem Cell*. 2007;1:263–70. <https://doi.org/10.1016/j.stem.2007.08.016>.
- Hu Y, Smyth GK. ELDA: extreme limiting dilution analysis for comparing depleted and enriched populations in stem cell and other assays. *J Immunol Methods*. 2009;347:70–8. <https://doi.org/10.1016/j.jim.2009.06.008>.
- Krivtsov AV, Twomey D, Feng Z, Stubbs MC, Wang Y, Faber J, Levine JE, Wang J, Hahn WC, Gilliland DG, Golub TR, Armstrong SA. Transformation from committed progenitor to leukaemia stem cell initiated by MLL-AF9. *Nature*. 2006;442:818–22. <https://doi.org/10.1038/nature04980>.
- Wang B, Wang M, Zhang W, Xiao T, Chen CH, Wu A, Wu F, Traugh N, Wang X, Li Z, et al. Integrative analysis of pooled CRISPR genetic screens using MAGECKFlute. *Nat Protoc*. 2019;14:756–80. <https://doi.org/10.1038/s41596-018-0113-7>.
- Stein EM, Aldoss I, DiPersio JF, Stone RM, Arellano ML, Rosen G, Meyers ML, Huang Y, Smith S, Bagley RG, et al. Safety and efficacy of Menin inhibition in patients (Pts) with MLL-rearranged and NPM1 mutant acute leukemia: a phase (Ph) 1, first-in-human study of SNDX-5613 (AUGMENT 101). *Blood*. 2021;138(Supplement 1):699.
- Krivtsov AV, Armstrong SA. MLL translocations, histone modifications and leukaemia stem-cell development. *Nat Rev Cancer*. 2007;7:823–33. <https://doi.org/10.1038/nrc2253>.
- Perner F, Stein EM, Wenge DV, Singh S, Kim J, Apazidis A, Rahnamoun H, Anand D, Marinaccio C, Hatton C, et al. MEN1 mutations mediate clinical resistance to menin inhibition. *Nature*. 2023;615:913–9. <https://doi.org/10.1038/s41586-023-05755-9>.
- Ebstein F, Kloetzel PM, Kruger E, Seifert U. Emerging roles of immunoproteasomes beyond MHC class I antigen processing. *Cell Mol Life Sci*. 2012;69:2543–58. <https://doi.org/10.1007/s00018-012-0938-0>.
- Basler M, Dajee M, Moll C, Groettrup M, Kirk CJ. Prevention of experimental colitis by a selective inhibitor of the immunoproteasome. *J Immunol*. 2010;185:634–41. <https://doi.org/10.4049/jimmunol.0903182>.
- Klein M, Busch M, Friese-Hamim M, Crosignani S, Fuchss T, Musil D, Rohdich F, Sanderson MP, Seenisamy J, Walter-Bausch G, et al. Structure-based optimization and discovery of M3258, a specific inhibitor of the

- immunoproteasome subunit LMP7 (beta5i). *J Med Chem.* 2021;64:10230–45. <https://doi.org/10.1021/acs.jmedchem.1c00604>.
37. Sanderson MP, Friese-Hamim M, Walter-Bausch G, Busch M, Gaus S, Musil D, Rohdich F, Zanelli U, Downey-Kopyscinski SL, Mitsiades CS, et al. M3258 is a selective inhibitor of the immunoproteasome subunit LMP7 (beta5i) delivering efficacy in multiple myeloma models. *Mol Cancer Ther.* 2021;20:1378–87. <https://doi.org/10.1158/1535-7163.MCT-21-0005>.
 38. Hartl M, Nist A, Khan MI, Valovka T, Bister K. Inhibition of Myc-induced cell transformation by brain acid-soluble protein 1 (BASP1). *Proc Natl Acad Sci U S A.* 2009;106:5604–9. <https://doi.org/10.1073/pnas.0812101106>.
 39. Hartl M, Schneider R. A unique family of neuronal signaling proteins implicated in oncogenesis and tumor suppression. *Front Oncol.* 2019;9:289. <https://doi.org/10.3389/fonc.2019.00289>.
 40. Marsh LA, Carrera S, Shandilya J, Heesom KJ, Davidson AD, Medler KF, Roberts SG. BASP1 interacts with oestrogen receptor alpha and modifies the tamoxifen response. *Cell Death Dis.* 2017;8:e2771. <https://doi.org/10.1038/cddis.2017.179>.
 41. Moorhouse AJ, Loats AE, Medler KF, Roberts SGE. The BASP1 transcriptional corepressor modifies chromatin through lipid-dependent and lipid-independent mechanisms. *IScience.* 2022;25:104796. <https://doi.org/10.1016/j.isci.2022.104796>.
 42. Lin CC, Huang YK, Cho CF, Lin YS, Lo CC, Kuo TT, Tseng GC, Cheng WC, Chang WC, Hsiao TH, et al. Targeting positive feedback between BASP1 and EGFR as a therapeutic strategy for lung cancer progression. *Theranostics.* 2020;10:10925–39. <https://doi.org/10.7150/thno.49425>.
 43. Tang H, Wang Y, Zhang B, Xiong S, Liu L, Chen W, Tan G, Li H. High brain acid soluble protein 1(BASP1) is a poor prognostic factor for cervical cancer and promotes tumor growth. *Cancer Cell Int.* 2017;17:97. <https://doi.org/10.1186/s12935-017-0452-4>.
 44. Uckelmann HJ, Haarer EL, Takeda R, Wong EM, Hatton C, Marinaccio C, Perner F, Rajput M, Antonissen NJC, Wen Y, et al. Mutant NPM1 directly regulates oncogenic transcription in acute myeloid leukemia. *Cancer Discov.* 2022. <https://doi.org/10.1158/2159-8290.CD-22-0366>.
 45. Stavropoulou V, Almosailleakh M, Royo H, Spetz JF, Juge S, Brault L, Kopp P, Iacovino M, Kyba M, Tzankov A, et al. A novel inducible mouse model of MLL-ENL-driven mixed-lineage acute leukemia. *Hemasphere.* 2018;2:e51. <https://doi.org/10.1097/HS9.0000000000000051>.
 46. Cosgun KN, Rahmig S, Mende N, Reinke S, Hauber I, Schafer C, Petzold A, Weisbach H, Heidkamp G, Purbojo A, et al. Kit regulates HSC engraftment across the human-mouse species barrier. *Cell Stem Cell.* 2014;15:227–38. <https://doi.org/10.1016/j.stem.2014.06.001>.
 47. Dahlmann B. Mammalian proteasome subtypes: their diversity in structure and function. *Arch Biochem Biophys.* 2016;591:132–40. <https://doi.org/10.1016/j.abb.2015.12.012>.
 48. Jayavelu AK, Schnoder TM, Perner F, Herzog C, Meiler A, Krishnamoorthy G, Huber N, Mohr J, Edelmann-Stephan B, Austin R, et al. Splicing factor YBX1 mediates persistence of JAK2-mutated neoplasms. *Nature.* 2020;588:157–63. <https://doi.org/10.1038/s41586-020-2968-3>.
 49. Bagger FO, Kinalis S, Rapin N. BloodSpot: a database of healthy and malignant haematopoiesis updated with purified and single cell mRNA sequencing profiles. *Nucleic Acids Res.* 2018. <https://doi.org/10.1093/nar/gky1076>.

Publisher's Note

Springer Nature remains neutral with regard to jurisdictional claims in published maps and institutional affiliations.

Ready to submit your research? Choose BMC and benefit from:

- fast, convenient online submission
- thorough peer review by experienced researchers in your field
- rapid publication on acceptance
- support for research data, including large and complex data types
- gold Open Access which fosters wider collaboration and increased citations
- maximum visibility for your research: over 100M website views per year

At BMC, research is always in progress.

Learn more biomedcentral.com/submissions



11. Acknowledgments

First of all, I would like to thank Prof. Florian Heidel for giving me the opportunity of doing my PhD project in his group and for being an incredible and supportive supervisor, always bringing in new ideas and pushing me in the correct direction. Moreover, I wish to show gratitude to the members of my thesis committee, Prof. Elke Krüger and Prof. Jan Krönke, for all the helpful comments and suggestions in regard to the project. I am also undoubtedly thankful to Dr. Tina Schnöder, who did not only teach me how to properly work in a laboratory and was there at any time to solve any question, but whose help goes beyond any work-related matter. Besides, I wish to show my appreciation to my two PhD colleagues, Jane Hsu and Theresa Eifert, that apart from helping with experiments, made lab work and life so much fun. I want to extend my thanks to all the other members of the Heidel lab and all collaborators that helped with the project, with special thanks to Dr. Florian Perner and Dr. Ashok Jayavelu, and to the funding organizations, the Deutsche Forschungsgemeinschaft (DFG) and the Wilhelm Sander-Stiftung, that support our research. Finally, I would like to acknowledge the patients that donated samples for our project and enabled this research to be possible.